Materials Science & Engineering R 166 (2025) 101024

Contents lists available at ScienceDirect

Materials Science & Engineering R

journal homepage: www.elsevier.com/locate/mser

Carbon dots for reactive oxygen species modulation

Guopeng Xu [a], Yiheng Tang [a], Danfeng Xiong [a], Wenkun Zhang [a], Ziyu Liu [b], Paul K. Chu [c], Guomin Wang [a,*]

[a] State Key Laboratory of Cardiovascular Diseases and Medical Innovation Center, Shanghai East Hospital, Shanghai Tenth People's Hospital, School of Medicine, Tongji University, Shanghai 200070, PR China
[b] Beijing Advanced Innovation Centre for Biomedical Engineering, School of Engineering Medicine, Beihang University, Beijing 100191, PR China
[c] Department of Physics, Department of Materials Science and Engineering, and Department of Biomedical Engineering, City University of Hong Kong, Tat Chee Avenue, Kowloon 999077, Hong Kong

ARTICLE INFO

Keywords:
Carbon dots
Reactive oxygen species
ROS-modulators
Biomedicine

ABSTRACT

Reactive oxygen species (ROS) manipulation is emerging as a pivotal focus in biomaterials design. Carbon dots (CDs), with their superior biocompatibility, facile synthesis, exceptional electronic properties, and abundant active sites, are gaining significant attention as ROS modulators (CDRMs). However, unclear mechanisms of action and challenges in controlling activity and selectivity hinder the advancement of CDRMs for sophisticated biomedical applications. While existing reviews have summarized the synthesis and biomedical applications of CDs, none have systematically addressed their roles and mechanisms in ROS modulation. Additionally, a universal principle for designing efficient and selective CDRMs is urgently needed to advance their clinical translation. This review explores the origins of activity in CDRMs, elucidates modulation mechanisms, and provides in-depth insights into tailoring CDRMs for ROS upregulation, downregulation, and bidirectional manipulation. Strategies such as nanozyme-catalyzed, physical field-energized, and precursor-inherited ROS management are highlighted, followed by an analysis of methods to optimize CDRM activity and selectivity, addressing critical gaps in current literature. Furthermore, the applications of CDRMs in cancer therapy, wound healing, and inflammation-related diseases are summarized and analyzed. Finally, we discuss existing obstacles, such as low efficacy and selectivity, and propose strategies to enhance the clinical translation of CDRMs, offering a forward-looking perspective to guide future research and innovation in this promising field.

1. Introduction

Reactive oxygen species (ROS) are chemically reactive molecules generated through intracellular metabolism [1–3]. They can be classified into two categories: free radicals containing one unpaired electron, such as superoxide ion ($O_2^{\cdot-}$) and hydroxyl radical (·OH), and non-radicals without unpaired electrons, including singlet oxygen ($^1O_2$) and hydrogen peroxide (H_2O_2) [4–7]. Importantly, as intracellular second messenger within cells, ROS play a pivotal role in regulating cell fate by influencing gene transcription, signal transduction, and cell survival [8–12]. When confronting invaders such as pathogens or cancer cells, the microenvironment becomes saturated with ROS, which activate phagocytes to rapidly eliminate harmful factors, thereby preventing infectious or tumorous diseases [13–18]. However, excessive ROS accumulation can irreversibly evoke oxidative stress damage to the normal cells causing serious inflammation-related diseases [19–23]. Therefore, ROS function as a double-edged sword with both physiological and pathological effects, and their precise regulation through the development of smart modulators could offer valuable strategies for treating various ROS-related disorders, including infected wounds, malignant tumors, and inflammatory diseases.

Nanotechnology has significantly advanced nanomedicine by offering meticulously designed nanoplatforms that can precisely regulate the microenvironment in the diseased site [24–27]. Among various nanomaterials, carbon dots (CDs) have gained growing attention for their distinctive advantages, including intrinsic fluorescence, enzyme-like activity, abundant surface functional groups, efficient electron transfer capabilities, semiconductor-like electronic property, and excellent biocompatibility [28–32]. CDs are a class of luminescent nanomaterials, whose size are typically less than 10 nm with the major compositions of C, N and O elements [33–35]. CDs usually exhibit various biomedical functions, such as imaging, drug delivery, and sensing. Especially,

* Corresponding author.
E-mail address: wangguominhi@gmail.com (G. Wang).

https://doi.org/10.1016/j.mser.2025.101024
Received 5 March 2025; Received in revised form 23 May 2025; Accepted 26 May 2025

carbon-dot ROS-modulators (CDRMs) have recently shown promising potential in ROS modulation for biomedical healthcare [36–38]. By mimicking oxidase- or peroxidase- enzymatic catalysis, some CDRMs can upregulate intracellular ROS, inducing bacterial and tumor cell lethality through excessive oxidative stress [39–42]. Other CDRMs can imitate natural antioxidant enzymes and act as antioxidant precursors, thereby downregulating the intracellular ROS levels [43,44]. In addition to the aforementioned unidirectional regulation, CDRMs can also enable bidirectional ROS manipulation (i.e., pro-oxidation and anti-oxidation) through strategic application of exogenous energy and deliberate structure design, allowing for dynamical control of ROS levels in response to disease progression [45]. The above flexible ROS modulation is generally reported to operate through three primary mechanisms: i) formation of catalytic sites to emulate natural enzymes; ii) generation of active electrons and holes upon photo or ultrasound excitation; iii) design of surface functional groups acting as electron donors, acceptors and transfer vehicle to facilitate redox reaction. Currently, numerous CDs with ROS regulation behaviors have been dispersedly developed, and some review articles have summarized their synthesis and biomedical applications. Regrettably, the underlying mechanisms of ROS management remain unclear and lack in-depth categorical analysis, including the active sites, energy transfer, substrate transformation process, and ROS modulation selectivity. Furthermore, a universal theory based on existing research is yet to be established. However, such a theory could significantly enhance the ROS-modulating activity and selectivity in future design of CDs. Therefore, a systemic summary and insightful discussion on the mechanism and structure-performance relationship of CDRMs is urgently needed to support their successful application in biomedical fields.

This review focuses on the state of the art in research on CDRMs, emphasizing their working mechanisms across various ROS regulation modes, and ultimately culminating in an extensive analysis of their current biomedical applications. Through comprehensive analysis and in-depth investigation, we aim to propose a foundational theory to guide the structural design of more efficient and selective CDRMs. CDRMs are categorized into three types based on their role in ROS modulation: upregulation, downregulation, and bidirectional regulation. For CDRMs with ROS up-regulation capability (Fig. 1a), we examine the mechanisms by which physical fields/enzymatic catalysis stimulate ROS generation or selectively enhance specific ROS types. Additionally, we review the operational principles of pro-oxidant enzyme-like CDRMs, providing practical examples from recent studies. For CDRMs with ROS down-regulation properties (Fig. 1b), we highlight those functioning as antioxidant enzymes or their precursors, offering a detailed overview of the mechanisms involved in ROS removal. Beyond these unidirectional influences, we focus on CDRMs capable of bidirectional ROS regulation (Fig. 1c), which hold promise for strategic, on-demand ROS modulation. Based on this theoretical framework, we summarize key biomedical applications, including chronic wound healing, malignant tumor treatment, and inflammatory disease management (Fig. 1d). Finally, we discuss emerging challenges and future prospects, emphasizing the need to establish structure-property relationships, enhance selectivity, and achieve precise ROS modulation.

2. Definition, classification, synthesis, and functionalization of CDRMs

CDs can be categorized into fluorescent, catalytic, photoelectric, and multifunctional types, with many depending on ROS regulation for their functionality. Given the pivotal role of ROS in maintaining cellular function and health at optimal levels as well as their potential to cause harm when imbalanced, this review focuses on the ROS regulation capabilities of CDs, setting it apart from the predominantly function-oriented perspectives of existing reviews. This section begins with an overview of the definition, chemical classification and structural characteristics of CDs, followed by a summary of general fabrication methods. Subsequently, we outline strategies to functionalize CDRMs, including doping and surface modification, aimed at enhancing performance and expanding their biomedical functionalities.

2.1. Definition, classification and structural characteristics

CDs, a collective term for various nanosized carbon materials, were first identified in 2004 by Scrivens et al. [46] as photoluminescent impurities in single-walled carbon nanotubes. In recent years, CDs have garnered significant attention in the biomedical field due to their

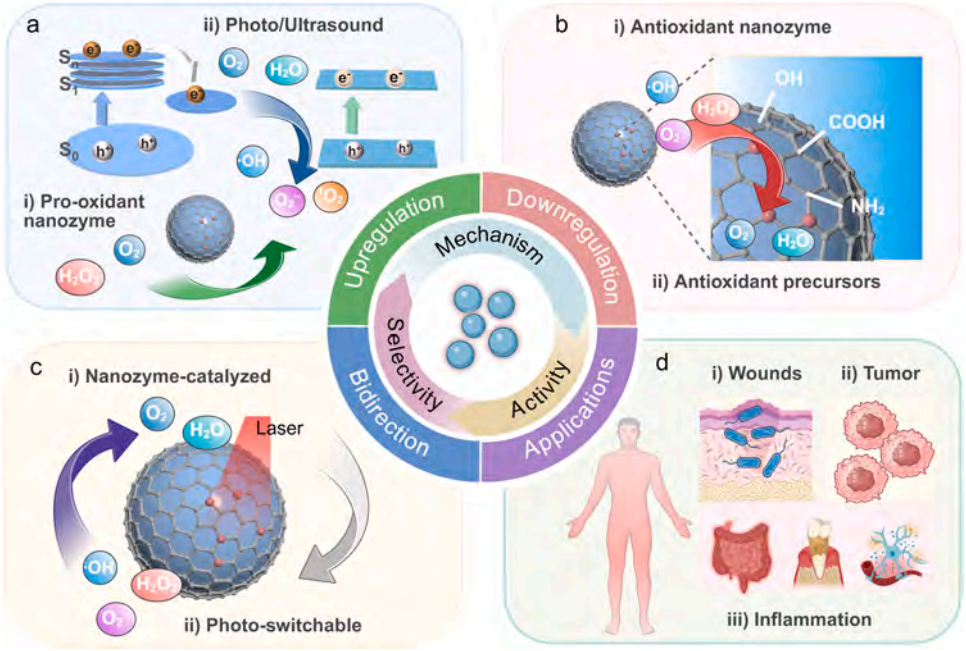

Fig. 1. Overview of CDRMs to manage intracellular ROS, including action mechanisms, activity modulation, and selectivity improvement. (a) Unidirectional ROS up-regulation, (b) Unidirectional ROS down-regulation, (c) Bidirectional ROS regulation, (d) Biomedical applications.

multifunctionality, encompassing not only their fluorescent properties but also their unique physicochemical features that enable ROS modulation, establishing them as CDRMs [47,48]. In this context, CDRMs are defined as a distinct subclass of CDs that not only retain the fundamental physicochemical characteristics such as size-dependent effects, photoluminescence, and biocompatibility, but also exhibit intrinsic catalytic activity or responsiveness to exogenous physical fields, enabling the modulation of ROS levels.

While the intrinsic "black box" nature of CDRMs poses challenges in achieving a fully accurate classification and structural definition, ongoing research and deeper understanding are gradually clarifying their structural characteristics and commonalities. Typically, CDRMs consist of a carbonized core with sp^2/sp^3 carbon skeletons, surrounded by a shell rich in functional groups or polymer chains [49,50]. This structural framework allows for significant diversity in physicochemical properties, including morphological structure, core crystallinity, and shell configuration, which can vary based on synthetic conditions (e.g., reaction time, temperature, pH, and solvent) and precursor selection. Based on these variations, CDRMs can be further categorized into graphene quantum dots (GQDs), carbon quantum dots (CQDs), and carbonized polymer dots (CPDs) [51–53].

GQD are the earliest reported and, to date, the most extensively studied type of CDRMs. When carbon materials are subjected to relatively harsh conditions, the resulting nanofragments are classified as GQDs (Fig. 2). These anisotropic structures have lateral dimensions of less than 10 nm and a height of no more than five graphite layers. GQDs typically feature sp^2-structured carbon cores with well-defined graphene lattices. Their edges or interlayer defects are rich in functional groups, such as carboxyl (-COOH), hydroxyl (-OH), and amino ($-NH_2$) groups, which confer unique properties like quantum confinement and edge effects [54,55]. The ROS modulation capability of GQDs arises synergistically from their size-dependent quantum confinement effects, isolated π-domains within the core, and edge effects contributed by the functional groups.

CQDs are usually obtained via the hydrothermal carbonization of organic small molecules. Although CQDs share similarities with GQDs in having a graphene-like crystalline sp^2-hybridized carbon core (Fig. 2), they typically feature a sp^3-hybridized surface shell enriched with oxygen- and nitrogen-based functional groups and polymer chains. Another distinction is that CQDs exhibit a quasi-spherical morphology, often accompanied by additional graphite layers within the core. These layered structures can be distinctly observed through high-resolution transmission electron microscopy, revealing their characteristic lattice spacing.

The concept of CPDs was first introduced by Yang's group in 2018 [56,57]. Distinct from the other three subtypes, CPDs CPDs are characterized by highly dehydrated, cross-linked polymer backbones or lightly graphitized carbon cores [58,59], which are encapsulated by externally entangled polymer chains bearing diverse chemical functionalities (Fig. 2). While both CQDs and CPDs contain functional groups and polymer chains, CPDs exhibit a higher abundance and complexity of these surface moieties.

The ROS modulation ability of CDRMs is closely related the abundant surface functional groups and unique structure such as crystallinity and edge effect. Among the three subtypes of CDRMs, GQDs are the most distinguishable due to their unique precursors, production methods, and morphological structure (Table 1). In contrast, the structural definitions of the other three types remain incomplete and are yet to reach a consensus, leading to their names often being used interchangeably.

2.2. Synthetic methods and techniques

Based on the differences in carbon sources, methods for preparing CDRMs can be broadly classified into two major approaches: "top-down" and "bottom-up". The top-down approach utilizes bulk carbon materials

Table 1
Structural characteristics, synthesis, and application difference of CDRMs.

Category	Graphene quantum dots (GQDs)	Carbon quantum dots (CQDs)	Carbonized polymer dots (CPDs)	Ref.
Size	< 10 nm	< 10 nm	< 10 nm	[50, 58]
Morphology	Anisotropic	Quasi-spherical	Quasi-spherical	[53, 55]
Core	The highest sp^2 fraction	The crystalline sp^2-sp^3 hybridization	Slightly graphitized structure	[28, 52]
Shell	Functional groups	Functional groups and little polymer chains	Functional groups and abundant polymer chains	[57, 59]
Precursor	Bulk carbon materials	Small molecules	Small molecules or polymers	[46, 51]
Synthesis	Top-down	Top-down or bottom-up	Bottom-up	[48, 60]
Application	ROS up- and downregulation	ROS up- and downregulation	ROS up- and downregulation	[61, 62]

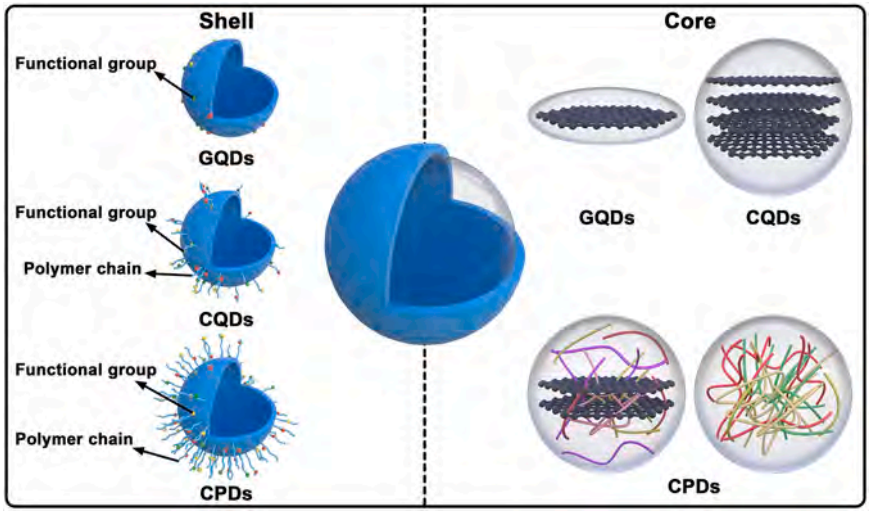

Fig. 2. Classification and structural characteristics of CDRMs in terms of morphology, crystallinity, and shell configuration. Reproduced with permission from ref. [52]. Copyright 2023, Elsevier.

as precursors, exfoliating them into nanoscale CDRMs, whereas the bottom-up approach begins with small molecules, polymers, or biomass as precursors, followed by processes such as dehydration, condensation, and localized carbonization.

2.2.1. Top-down synthesis

In the top-down synthesis pathway, the precursors are relatively limited, primarily involving graphite, graphite oxides, carbon fibers, and carbon nanotubes with sp^2 structures (Fig. 3a). GQDs are commonly synthesized through this approach, which employs various methods to efficiently fragment bulk carbon materials, including physical and chemical exfoliation.

Physical methods, such as arc discharge, mechanical milling, and laser ablation were developed earlier [48,60,63,64]. The arc discharge method typically places an anode a few millimeters away from a graphite rod that could be evaporated by an electric arc to produce unpurified CDs deposited on the chamber walls as a soot. Although this method achieves excellent fluorescence performance, it is limited by low yield efficiency and poor size controllability of the resulting CDRMs. Mechanical milling addresses some of these issues by enabling modulation of ball size, collision frequency, and grinding time, to achieve more controllable results. However, the above methods often require the complex synthesis processes. Laser ablation is emerging as promising alternative because it seldom requires harsh exfoliation conditions and is less time-consuming. CDRMs produced through laser ablation often exhibit reduced fluorescent performance due to rapid heating and highly concentrated energy during the process. Chemical exfoliation methods can be categorized into chemical oxidation and electrochemical oxidation, both relying on strong oxidants (e.g., concentrated HNO_3, H_2SO_4, and KOH) [52,65]. The chemical oxidation method treats bulk carbon materials with strong acids under hydrothermal or solvothermal conditions. Meanwhile, electrochemical oxidation applies high voltage to carbon precursors acting as working electrodes in an electrolyte, exfoliating large carbon structures into smaller nanoparticles (NPs). Despite the emergence of various exfoliation methods mentioned above, most remain unsuitable for large-scale production due to the nature requirement of harsh synthesis conditions, and complex post-treatment requirements for top-down synthesis.

2.2.2. Bottom-up synthesis

Given the importance of reducing industrial manufacturing costs and improving synthesis purity for the widespread application of CDRMs in biomedical and other fields, the bottom-up method has gained greater popularity due to its notable advantages, including simpler operation processes, fewer purification steps, and a broader range of raw materials. The bottom-up synthesis approach employs small organic molecules, aromatic compounds, organic polymers, and biomass as precursors, which are typically rich in functional groups such as -OH, -COOH, $-NH_2$, and -SH (Fig. 3**b**). These precursors are usually sealed in an autoclave and heated above their boiling points to undergo hydrothermal or solvothermal reactions, during which dehydration and crosslinking processes promote the formation of carbonized structures [54,66,67]. During bottom-up synthesis, the structure, size, and components of CDRMs can be fine-tuned by selecting suitable precursors and varying reaction parameters such as solvents, temperature, and time, so as to obtain a better ROS-modulating performance. For example, Kim et al. [68] synthesized multicolor emission CQDs, including blue (B-CQDs), green (G-CQDs), and yellow (Y-CQDs), by adjusting the ratio of sulfuric and phosphoric acids in the reaction. Under near-infrared light irradiation, Y-CQDs demonstrated the most ·OH generation effectively killing bacteria, attributed to their larger polyaromatic sp^2 domains and more oxidized surfaces. Similarly, Su et al. [69] used natural turmeric as a carbon source to prepare CDRMs (ST-JHCQDs) under various reaction temperature. As the carbonization temperature increased, the antibacterial performance decreased due to reduced ROS generation under blue light irradiation.

Although hydrothermal and solvothermal methods are eco-friendly and offer strong operability, they can be time-consuming. Microwave-assisted synthesis offers a faster alternative, leveraging electromagnetic fields to interact with carbonaceous molecules in confined spaces and resulting in more uniform heating and faster carbonization and nucleation of CDRMs. Another widely used bottom-up method is pyrolysis, which involves the direct condensation and decomposition of organic precursors under non-enclosed conditions, leading to irreversible changes in physical and chemical properties. Pyrolysis typically requires high-temperature calcination under the protection of inert gas [70,71], during which most functional groups decompose into gases, reducing the heteroatom doping content in the synthesized CDRMs. Among various synthesis methods for bottom-up synthetic techniques, hydrothermal and solvothermal techniques still remain the mainstream and should be continuously refined to improve synthesis purity and clarify formation mechanisms of CDRMs. Furthermore, integrating microwave-assisted synthesis with hydrothermal or solvothermal approaches shows promise for saving time and producing CDRMs with enhanced ROS-modulating performance.

2.3. Strategies for functionalization of CDRMs

Functionalization plays a crucial role in tailoring the physicochemical properties of CDRMs, enhancing their activity and selectivity in ROS regulation, lesion targeting, and multifunctional disease therapies. Two widely used strategies are heteroatom doping, which is incorporated during synthesis, and surface modification, typically performed post-synthesis. The following sections will detail the fabrication processes of these approaches and their respective impacts on the properties of CDRMs.

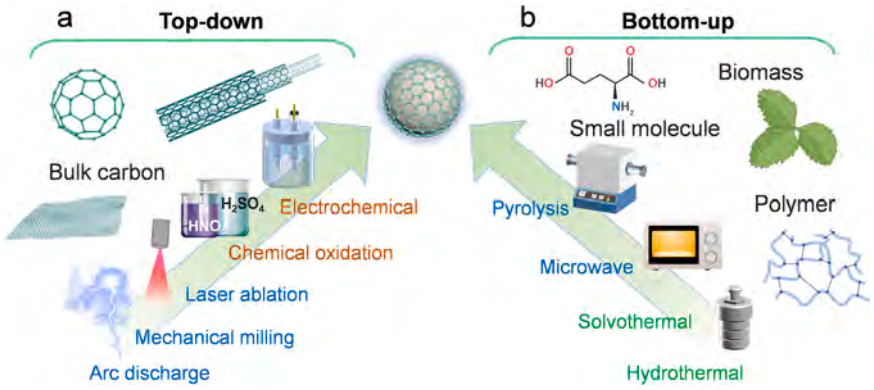

Fig. 3. The synthetic pathway and techniques of CDRMs. (a) The top-down preparation. (b) The bottom-up synthesis.

2.3.1. Heteroatom doping

Doping is a highly effective strategy for tuning the physical and chemical properties of CDRMs. Doping elements can be broadly classified into non-metallic (e.g., N, S, P) and metallic (e.g., Fe, Ce, Cu, Co, Mn, Se, Au) categories (Fig. 4a). The standard synthesis of doped CDRMs involves incorporating carbon precursors containing the required doping elements, with subsequent steps following conventional synthesis procedures outlined in *Section 2.2*. For metallic doping, organometallic complexes or metal salts are often employed alongside carbon sources.

Incorporating heteroatoms into the carbon framework creates surface active sites and defects, thereby improving the enzymatic and photocatalytic processes. N, with its five valence electrons, similar atomic size to carbon, and frequent presence in precursor materials, is the most extensively studied non-metallic dopant for enhancing surface catalytic activity, charge transfer, and selectivity of CDRMs. [72,73]. On the other hand, metallic doping is usually prioritized to enhance catalytic activity, optoelectronic performance, or imaging functions. For instance, Fe, Cu, and Ce are frequently incorporated to replicate the catalytic sites of natural oxidoreductases for intracellular ROS modulation [74–76]. Jiang et al. [77] synthesized Mn-doped CDs via a hydrothermal method using EDTA-2Na as a precursor. These resulting CDs exhibited superior oxidase activity by generating $O_2^{\cdot-}$ under light irradiation, which was attributed to the reduced bandgap, influenced by the intermediate energy levels, spin density, and charge distribution. Cheng et al. [78] employed a one-step microwave-assisted method to synthesize Gd/Ru bimetallic-doped CDs, which exhibited both $^1O_2$ generation upon 650 nm laser exposure and magnetic resonance imaging (MRI) capabilities. Despite these advancements, the potential biotoxicity from ion release in metal-doped CDRMs warrants attention. Furthermore, it is crucial to rationally design the doped structures, particularly by optimizing the coordination ratio and utilizing secondary dopants, to improve stability.

2.3.2. Surface modification

While doping modifies the core structure affecting intrinsic properties, surface modification can tailor the external surface of CDRMs by attaching various of functional groups such as small drug molecules, ions, nanocluster or NPs [44,79,80]. The primary strategies for surface modification include amide coupling, electrostatic assembling, and in-situ reduction, with each method impacting the properties of CDRMs in distinct ways (Fig. 4b).

Amide coupling reactions involve the condensation of a carboxylic acid with an amine to form an amide and release water. However, this reaction is thermodynamically unfavorable and requires activation of the carboxyl group or deprotonation of the amine [81,82]. This method is typically used to modify the surface of CDRMs with small molecules or targeting agents like folic acid. However, the effect of this surface modification on ROS modulation is not yet fully explored, and a balance must be struck between imparting new functionalities (e.g., fluorescence modulation, lesion targeting and response) and maintaining ROS-regulating ability. Typically, CDRMs are either positively or negatively charged [83,84], which paves the way for electrostatic assembly between CDRMs and ions or molecules. Another electrostatic surface modification method for CDRMs is complexation, where coordination bonds form between ions and the functional groups on the surface. For instance, Park et al. [85] designed a CDs using o-phenylenediamine (OPD) as a precursor, which introduced nitrogen-containing polyaromatic groups on the CD surface. These functional groups exhibited strong absorption and coordination abilities with Cu^{2+} ions. The in-situ reduction method is often employed to integrate metal nanoclusters or nanoparticles (NPs) onto CDRMs to enhance enzymatic activity, electron transfer, and physical field-responsive properties. This process involves the absorption of metal compounds (e.g., $HAuCl_4$, $PdCl_2$, H_2Cl_6Pt, and $AgNO_3$) and their subsequent in-situ reduction using strong reductive agents (e.g., $NaBH_4$ and ethanol). Sakdaronnarong et al. [86] demonstrated that Pt NPs could be synthesized on CD surfaces to improve enzyme-like activity while the incorporation of silver (Ag) NPs could diminish the catalytic activity. In some cases, the above surface modifications might also enhance the stability and hydrophilicity of CDRMs, improving their bioavailability and efficacy in biomedical applications.

Above all, the bulk properties such as electronic structure, catalytic activity, and ROS modulation, as well as surface properties, including targeting ability, drug delivery, biocompatibility, and fluorescence, can be finely tuned by synergistically combining doping and surface modification, depending on the specific application.

3. Upregulation of ROS by CDRMs

CDRMs themselves rarely generate ROS directly. Interestingly, the pristine sp^2/sp^3 hybridized carbon core, unique internal properties, and diverse surface functional groups of CDRMs enable them to expose abundant catalytic sites mimicking oxidase (OXD) and peroxidase (POD) or be excited by external physical stimuli. All these properties contribute to ROS generation, the fundamental cause of which lies in the abundant supply of active electrons to catalyze other molecules serving as substrates. In this section, we first discuss ROS upregulation triggered by the catalytic activities of CDRMs. Additionally, we summarize ROS upregulation strategies based on physical stimuli such as light and ultrasound. Each strategy is examined by exploring the mechanisms

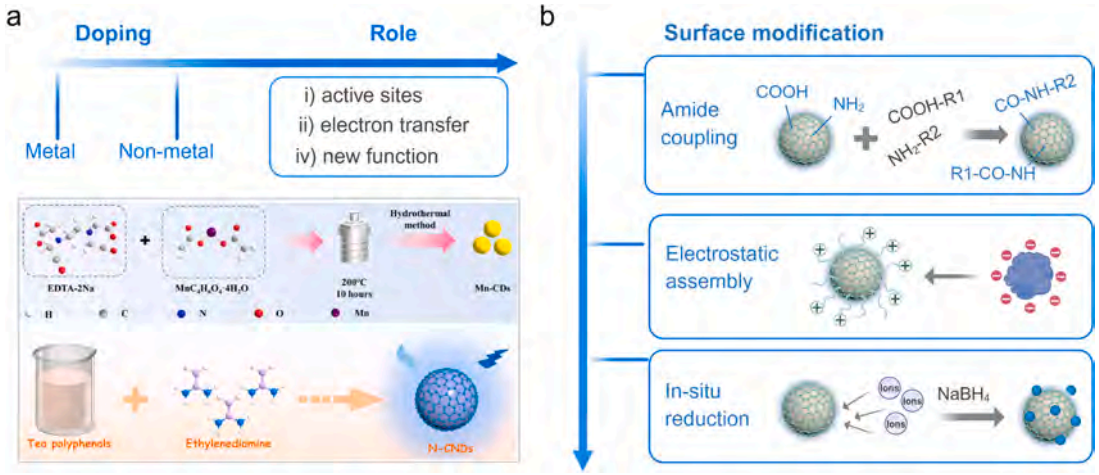

Fig. 4. The functionalization of CDRMs. (a) Doping and its effect on CDRMs. Reproduced with permission from ref. [77,87]. Copyright 2023, Elsevier. (b) Methods of surface modification.

underlying free electron production, followed by a discussion of activity modulation and selectivity improvement approaches.

3.1. Nanozyme-catalyzed ROS upregulation

The phenomenon of nanozyme-catalyzed ROS production was first reported in 2007 when Yan et al. [88,89] discovered the intrinsic horseradish peroxidase (POD)-mimicking activity of ferromagnetic Fe_3O_4 NPs. In 2013, Wang et al. [90] introduced the term "nanozyme" to describe various nanomaterials with enzymatic activities. Compared to natural enzymes, nanozymes offer advantages in terms of lower preparation costs, enhanced catalytic stability, and ease of surface modifications. Among these, carbon dots stand out as promising nanozymes due to their small size, excellent biocompatibility, and diverse precursors. CDRMs can mimic natural POD and OXD activities, generating ·OH, $O_2^{\cdot-}$, and $^1O_2$ using H_2O_2 and O_2 as substrates. Although reaction substrates of POD and OXD are similar with that of photo-energized ROS generation, the enzymatic catalysis requires no external energy field. This section delves into the origins of the enzymatic activity of CDRMs and the corresponding mechanisms. Additionally, strategies for enhancing enzyme-like activity are discussed, including the application of physical fields, engineering single-atom nanozymes, doping with synergistic dual elements, modulating the coordination environment, and constructing cascaded reactions. Furthermore, current methodologies for achieving selective ROS generation are also highlighted.

3.1.1. Active sites and catalytic mechanisms

Both the POD- and OXD-like catalytical properties of CDRMs are largely dependent on the active sites present within the CDRMs. In a typical POD-like catalytic process, the first substrate, hydrogen peroxide (H_2O_2), is catalyzed to generate highly oxidative species such as hydroxyl radicals (·OH) or superoxide ($O_2^{\cdot-}$), which then further oxidize the second substrates. Similarly, in OXD catalysis, molecular oxygen (O_2) acts as the first substrate, producing $O_2^{\cdot-}$ or singlet oxygen ($^1O_2$), which can oxidize the second substrates, completing the catalytic process.

Elemental doping is a widely used strategy to incorporate catalytic sites into carbon dots with metal/non-metal dopants. Various metal elements, such as Fe, Cu, Mn, Ce, Co, and others, have been reported to enhance the enzymatic catalysis of CDRMs, facilitating the upregulation of ROS. A common method for doping is the hydrothermal technique, which uses metal salts (e.g., $FeCl_3$, $FeSO_4$, $CuCl_2$, $MnCl_3$, and $Ce(NO_3)_3$) as doping precursors to synthesize CDRMs exhibiting POD or OXD activities. In this process, the doped metal ions coordinate with nitrogen (N) elements in the CDs, forming chemical bonds that are believed to be responsible for substrate adsorption and electron transfer, key steps in enzymatic redox catalysis. For example, Li et al. [91] prepared Fe, N-doped CDs (Fe/N-CDs) exhibiting superior POD-like activity by hydrothermally carbonizing $FeSO_4{\cdot}7\,H_2O$ and L-histidine (Fig. 5a). They demonstrated that H_2O_2 molecules were adsorbed onto the Fe-N_4 sites of Fe/N-CDs, where they were activated for homolytic decomposition into two hydroxyl radicals (·OH), which then generated ·OH upon desorption. Similarly, Jin et al. [92] found that the coordination of Cu with N could significantly enhance the number of active sites by forming Cu^+/Cu^{2+} redox pairs, which triggered a Fenton-like reaction leading to the formation of ·OH. These radicals then rapidly transformed into $O_2^{\cdot-}$ and $^1O_2$, completing the catalytic cycle.

Although various metal elements endow CDRMs with enzymic property, the enzymatic activity is found to correlate linearly with the stability constants of the metal ions. This observation is supported by Li et al. [93], who synthesized EDTA-functionalized CDs-metal nanozymes (CDs_{EDTA}-Me) with different metal ions (Fe^{3+}, Cu^{2+}, and Co^{2+}). They found that CDs_{EDTA}-Fe exhibited the highest POD-like activity (Fig. 5b). pH also plays a critical role in modulating the catalytic activity of CDRMs. Acidic environments generally promote POD and OXD-like activities, while neutral or alkaline conditions tend to diminish enzymatic properties. Therefore, developing CDRMs that maintain enzymatic activity under neutral conditions is especially promising for biomedical applications. For example, Zhang et al. [94] prepared CDs-Fe with

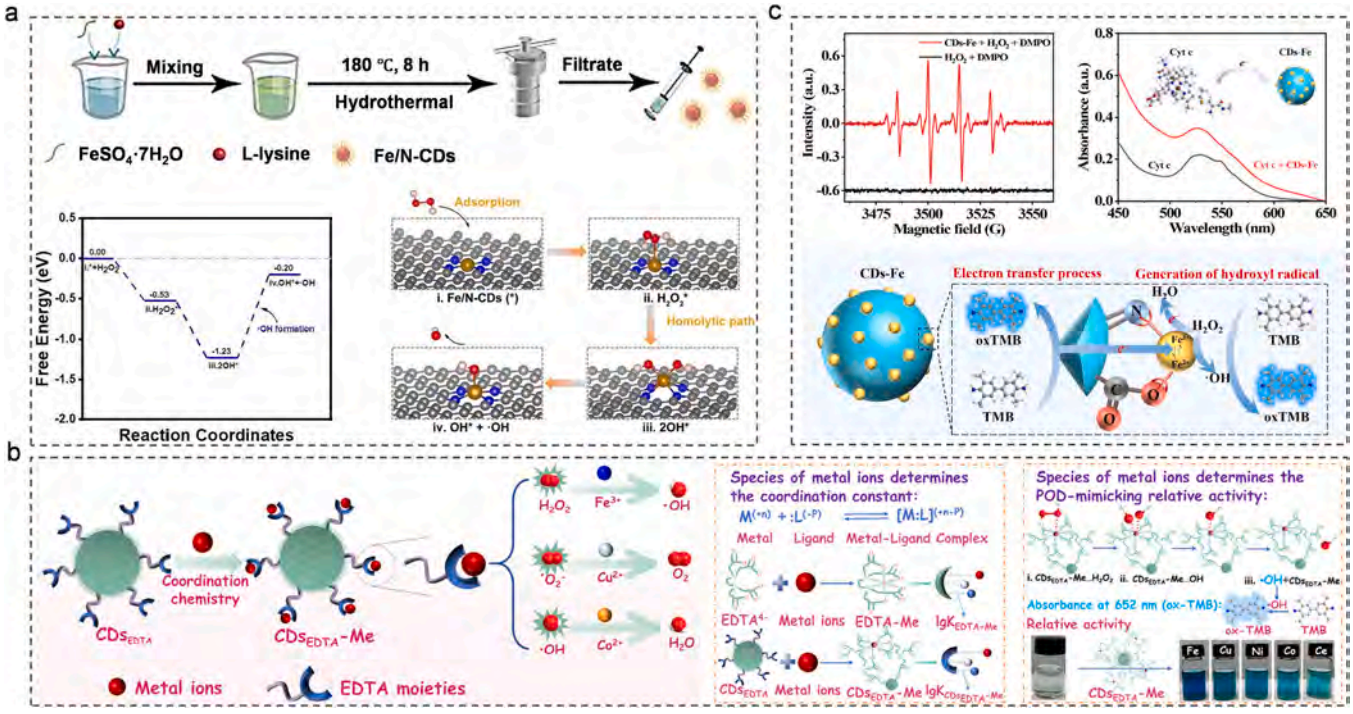

Fig. 5. Catalytic sites and corresponding mechanisms of nanozyme-catalyzed ROS upregulation. (a) The reaction pathway of POD-like Fe/N-CDs. [91]. Copyright 2023, Elsevier. (b) Differences in enzyme-like activity caused by various metal ions with the same coordination structure. [93]. Copyright 2024, American Chemical Society. (c) POD-like activity of CDs-Fe and potential catalytic mechanisms under neutral pH. [94].Copyright 2024, Elsevier.
(a) Reproduced with permission from ref. (b) Reproduced with permission from ref. (c) Reproduced with permission from ref.

Fe^{3+}/Fe^{2+}species through redox and coordination between aloe leaves-derived CDs which contain oxygen/nitrogen-rich functional groups, and Fe^{3+} (Fig. 5c). These CDs-Fe demonstrated excellent POD-like activity under neutral pH, owing to the synergistic effect of electron transfer processes and Fenton reaction-initiated ·OH generation. Specifically, electrons from substrates were captured by coordinated Fe^{3+}, reducing it to Fe^{2+}. The accumulated electrons at Fe^{2+} were then transferred to H_2O_2, with Fe^{2+} being oxidized back to Fe^{3+}, facilitating an effective Fe^{3+}/Fe^{2+} redox cycle and accelerating the electron transfer between substrates and CDs-Fe.

In addition to metal doping, non-metal elements N, S, and P are also commonly incorporated into CDRMs, due to their lower biotoxicity compared to metal-doped enzymes. For example, Gong et al. [87] fabricated low-cost, biocompatible, and water-dispersible metal-free nitrogen-doped carbon nanodots (N-CNDs) with OXD-mimicking activity, exhibiting a high maximum reaction rate (1.59 μM/s) and a low Michaelis constant (0.421 mM). The surface functional groups of the CDRMs are another critical factor, as they serve as enzymatic catalytic centers. Functional groups such as hydroxyl, carboxyl, and amine can adsorb and bind substrates through electrostatic interactions, promoting electron transfer between CDRMs and substrates, which is essential for initiating POD/OXD reactions. In the work by Huang et al. [43], they synthesized a type of metal-free CDs with multiple enzyme-like activities such as POD and CAT, that could be attributed to the abundant surface functional groups.

Despite considerable progress, our understanding of the catalytic mechanisms in CDRMs remains limited, mainly due to the complex substrate decomposition pathways and the elusive nature of the active sites. Although much evidence highlights the crucial role of doped metal and non-metal ions in enzymatic catalysis, a deeper understanding of substrate binding, transformation, and interaction with these active sites is still needed. For example, surface defects often form during doping, which may influence substrate adsorption and electron transfer, thereby affecting the enzymatic activity of CDRMs. Moreover, the depletion of catalytic sites remains a challenging issue that cannot be ignored. Additionally, components in the solution, such as phosphate ions, may

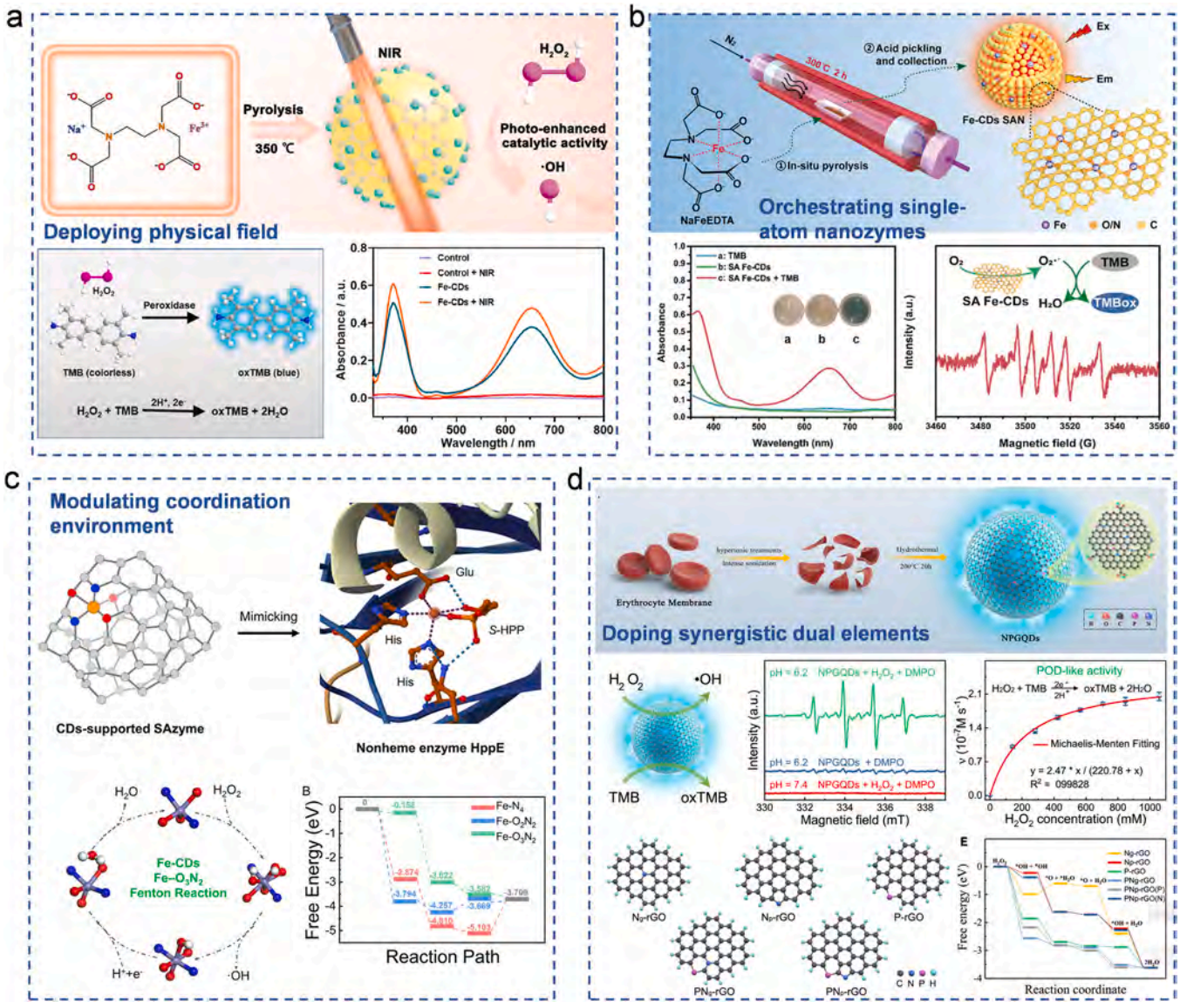

Fig. 6. Activity modulation of nanozyme-catalyzed ROS upregulation. (a) Deploying physical fields. [95]. Copyright 2022, Elsevier. (b) Orchestrating single-atom nanozymes. [105]. Copyright 2022, Wiley. (c) Modulating the coordination environment. [108]. Copyright 2023, American Chemical Society. (d) Synergistic dual elements doping. [109]. Copyright 2024, Elsevier.
(a) Reproduced with permission from ref. (b) Reproduced with permission from ref. (c) Reproduced with permission from ref. (d) Reproduced with permission from ref.

inhibit the ROS upregulation ability of CDRMs, though the underlying mechanism is yet to be fully explained. It is also worth noting that the OXD-like catalytic mechanisms of CDMRs have been less extensively studied, but the principles established for POD-like CDRMs may also apply to OXD-like reactions.

3.1.2. Activity modulation

3.1.2.1. Deploying physical field. The semiconductor-like electronic properties of CDRMs enable them to be excited by photons with appropriate energy, resulting in enhanced enzyme-mimicking activity. The photothermal effect and hot carriers are believed to be the primary mechanisms behind the activity enhancement of CDRM nanozymes. Photon excitation of CDRMs generates hot carriers (e.g., e^--h^+ pairs), which release their energy as localized heat through non-radiative relaxation. This localized heat increases the kinetic energy of substrates, optimizes the absorption surface, reduces the activation energy of catalytic reactions, and ultimately enhances enzymatic catalysis. For example, Zhou and Liu et al. [95] synthesized Fe-CDs (~3 nm) nanozymes with excellent photothermal-enhanced enzymatic properties via a simple one-pot pyrolysis approach (Fig. 6a). The Fe-CDs exhibited significantly boosted POD-like activity upon 808 nm laser irradiation, likely due to increased electron transfer efficiency from the mild photothermal effect. The larger polyaromatic sp^2 domain and oxidized surface contribute to higher photothermal conversion efficiency (η). Zhang et al. [96] used a graphite plate as the raw material and employed a pulse electrolysis method to obtain high-purity CDs. These CDRMs featured a highly π-conjugated sp^2-hybridized graphite structure, achieving an η as high as 64.3 % at a concentration of 500 μg/mL, with the temperature rising to 82.2°C under NIR irradiation. In addition to internal structure design, adjusting the adsorbed substrates can further synergize with enzymatic catalysis to boost ROS production. For instance, Li and Xu et al. [97] created a heterointerface between POD-mimicking Fe-CDs and hot electron-generating nanorods (GNRs) through simple electrostatic self-assembly. The electric field formed at the heterointerface induced rapid migration of hot electrons from the GNRs to the Fe-CDs upon 808 nm laser excitation, increasing the POD-like activity by 3.14 times. Similarly, Wang et al. [98] synthesized Mn-doped CD nanozymes (Mn-CDs), which exhibited 1.81 times higher enzymatic activity under laser excitation compared to that in the dark.

While these strategies focus on enhancing POD activity through photocatalysis, non-metal incorporation, such as P-doping in P-CDs, has been found to enhance photocatalytic OXD-like activity more effectively [99]. This improvement is attributed to the higher crystallinity conferred by P-doping. Ultrasound, as another physical field, can also boost the enzymatic activity of CDRMs, owing to their ultrasound-responsive properties discussed in *Section 3.3*. However, corresponding investigations are still in the early stages.

3.1.2.2. Orchestrating single atom nanozymes. Single-atom nanozymes (SAzymes) have recently garnered significant attention due to their promising catalytic properties [100,101]. Although their coordination structure resembles that of metalloenzymes, the atomically dispersed active sites in SAzymes result in highly efficient atom utilization [102–104], leading to enzymatic activities that can match or even surpass those of natural enzymes. For instance, Lin et al. [105] designed single-atom Fe-doped carbon dots (SA Fe-CDs), which demonstrated exceptional OXD activity through a simple in situ pyrolysis process (Fig. 6b). The atomically dispersed Fe sites were capable of catalyzing the oxidation of TMB with a rapid response and high affinity, as evidenced by a V_{max} of 10.4 nM/s and a K_m of 168 μM. Similarly, Kang et al. [106] reported the development of a single-atom Cu catalyst, coordinated in the form of CuN_2O_2, decompose H_2O_2 with the V_{max} of 656 nM/s, 6.56 times faster than natural horseradish peroxidase (HRP).

Despite the enhanced enzymatic activity, several challenges hinder the practical application of SAzymes. One significant issue is their poor dispersibility in aqueous solutions and potential toxicity, which could be addressed by incorporating abundant surface functional groups. Additionally, the traditional hydrothermal synthesis of SAzymes presents difficulties; the harsh conditions (e.g., high temperature and pressure) often lead to aggregation of the atoms, preventing their stabilization in a monatomic state. Moreover, the complex chemical reactions and phase transitions that occur during hydrothermal synthesis may impede the precise control of the homogeneous formation and distribution of single-atom sites.

3.1.2.3. Modulating coordination environment. The challenges associated with the application of single-atom nanozymes (SAzymes) can be partially addressed through modulation of their coordination environment, which influences both structural stability and catalytic activity. By optimizing the bond types, the number of coordinating atoms, and the stereochemical structure within CDRMs, precise control over catalytic behavior can be achieved. For instance, Zhang et al. [107] developed a carbon dot-supported Fe SAzyme (ph-CDs-Fe SAzyme) with a high content of pyrrolic nitrogen using a ligand-assisted strategy. The coordination and dilution effects of phenanthroline promoted local coordination with Fe atoms and prevented their aggregation, thereby enhancing peroxidase-like (POD) catalysis by mimicking the coordination structure of ferriporphyrin in natural PODs. Additionally, compared to planar active sites, three-dimensional active sites can offer higher catalytic kinetics. For example, Xu et al. [108] synthesized CD-supported Fe-SAzymes (Fe-CDs) with twisted, nonplanar Fe-O_3N_2 active sites (Fig. 6c), which closely resemble the non-heme iron center in Hydroxypropyl-1-phosphonate (S-HPP) epoxidase. These Fe-CDs exhibited remarkable POD-like activity (750 units/mg), outperforming conventional SAzymes with planar Fe-N_4 active sites.

3.1.2.4. Doping synergistic dual elements. The interactions between different atoms in doped systems can lead to the rearrangement of electronic structures and energy levels, which may synergistically enhance the catalytic performance of CDRM nanozymes. Furthermore, the presence of two atomic species can improve structural stability and reduce activation energy, thereby accelerating the overall reaction rate. For example, Wang et al. [109] synthesized N/P co-doped graphene quantum dots (NPGQDs) as metal-free nanozymes, which enhanced POD activity in two key ways (Fig. 6d). First, the synergistic electron effect between N, which has a higher electronegativity, and P, with a lower electronegativity, generated highly localized states near the Fermi level. Additionally, the N/P co-doping improved substrate adsorption and reduced the energy barrier, creating superior conditions for enzymatic activity compared to single heteroatom doping.

Diatomic doping with metal elements can also accelerate surface electron transfer in CDRM nanozymes, promoting more effective catalysis. For instance, Shen et al. [110] developed bimetallic Mn and Ce co-doped carbon dots (CDs), while Zhang et al. [111] prepared Co, N-doped CDs nanozymes, both of which exhibited superior OXD activity due to the synergistic electronic effects. These advantages make diatomically doped CDRM nanozymes promising candidates for advanced ROS upregulation. However, when incorporating a second dopant into the lattice structure of CDRM nanozymes, it is crucial to carefully screen the choice of dopant. Inappropriate atoms could inadvertently hinder POD/OXD-like activity, negating the desired catalytic enhancement.

3.1.2.5. Constructing cascaded reactors. The reaction rate in enzymatic catalysis is influenced by both enzymatic activity and substrate concentration. A sufficient concentration of reactants increases the probability of collisions between the substrate and active sites, thereby enhancing the enzymatic reaction rate. To elevate the concentration of key reactants like O_2 and H_2O_2, the strategy of designing cascaded reactors has been proposed. This approach aims to boost OXD and POD

catalysis. For example, glucose oxidase (GOX) decomposes glucose into gluconic acid and H_2O_2, and is often combined with POD-like CDRM nanozymes to improve ROS generation efficiency. Wang et al. [112] engineered a glucose-responsive, photothermal nanozyme (GOX/MPDA/Fe@CDs), consisting of GOX, Fe@CDs, and mesoporous polydopamine (MPDA). By utilizing endogenous high blood glucose, GOX/MPDA/Fe@CDs could self-supply H_2O_2, which was then catalyzed to generate a large amount of intracellular ·OH. Similarly, Shen et al. developed a bimetallic-supported CDs nanozyme based on Cu and Fe, which exhibited both alcohol oxidase (AOX) and POD-like activity. In this system, methyl mercaptan (CH_3SH) was catalyzed to H_2O_2, providing sufficient substrate for the subsequent POD process.

OXD-like catalysis can also be enhanced by constructing cascaded reactors. For instance, catalase (CAT), a natural enzyme, catalyzes the conversion of H_2O_2 into O_2 [113,114], providing a key substrate for the OXD process in CDRMs. However, the complex operation and reduced activity of natural enzymes can limit their applicability. Therefore, engineering structures with optimal catalytic environments can support the self-cascaded catalysis of CDRM enzymes, improving overall efficiency.

3.1.3. *Selectivity modulation*

Catalytic selectivity is as crucial as catalytic activity in assessing enzymatic performance. Despite significant advancements in enhancing the enzymatic activity of CDRMs, modulating selectivity remains challenging due to insufficient specificity toward both reaction pathways and substrates.

One major challenge in reaction pathway specificity arises from the multifunctionality of some CDRM nanozymes, which may exhibit competitive catalytic activities using the same substrate to produce different ROS. For example, certain CDRMs possess both POD and CAT activities, utilizing H_2O_2 as a substrate to generate ·OH and O_2, respectively. This competition can be mitigated by adjusting active sites or regulating electron transfer. Ji and Chen et al. [115] demonstrated that Fe-SAzymes with neighboring active sites suppressed the competitive POD reaction while increasing CAT selectivity by up to sixfold compared to those with randomly dispersed active sites. The neighboring active sites acted as a molecular tweezer, trapping and decomposing H_2O_2 into O_2 through hydrogen bond cooperation near the end-bridge. Similarly, Wang et al. [116] reconstructed Cu active sites by integrating nanoceria (CeO_2), which significantly inhibited hydroxyl radical antioxidant capacity (HORAC) while enhancing POD-like activity. Given that enzymatic catalysis depends on electron transfer between nanozymes and reaction substrates, inhibiting or blocking electron transfer with unfavorable substrates is a promising strategy for improving catalytic selectivity. For instance, Li and Xu et al. [117] proposed an "electron lock" strategy to control the catalytic pathways of CDRM nanozymes (Fig. 7a). By tuning the CB potential of FeCDs to match specific catalytic reaction energy barriers, they achieved a switchable electron lock that enabled activatable OXD and selective POD activity, with substrate affinity 123 times higher than that of natural HRP.

The challenge of achieving substrate selectivity in CDRMs lies in their rough surfaces, which lack binding pockets for specific substrate recognition and binding. For example, POD-like nanozymes in the presence of H_2O_2 can oxidize various organic substrates such as TMB, OPD, and ABTS. To emulate the substrate specificity of natural enzymes, strategies such as molecular imprinting, physical adsorption, and surface modification have been developed [118]. These approaches focus on artificially creating binding sites and secondary interactions—such as hydrogen bonding, ionic bonding, hydrophobic interactions, and van der Waals forces—to establish structural complementarity between nanozymes and substrates, thereby achieving selective recognition and binding. Furthermore, the recognition of chiral molecules offers additional potential for enhancing substrate selectivity. Chiral CDRM nanozymes are typically prepared either by surface modification with chiral molecules or by directly using chiral molecules as reaction precursors. For example, Yang et al. [119] designed cysteine-derived chiral CDs (Fig. 7b) and found that D-CDs outperformed L-CDs in catalyzing the topological transition of plasmid DNA from a supercoiled to a nicked open-circular configuration. All-atom molecular dynamics (MD) simulations revealed that the strong affinity between double-stranded DNA and D-CDs was the enantioselective origin of the DNA's topological rearrangement.

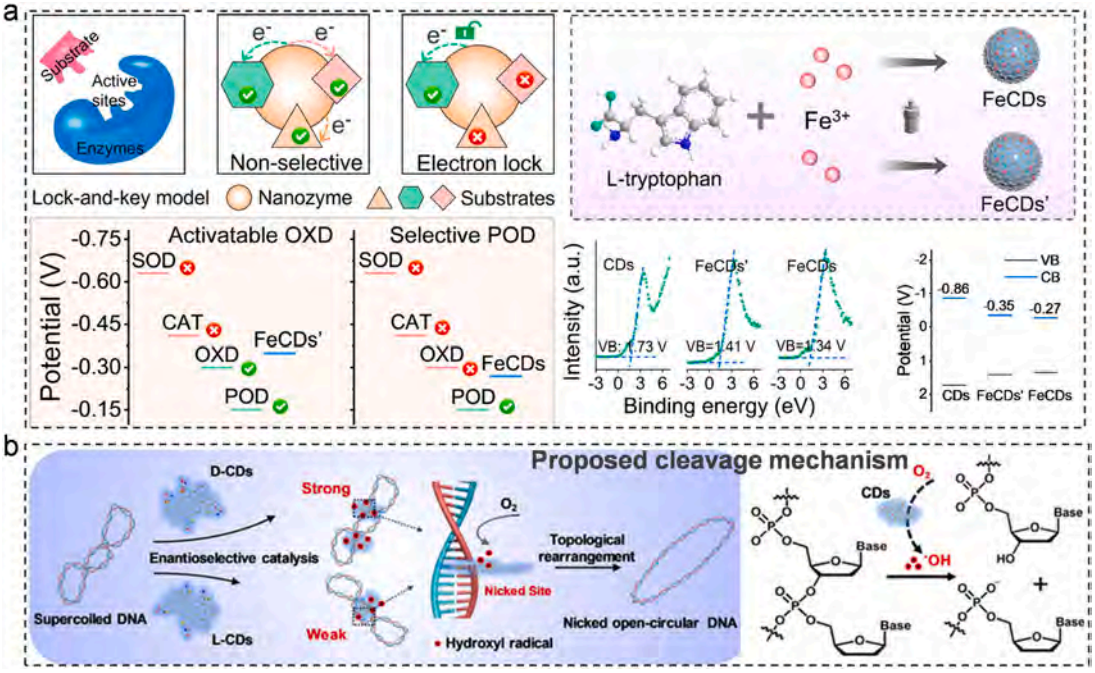

Fig. 7. Selective upregulation of ROS through nanozyme catalysis. (a) The "Electron lock" effect to manipulate catalytic reaction pathway. [117]. Copyright 2024, American Chemical Society. (b) Leveraging the recognition ability of chiral molecules to achieve substrate selectivity. [119]. Copyright 2022, Wiley.
(a) Reproduced with permission from ref. (b) Reproduced with permission from ref.

Overall, research into the selectivity modulation of CDRM nanozyme is still in its early stages. More convenient strategies are needed to address weak pathway and substrate selectivity in CDRM nanozymes. These include mimicking the precise catalytic microenvironment of natural enzymes and employing machine learning to predict and screen for optimal reaction selectivity. Additionally, establishing robust criteria and methods for accurately evaluating and comparing catalytic specificity across various enzymatic reactions and substrates will be critical to advancing the field.

3.2. Light-driven ROS upregulation

3.2.1. Action mechanisms

Light can be provided by lasers, xenon lamps, or light-emitting diodes. However, the penetration of external light sources into deep tissue is limited due to absorption and scattering by biological tissues. Interestingly, this limitation can be overcome by utilizing chemiluminescence. Chemiluminescence is a unique phenomenon initiated by a series of chemical reactions, where the energy released during redox processes excites a substance from its ground state to an excited state, and then returns to emit light. For example, Fan et al. [120] used a luminol-H_2O_2-horseradish peroxidase reaction to generate intracellular chemiluminescence, thereby activating CDs-based $^1O_2$ generation without the need for external light. Substrate molecules typically include H_2O_2, H_2O and O_2. Currently, photo-energized ROS generation is primarily supposed to arise from the photosensitizing and photocatalytic properties of CDRMs, both of which are closely linked to photon absorption and subsequent electron transitions.

Photosensitizing theory considers CDRM as photosensitizers, whose electrons could absorb one or multiple photons, transitioning from the ground singlet state (S_0) to the excited singlet state (S_1) (Fig. 8a). The unstable electrons in the S_1 state may undergo intersystem crossing (ISC) to the excited triplet state (T_1). Those energetic electrons in T_1 enable ROS production via two distinctive reaction processes. In type I process, some electrons in T_1 may be transferred to surrounding molecules, such as H_2O_2, or O_2, to generate··OH or H_2O_2, as shown in Equations.

$$O_2+e^-\rightarrow O_2^{\cdot-} \quad (1)$$

$$O_2+2e^-+2H^+\rightarrow H_2O_2 \quad (2)$$

$$H_2O_2+e^-\rightarrow \cdot OH+OH^- \quad (3)$$

In the type II process, energy transfer typically occurs between electrons in T_1 and O_2 adsorbed on the surface of CDRMs. During energy relaxation in the energetic electrons, the spin state of O_2 transitions from triplet to singlet state. This energy transfer results in the generation of $^1O_2$, as shown in Eq. 4, which has a longer lifetime in air (2.80 s) compared to ·OH. For active electrons on CDRMs, the probability of colliding with oxygen adsorbed on the surface is significantly higher than that of colliding with surrounding molecules, making the type II process the dominant mechanism for ROS production in the photosensitizing theory [121].

$$^3O_2+e^- \text{ (energy transfer)} \rightarrow {}^1O_2 \quad (4)$$

The photocatalytic theory primarily depends on the semiconductive properties of CDRMs (Fig. 8b). A typical photocatalytic process involves three sequential steps. 1) Excitation: Upon light irradiation, electrons in CDRMs are excited and transmitted from the valence band (VB) to the conduction band (CB), leaving behind positively charged holes (h^+) in the VB. These photo-excited electrons and holes, collectively called carries, exhibit reductive and oxidative ability, respectively; 2) Migration: The above carriers migrate in opposite directions within the CDRMs, eventually reaching reactive sites on the surface; 3) Reaction: At the surface of CDRMs, electrons reduce molecules to produce $O_2^{\cdot-}$ (Eq. 1) and H_2O_2 (Eq. 2). Simultaneously, holes oxidize other molecules to form ·OH ($H_2O+h^+\rightarrow\cdot OH$). Among these ROS, ·OH is most reactive due to its superior electron-capturing capability. It is worth noting that the above process requires the photon energy ($h\nu$) of incident light to exceed the bandgap energy (E_g) of the CDRMs. Furthermore, the effectiveness of the reduction and oxidation reactions is determined by the potentials of the CB and VB. A sufficiently negative CB potential enables effective electron transfer for reduction, while a sufficiently positive VB potential supports efficient oxidation by holes.

The photosensitizing theory explains ROS generation by defining CDRMs as photosensitizers, while the photocatalytic theory strictly considers CDRMs as semiconductors. Both theories are valid, as the complex structure of CDRMs characterized by uncontrollable sp^2/sp^3 hybridization, defects, and surface functional groups endows them with both photosensitizing and photocatalytic properties. However, it remains challenging to precisely determine the origin of their activity at the atomic level. Therefore, comprehensive structural studies and detailed mechanistic investigations are essential to achieve a deeper understanding of photo-energized ROS generation by CDRMs.

3.2.2. Activity modulation

Building on the fundamental understanding of the mechanisms behind photo-energized ROS production, several strategies have been proposed to enhance ROS generation in CDRMs. For the photocatalytic theory, these strategies include increasing the number of photo-generated carriers, extending the absorption range of incident wavelengths, and inhibiting carrier recombination.

3.2.2.1. Increasing carrier amounts. According to the formula of carrier generation ($h\nu\geq E_g$), reducing the bandgap (E_g) decreases the energy required to excite CDRMs. A smaller bandgap allows for the generation of more carriers under the same irradiation time and excitation wavelength. The bandgap of CDRMs is influenced by their structure, size, and surface defects. For example, Wang et al. [122] utilized sonication-assisted thermal exfoliation to prepare GOQDs capable of generating $^1O_2$ upon irradiation by white light (Fig. 9a). The production of $^1O_2$ doubled when the GOQDs were chemically reduced by hydrazine hydrate. This enhancement occurred because the chemical treatment reduced the bandgap of GOQDs from 3.2 eV to 2.6 eV, increasing the

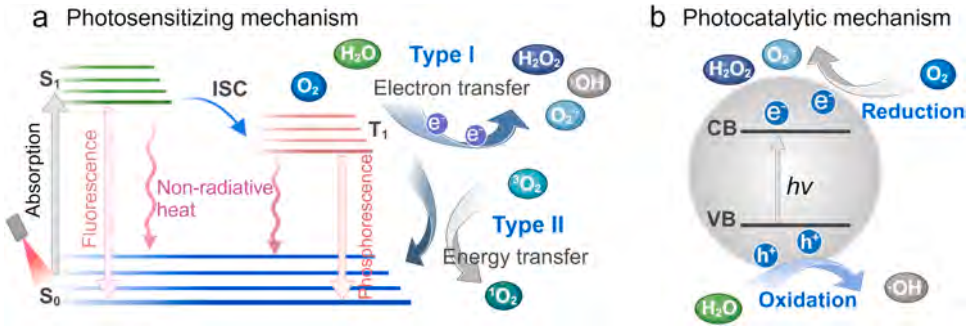

Fig. 8. Action principles of photo-energized ROS upregulation. (a) Photosensitization mechanism. (b) Photocatalytic mechanism.

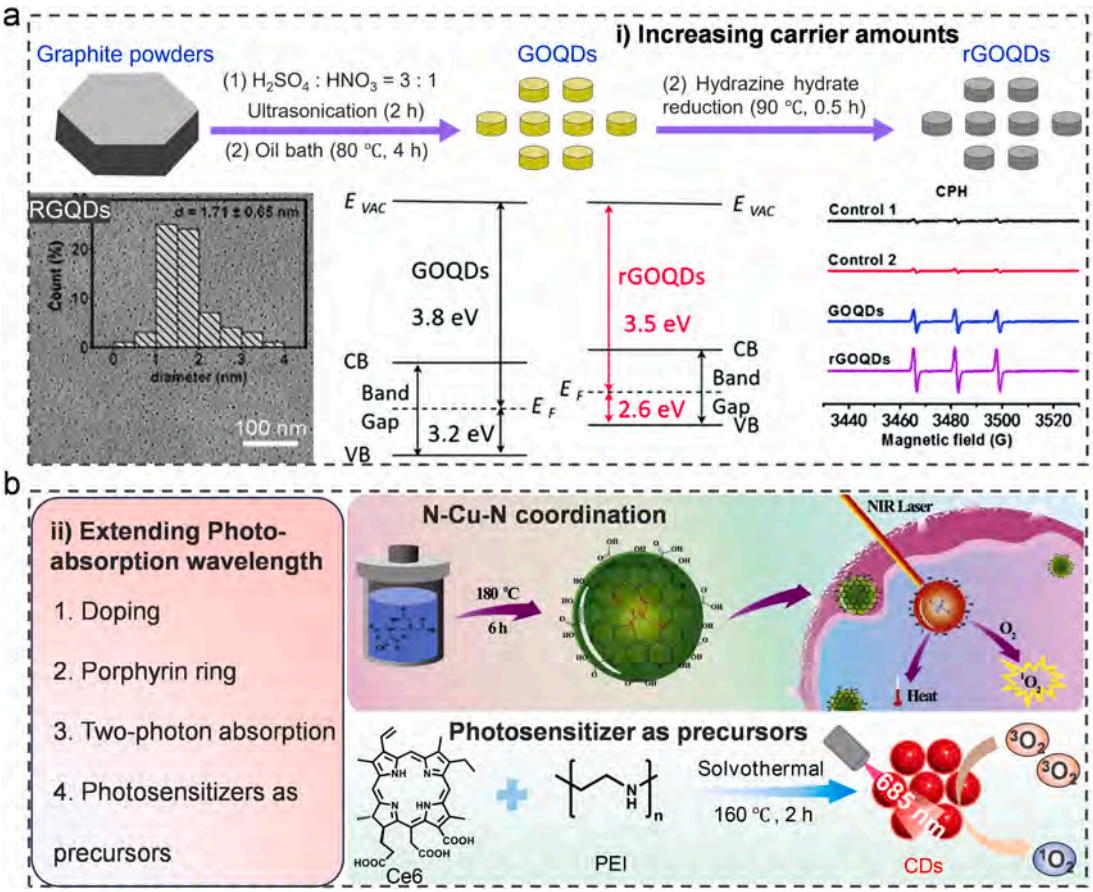

Fig. 9. Activity modulation of photo-energized ROS upregulation. (a) Increasing carrier amounts. [122]. Copyright 2018, Royal Society of Chemistry. (b) Extending photo-absorption wavelength. [125]. Copyright 2018, Elsevier. [128]. Copyright 2023, Elsevier.
(a) Reproduced with permission from ref. (b) Reproduced with permission from ref. (c) Reproduced with permission from ref.

generation of electron-hole (e^--h^+) pairs. Similarly, Leblanc et al. [123] reported that CDs with smaller sizes exhibited a reduced bandgap, potentially due to elevated impurity levels associated with a higher O content.

3.2.2.2. Red-shift of the excitation wavelength. Typically, the excitation wavelength of CDRMs is located in ultraviolet or visible light region. Enlarging the absorption wavelength allows electrons to be excited by photons with lower energy, thereby enhancing the utilization efficiency of incident light. The excitation wavelength is closely tied to the structure and composition of CDRMs. Numerous red to near-infrared (NIR)-responsive CDRMs have been developed through strategies such as heteroatom doping, porphyrin ring incorporation, two-photon absorption cross-section expansion, and precursor photosensitization. For instance, Wu et al. [124] demonstrated that P doping resulted in a red-shift in the maximum excitation wavelength of CQDs compared to S-CQDs. Similarly, metallic doping with Cu^{2+} increased the potential for NIR absorption in CDRMs [125] (Fig. 9b). An optimal Cu^{2+} content enabled effective O_2 photosensitization to generate $^1O_2$ upon 808 nm laser irradiation. Wang and Yu et al. [126] synthesized CDRMs, in which the porphyrin ring structure is cross-linked with p-phenylenediamine by amide condensation to form a larger π-electron domain. The conjugated domain effectively extended the photo-responsive wavelength range of CDRMs, enabling $^1O_2$ generation under 638 nm laser excitation. Zhang et al. [127] hydrothermally synthesized CDRMs using 1,3,6-trinitropyrene and Na_2SO_3, which could generate $^1O_2$ upon 800 nm irradiation via a two-photon excitation expansion mechanism. Besides, small molecular photosensitizers such as chlorin e6 (Ce6), Cyanine 7 (Cy7), and methylene blue have been employed to synthesize CDRMs with red or NIR absorption property. For example, Zheng et al. [128] utilized Ce6 and polyethylene imine (PEI) as precursors to synthesize CDs (Fig. 9b), which were activated by a 685 nm laser to generate $^1O_2$. The characteristic absorption peak at 662 nm was attributed to the n-π* transition of C═O and C═N bonds.

3.2.2.3. Inhibiting carrier recombination. The generation of electron-hole pairs (e^--h^+) is a crucial step in initiating ROS production. However, these photo-generated carriers are highly reactive and often recombine quickly, returning to their original states. To address this, several strategies have been developed to reduce carrier recombination, including extending the lifetime of active electrons and consuming the generated holes.

Heteroatom doping is commonly used to generate surface defects that can effectively trap photo-generated electrons, thereby inhibiting their recombination with holes. Chen et al. [129] reported that Cu-N coordination increased the decay time of NCDs from 2.2 to 3.6 ns (Fig. 10a), which in turn enhanced ROS production. Surface modification with molecules can also create space for electrons, preventing recombination. For instance, Duan et al. [130] modified the surface chemistry of carbon quantum dots (CQDs) by selectively substituting surface carbonyl groups (C═O) with phenylhydrazine (PH). This modification significantly decreased photoluminescence (PL) intensity, demonstrating PH could effectively inhibit the recombination of photo-induced carriers (Fig. 10b). Constructing heterojunctions with metal nanoclusters and semiconductors is another effective strategy to create a more negative conduction band (CB) potential, which can accept more electrons. Yuan et al. [131] found that conjugated AuAg nanoclusters (AuAg NCs) in CDs promoted charge carrier separation by

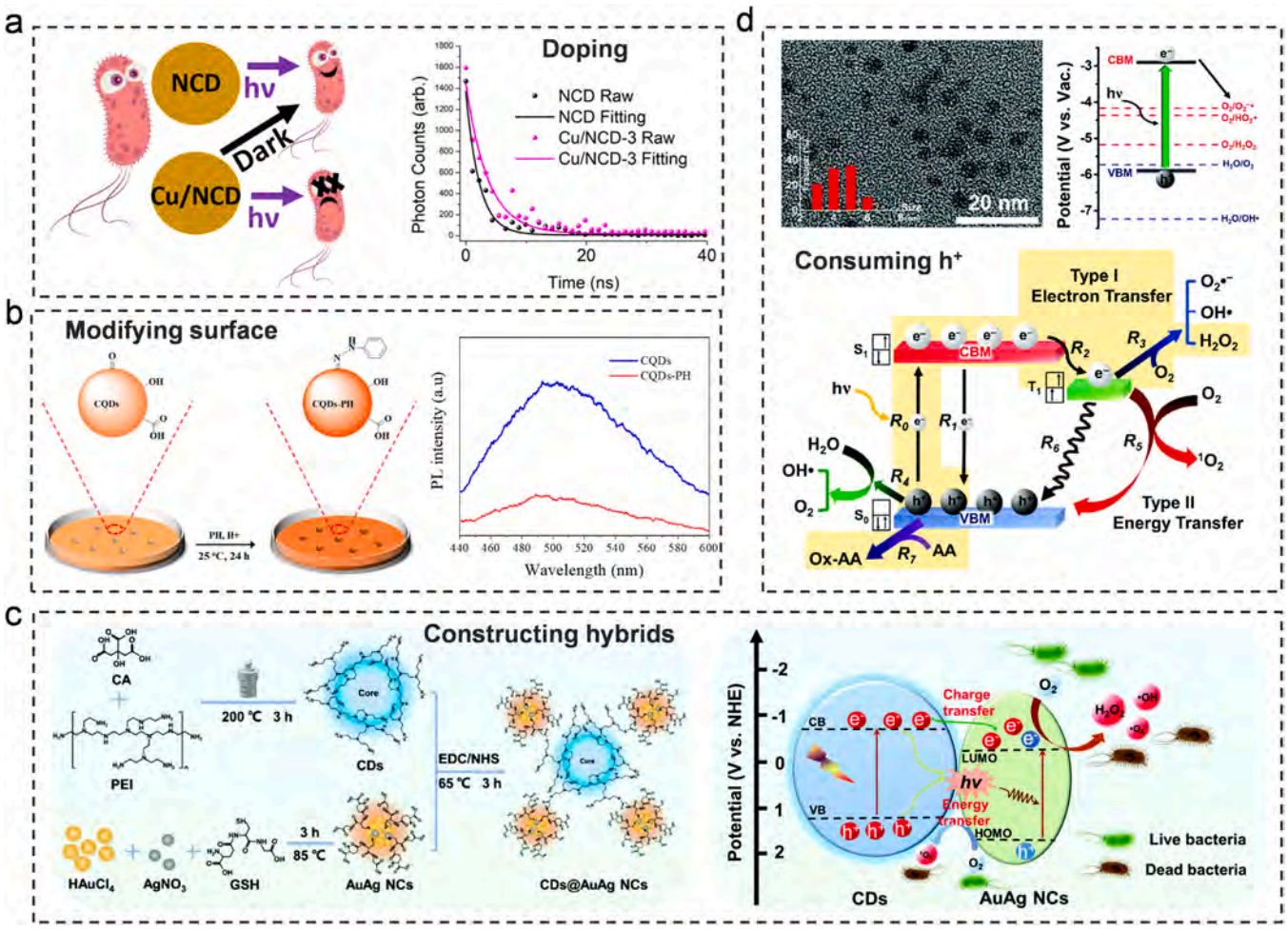

Fig. 10. Strategies to inhibit carrier recombination for modulating activity of photo-energized ROS upregulation. (a) Doping. [129]. Copyright 2020, American Chemical Society. (b) Surface modification. [130]. Copyright 2023, Elsevier. (c) Construction of hybrids. [131]. Copyright 2022, Royal Society of Chemistry. (d) Consumption of photo-generated h^+. [132]. Copyright 2021, Royal Society of Chemistry.
(a) Reproduced with permission from ref. (b) Reproduced with permission from ref. (c) Reproduced with permission from ref. (d) Reproduced with permission from ref.

increasing the negative CB potential (Fig. 10c).

Additionally, the use of reductive molecules can react with oxidative holes, indirectly extending the lifetime of electrons. Teng et al. [132] utilized ascorbic acid (AA) to scavenge photo-generated holes in nitrogen-doped graphene oxide dots (NGODs) (Fig. 10d). The results showed that NGODs effectively produced H_2O_2 under white-light irradiation, with the production rate directly proportional to the concentration of AA.

The above strategies summarize the modulation of ROS production from the perspective of photocatalytic theory. In contrast, approaches based on photosensitizing theory primarily focus on improving the efficiency of intersystem crossing (ISC) from the singlet state (S_1) to the triplet state (T_1), incorporating photosensitizers, minimizing non-radiative decay, and enhancing substrate adsorption.

3.2.2.4. Boosting ISC efficiency. Efforts to enhance intersystem crossing (ISC) efficiency focus on reducing the ISC energy gap (ΔE_{st}), which facilitates electron transfer from the singlet state (S_1) to the triplet state (T_1). A smaller ΔE_{st} makes the transition from S_1 to T_1 more favorable, increasing the population of the triplet state and thereby enhancing energy transfer to adjacent O_2 for efficient $^1O_2$ generation. Wang et al. [133] synthesized three types of Hypericum perforatum extract-derived red-emissive CDs (h-RCDs) with tunable ROS generation properties (Fig. 11a). By modifying the reaction solvents to reduce ΔE_{st}, the $^1O_2$ quantum yield of h-RCDs was significantly improved from 0.02 to 0.42. Similarly, Wu et al. [134] demonstrated that graphitic N in N-CDs possessed the smallest ΔE_{st}, which is highly conducive to triplet state activation.

3.2.2.5. Loading photosensitizes. The composite of CDRMs and photosensitizers is typically fabricated through electrostatic interactions and amide coupling reactions, as discussed in detail in *Section 2.3.2*. Utilizing CDRMs as carriers addresses the solubility and stability challenges of photosensitizers. Additionally, the electron or energy transfer processes between CDRMs and the photosensitizers significantly enhance ROS generation. For instance, hemin, a photosensitizer capable of absorbing UV–visible light in the range of 220–500 nm, was utilized by Sheng et al. [135] to construct CDs/hemin nanoplatforms (HCDs). Notably, they observed a fluorescence resonance energy transfer (FRET) effect between the two components, which improved the overall photoactivity and foster the generation of $^1O_2$ under 650 nm laser irradiation (Fig. 11b).

3.2.2.6. Diminishing non-radiative decay. Non-radiative decay consumes energetic electrons by generating localized heating, thereby reducing the efficiency of ROS generation. By minimizing energy dissipation into heat, a greater proportion of energetic electrons can participate in reactions with substrates, leading to enhanced ROS production. Bi et al.

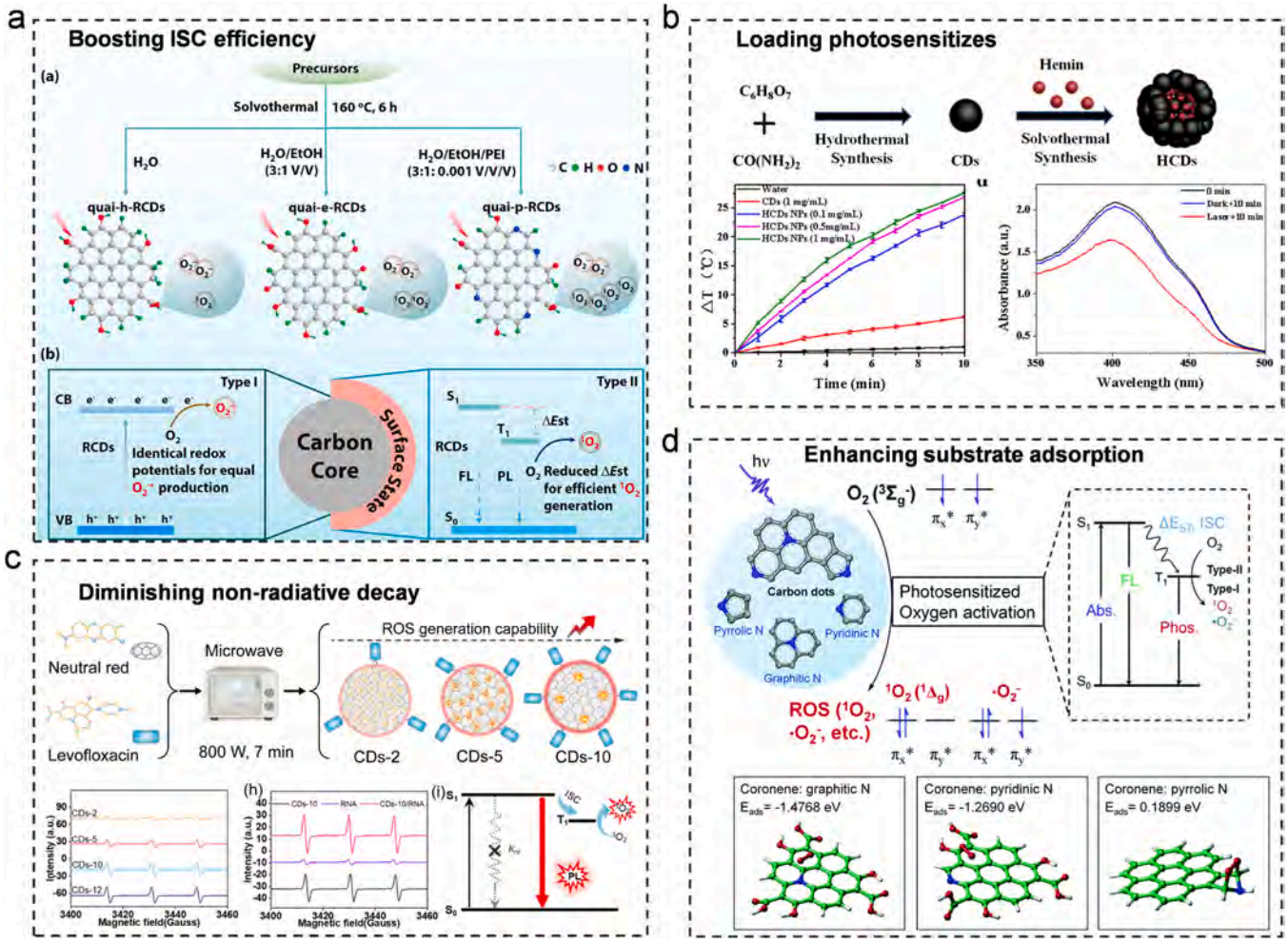

Fig. 11. Activity modulation of photo-energized ROS upregulation. (a) Enhancement of ISC efficiency. [133]. Copyright 2022, Elsevier. (b) Loading of photosensitizers. [135]. Copyright 2019, Elsevier. (c) Reduction of non-radiative decay. [136]. Copyright 2023, American Chemical Society. (d) Enhancement of substrate adsorption. [134]. Copyright 2020, Royal Society of Chemistry.
(a) Reproduced with permission from ref. (b) Reproduced with permission from ref. (c) Reproduced with permission from ref. (d) Reproduced with permission from ref.

[136] synthesized CDs with tunable ROS generation efficiencies using levofloxacin and neutral red as precursors (Fig. 11c). By adjusting the molar ratio of levofloxacin to neutral red from 2:1 (CDs-2) to 10:1 (CDs-10), the $^1O_2$ generation rate increased by 3.5 times. The radiative decay (k_r) of CDs-10 was measured as 1.8 times higher than that of CDs-2, while the non-radiation (k_{nr}) decay decreased approximately 40 %, suggesting that the enhanced ROS generation is likely due to the suppression of non-radiative decay pathways via a rigidifying effect.

3.2.2.7. Enhancing adsorption of reaction substrates. The adsorption of reaction substrates is crucial for efficient ROS generation, as desorbed substrates prevent photo-generated carriers on the surface of CDRMs from reacting effectively. The abundant functional groups on CDRMs play a pivotal role in substrate adsorption. Wu et al. [134] demonstrated that pyrrolic N serves as the primary site for O_2 adsorption, effectively reducing the distance between O_2 and CDs, thereby facilitating photosensitization (Fig. 11d). Additionally, heteroatom doping has proven effective in decreasing the adsorption energy of reaction substrates, thus enhancing photo-induced ROS generation. The incorporation of heteroatoms modifies the electronic structure of CDRMs and creates defect sites, which can weaken the interaction between substrates and CDRMs. Furthermore, heteroatoms alter the bonding characteristics of CDRMs, disrupting surface bonding. This perturbation might lead to the formation of more polarized or covalent bonds, ultimately changing the adsorption energy of the substrates and improving their reactivity.

Although numerous valuable strategies have been proposed to enhance the photo-energized ROS generation of CDRMs, many challenges remain. For example, it is yet to be determined whether the selective deactivation of a functional group could precisely elucidate its specific contribution to the photoactivity of CDRMs. Additionally, optimizing the electron transfer rate between photo-generated carriers and reaction substrates continues to be a significant challenge. Furthermore, while a diverse array of doping types exists, identifying those most effective for enhancing ROS generation remains unclear and demands more systematic exploration.

3.2.3. Selectivity modulation

CDRMs can generate four common types of ROS—$O_2^{\cdot-}$, ·OH, $^1O_2$, and H_2O_2—with the assistance of light. However, achieving controllable production of specific ROS remains challenging. Fundamental theories suggest that precise control of ROS generation can be realized by adjusting factors such as the CB/VB, *ΔEst* and precursors.

According to the photocatalytic mechanism, the CB/VB potentials of CDRMs must be sufficiently negative/positive to surpass the transformation potential of substrates. This ensures that photo-generated electrons (e^-) and holes (h^+) can reduce or oxidize adsorbed substrates, respectively. Adjusting the CB/VB potentials to optimal levels

can facilitate the selective generation of specific ROS. For example, Song et al. [137] synthesized N-doped carbon dots (NCDs) via one-step hydrothermal treatment of tartaric acid and 3-aminophenol. The CB potential of these NCDs was more negative than the reduction potential of O_2 to $O_2^{\cdot-}$ (-0.33 eV vs. NHE), enabling efficient conversion of O_2 to $O_2^{\cdot-}$ under 488 nm excitation. This demonstrates that tuning CB/VB potential is a feasible strategy to regulate the production of specific ROS.

In addition, reducing the *ΔEst* has been shown to promote the generation of $^1O_2$ selectively. For instance, Wang and Ge et al. [133] synthesized three types of carbon dots (CDs)—h-RCDs, e-RCDs, and p-RCDs—with *ΔEst* values of 0.12, 0.07, and 0.04 eV, respectively. As *ΔEst* decreased, the selective production of $^1O_2$ increased, while the efficiency of $O_2^{\cdot-}$ generation remained unchanged due to identical CB potentials determined by the core structure. Combining this approach with CB/VB modulation to suppress $O_2^{\cdot-}$, ·OH, and H_2O_2 formation presents a promising strategy for selectively producing $^1O_2$.

Precursors also play a significant role in determining the types of ROS generated by CDRMs. For instance, CDRMs derived from the dehydration and carbonization of photosensitizers tend to favor $^1O_2$ generation [138–140]. This behavior may be attributed to the partial retention of the photosensitizing and structural properties of the photosensitizers. Additionally, Shen and Zhou et al. [141] that the N-Cu-N coordination structure in Cu-CDs was more favorable for $^1O_2$ generation, which might be caused by the decreased energy for ISC.

3.3. Ultrasound-energized ROS upregulation

3.3.1. Action mechanisms

In addition to their photo-activated properties, CDRMs can also be excited by ultrasound to generate ROS, a process promising for biomedical engineering due to ultrasound's deep tissue penetration and minimal side effects. However, understanding the mechanisms of ultrasound-energized ROS production remains in its early stages because of the complexity involved. Sonoluminescence and sonochemistry are the two primary mechanisms responsible for ROS generation, both initiated by the cavitation effect (Fig. 12a).

Cavitation arises from interactions between CDRMs and ultrasound, leading to pressure fluctuations in the liquid and the formation of microbubbles (MB). These MB undergo nucleation, growth, and collapse, processes classified into stable or inertial cavitation [142]. Stable cavitation, induced by low-intensity ultrasound, involves small-scale oscillations without rupture, while inertial cavitation, triggered by high-intensity ultrasound, entails violent expansion, compression, and explosive collapse of bubbles. The collapse of MB near the surface of CDRMs can lead to sonoluminescence, where the emitted energy matches the excitation energy of CDRMs, generating e^--h^+ pairs. These pairs then react with adsorbed substrates (e.g., O_2, H_2O, and H_2O_2) to produce ROS, as outlined in *Section 3.2.1*. This mechanism parallels photosensitization, differing only in the energy source.

In sonochemistry, microbubble collapse converts ultrasound energy into localized heat (up to 10,000 K) and pressure (81 MPa), triggering

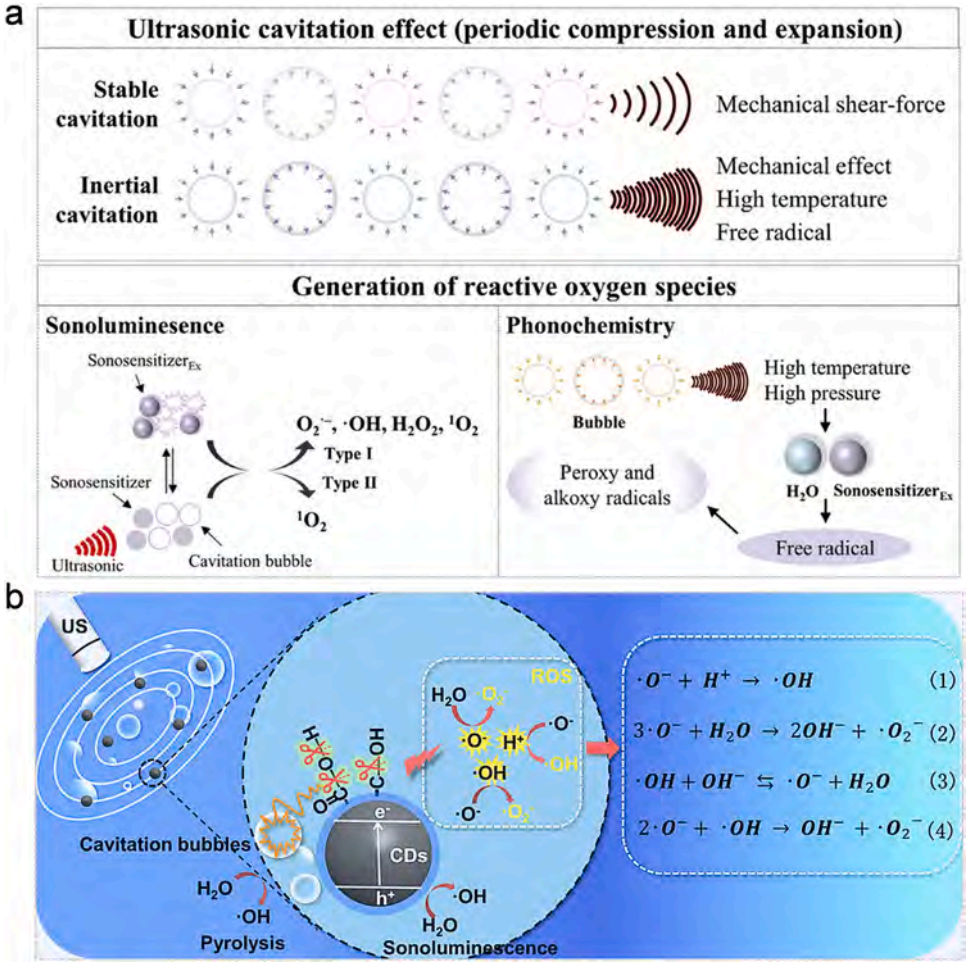

Fig. 12. Action mechanisms of ultrasound-energized ROS upregulation. (a) Cavitation-induced sonoluminescence and phonochemistry. [142]. Copyright 2024, Wiley. (b) Cavitation-evoked breakage of surface functional groups. [143]. Copyright 2021, Elsevier.
(a) Reproduced with permission from ref. (b) Reproduced with permission from ref.

water pyrolysis and generating ·OH radicals. CDRMs contribute to cavitation bubble formation and transfer energy from bubble collapse to their surfaces, leading to bond breakage in surface functional groups. This creates transient active species capable of reacting with the environment to form ROS. For example, Hu et al. [143] demonstrated that oxygen-containing groups (-COOH and -C-OH) on CD surfaces could transform into ROS upon ultrasound exposure (Fig. 12b). During cavitation collapse, oxygen free radicals ($\cdot O^-$) are generated, subsequently reacting with H^+ and H_2O to form $O_2^{\cdot-}$ and ·OH (e.g., $3\cdot O^- + H_2O \rightarrow 2OH^- + O_2^{\cdot-}$; $\cdot O^- + H^+ \rightarrow \cdot OH$). This transformation is reversible and pH-dependent, offering potential for controlled ROS generation in specific microenvironments.

Overall, both sonoluminescence and sonochemistry convert ultrasonic energy into forms that activate e^--h^+ pairs, pyrolyze water, or break surface bonds, all of which contribute to ROS generation.

3.3.2. *Activity modulation*

Although ultrasound-energized ROS production is a promising function of CDRMs, its low yield efficiency remains a significant limitation. Current strategies to enhance this process can be broadly classified into two categories: internal strategies, involving the modification of CDRMs, and external strategies, which incorporate sensitizers.

The internal strategy focuses on manipulating thermodynamic and dynamic factors to enhance ROS production. A narrow bandgap is a favorable thermodynamic factor, as it reduces the ultrasound energy required to generate e^--h^+ pairs. Additionally, extending the excited-state lifetime is a beneficial dynamic factor, as long-lived carriers can activate more adsorbed substrates for ROS generation. Constructing p-n junctions on CDRMs has proven to be an effective approach to narrowing the bandgap and prolonging carrier lifetimes [144]. A p-n junction is formed by combining p-type and n-type semiconductors, where the p-type semiconductor is rich in holes, and the n-type semiconductor contains more free electrons. By compositing semiconductors with different bandgaps into heterojunctions, energy-level alignment can be achieved, which affects the bandgap of the overall structure. Furthermore, the p-n junction increases carrier lifetime by providing a built-in electric field that facilitates the separation of ultrasound-excited e^--h^+ pairs and reduces recombination rates. For example, Shen et al. [62] developed a one-step microwave synthesis method to prepare CDs with different conductivity types (p, n, and p-n junction) by engineering them with sulfonic acceptors and/or nitrogen donors (Fig. 13a). The p-n junction group demonstrated enhanced $^1O_2$ production under ultrasound irradiation, attributed to its narrowed bandgap (1.62 eV) and long-lived triplet state (11.4 μs), which inhibited e^--h^+ pair recombination. Moreover, doping with impurity elements of varying valence states can convert p- or n-type semiconductors into p-n type semiconductors. For instance, Li et al. [145] synthesized Cu-doped CDs (Cu-CDs) using copper (II) acetylacetonate as the Cu source. Electrochemical measurements revealed that Cu doping transformed n-type CDs into p-n type semiconductors, reducing the bandgap from 2.93 to 1.58 eV. This modification prolonged the e^--h^+ pair lifespan (10.7 μs) and significantly boosted separation efficiency.

External strategies primarily focus on enhancing the cavitation effect to improve ultrasound-energized ROS generation. Lipid-shell gaseous microbubbles (MBs) are particularly effective at absorbing ultrasound energy. Incorporating sonosensitizers near MBs can significantly boost their ROS generation efficiency under ultrasound excitation. For example, Yeh et al. [146] developed carbon-dot-based microbubbles (C-dots MBs) by integrating CDs directly into the MB shell, forming novel sonosensitizer-like CDRMs (Fig. 13b). This design allowed the CDs to efficiently absorb the energy from inertial cavitation, leading to the production of higher amounts of $^1O_2$, ·OH, and H_2O_2 upon ultrasound

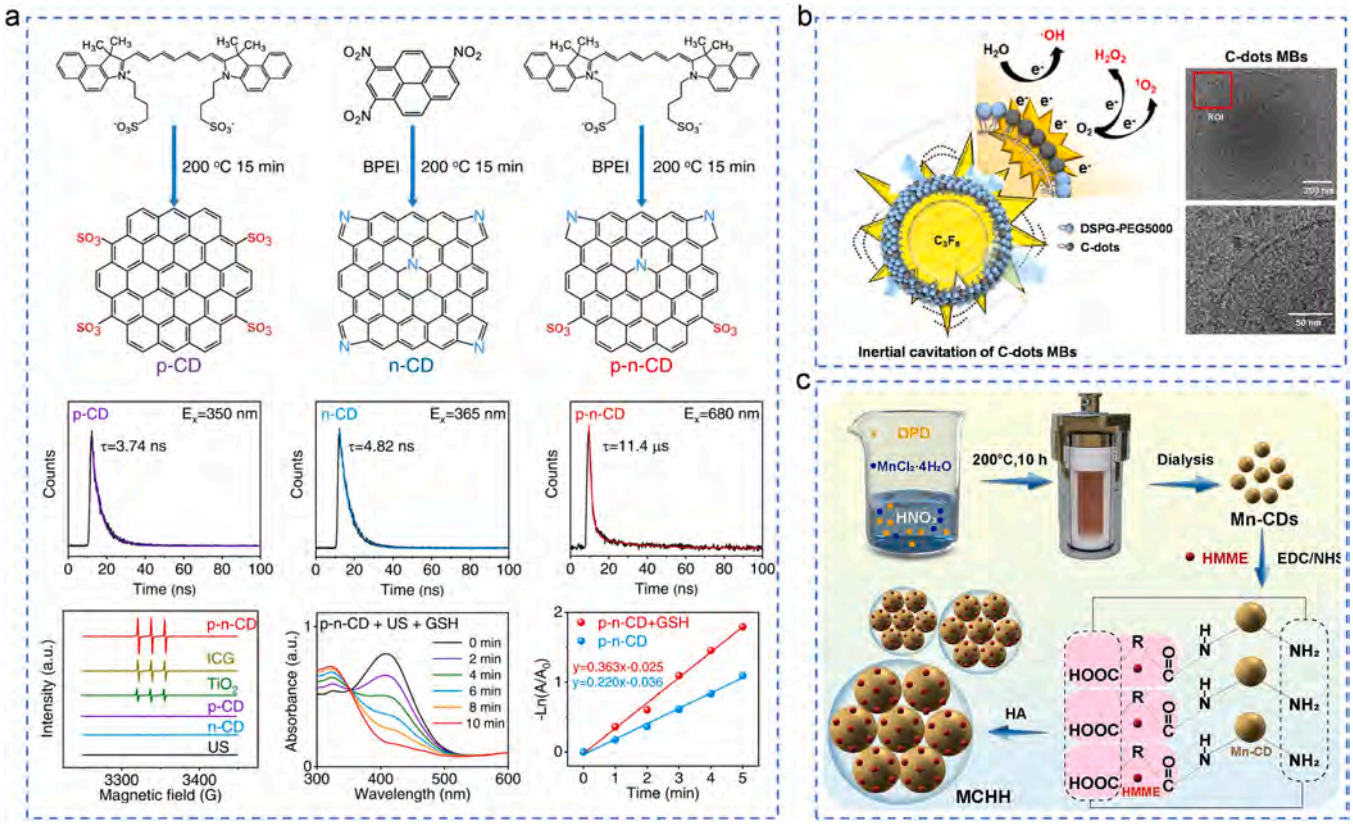

Fig. 13. Activity modulation of ultrasound-energized ROS upregulation. (a) Construction of p-n junction. [62]. Copyright 2022, Springer Nature. (b) Enhancement of cavitation effect. [146]. Copyright 2023, Elsevier. (c) Loading of sonosensitizers. [148]. Copyright 2024, Elsevier.
(a) Reproduced with permission from ref. (b) Reproduced with permission from ref. (c) Reproduced with permission from ref.

irradiation. Similarly, Liu et al. [147] loaded CDs into core-shell poly (methacrylic acid) nanoparticles with hollow structures (CDs@CS-PMAA), creating potent sonosensitizers. The hollow structure enhanced the cavitation effect, resulting in substantially increased $^1O_2$ production under ultrasound. In addition to constructing hollow structures, directly loading sonosensitizers onto CDs via chemical reactions is another effective approach to amplify the cavitation effect. A common method involves amide coupling reactions, which form stable bonds between carboxylic acids and amines. This strategy not only stabilizes the sonosensitizers but also extends their lifespan. For instance, Xue et al. [148] synthesized CD-based nanoclusters by covalently assembling Mn-doped CDs and simultaneously encapsulating the sonosensitizer hematoporphyrin monomethyl ether (HMME) (Fig. 13c). This assembly effectively prevented the aggregation of hydrophobic HMME molecules, enhancing their stability and functionality.

There is an urgent need to deepen our understanding of the mechanisms underlying ROS production by CDRMs under ultrasound excitation and to develop innovative strategies to overcome the limitations in ROS generation. Incorporating metal nanoparticles or nanoclusters (e.g., Pd, Pt, and Au) into CDRMs holds significant promise for enhancing ROS production by extending carrier lifetimes and modulating bandgaps. However, these approaches remain largely unexplored and require further research to achieve controllable ROS production.

4. Downregulation of ROS by CDRMs

Although significant research has focused on the upregulation of ROS by CDRMs, certain CDRMs with specific structure and components also demonstrate the ability to downregulate intracellular ROS. This capability is particularly promising for combating oxidative stress and its associated damage. By mimicking the active sites of natural antioxidant enzymes or directly reacting with ROS as reductant, CDRMs can scavenge various free radicals effectively. In this section, we will systematically examine the mechanisms underlying the antioxidant properties of CDRMs. Furthermore, we will summarize strategies to modulate their antioxidant activity and selectivity, aiming to develop CDRMs with potent and precise ROS downregulation capabilities.

4.1. Active sites and antioxidant mechanisms

4.1.1. ROS downregulation by mimicking natural enzyme

Catalase (CAT) and superoxide dismutase (SOD) are the primary antioxidant enzymes in cells, working synergistically to eliminate harmful ROS and protect normal cells from oxidative damage. SOD, a metalloenzyme, catalyzes the dismutation of superoxide ($O_2^{\cdot-}$) into O_2 and H_2O_2 through the reaction:

$$2\ O_2^{\cdot-} + 2H^+ \rightarrow H_2O_2 + O_2 \quad (5)$$

Subsequently, H_2O_2 could then be decomposed into H_2O and O_2 via the reaction:

$$2H_2O_2 \rightarrow 2H_2O + O_2 \quad (6)$$

The above reaction is specially catalyzed by CAT, which is an iron-containing enzyme. The following paragraphs will summarize current research on CDRMs that mimic the catalytic properties of CAT and SOD.

CDRM nanozymes exhibiting SOD-like activity rely heavily on their surface functional groups, such as hydroxyl and carboxyl groups, which bind and capture $O_2^{\cdot-}$ through electrostatic interactions or hydrogen bonding. Additionally, the conjugated π systems in CDRMs enable efficient electron transfer, oxidizing $O_2^{\cdot-}$ to molecular O_2. The reduced CDRM is then regenerated by reducing another $O_2^{\cdot-}$ to H_2O_2, thereby completing the catalytic cycle. For example, Yan et al. [61] synthesized CDRM nanozymes with a remarkable SOD-like activity of over 10,000 U/mg by oxidizing activated charcoal (Fig. 14a). The critical role of surface functional groups was demonstrated through chemical modifications. Deactivating carboxyl and hydroxyl groups with 1,3-propanesultone (PS) reduced the SOD-like activity to 1600 U/mg, which recovered to 4000 U/mg upon reactivating carboxyl groups. Similarly, deactivating the π-system by hydrothermal treatment in NaOH solutions, which decreased the carbonyl content, also weakened the SOD-like activity. These findings highlight that surface hydroxyl and carboxyl groups are essential for binding $O_2^{\cdot-}$ and facilitating electron transfer to the conjugated π-system, which generates O_2. Moreover, other functional groups such as -NH_2 and -SH) also contribute to binding $O_2^{\cdot-}$, promoting electron transfer, and accelerating the disproportionation of $O_2^{\cdot-}$ into O_2 and H_2O_2 [149]. However, these functional groups alone are insufficient for SOD-like activity. Effective catalysis depends on a match between the redox potential and structural compatibility of

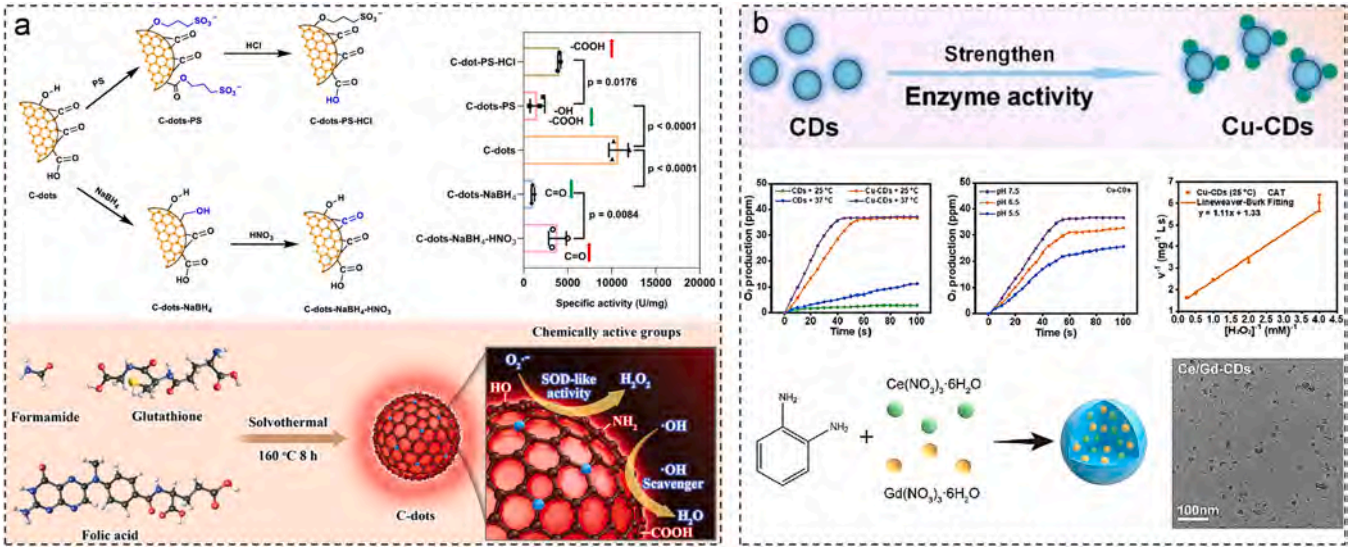

Fig. 14. Nanozyme-catalyzed ROS downregulation. (a) Surface fictionization to mimic active sites of SOD. [61]. Copyright 2023, Springer Nature. [149]. Copyright 2023, Wiley. (b) Metal elements doping to acquire active sites of CAT. [153]. Copyright 2022, American Chemical Society. [154]. Copyright 2023, Elsevier.
(a) Reproduced with permission from ref. (b) Reproduced with permission from ref. (c) Reproduced with permission from ref. (d) Reproduced with permission from ref.

CDRMs with the substrate. In addition to introducing antioxidant functional groups, another promising strategy for constructing SOD-like CDRM nanozymes involves incorporating redox pairs (e.g., Ce^{3+}/Ce^{4+} and Fe^{2+}/Fe^{3+}). These redox pairs enhance electron transfer, facilitating efficient disproportionation of $O_2^{\cdot-}$.

Inspired by the active sites of natural CAT, which are formed by Fe coordination to amino acid residues, CAT-like CDRMs are typically constructed by doping metal elements (e.g., Fe, Cu, and Ce) into CDs [150–152]. The catalytic process involves the interaction of active sites with H_2O_2 molecules and subsequent electron transfer, triggering the disproportionation reaction. The efficient valence cycling of doped metal ions is crucial for achieving excellent radical scavenging efficiency. For instance, Yang et al. [153] synthesized Cu-doped CD nanozymes (Cu-CDs) using $CuCl_2{\cdot}2\,H_2O$ as the doping source (Fig. 14b). These Cu-CDs rapidly catalyzed H_2O_2 to generate O_2 across various pH levels, including 5.5, 6.5, and 7.5. In contrast, pure CDs without doping exhibited minimal catalytic activity, underscoring the importance of Cu doping in forming active sites. Additionally, Huang and Xin et al. [154] developed Ce and Gd bimetallic ion-doped CD nanozymes (Ce/Gd-CDs) with remarkable CAT-like activity, efficiently catalyzing the disproportionation of H_2O_2 to generate visible bubbles of O_2. While acidic conditions generally hinder the CAT-mimicking activity of CDRM nanozymes, this limitation can be addressed by the synergistic effect of elemental doping and localized surface plasmon resonance, enabling efficient O_2 generation even under acidic conditions [155].

4.1.2. *CDRMs directly reacting with ROS as reductant*

Many small molecules and natural biomass materials are rich in active antioxidant groups, enabling them to efficiently scavenge various types of ROS. However, their practical applications are significantly limited by poor solubility, physiological instability, and low bioavailability. Excitingly, carbonizing these antioxidant materials into CDs can preserve the antioxidant groups while incorporating the advantages of CDs, such as excellent water solubility, high biocompatibility, and low toxicity. Notably, the antioxidant activity can be significantly enhanced when antioxidant molecules are meticulously formulated into CDs [156]. In principle, with the selection of an appropriate solvent, any material containing antioxidant sites can serve as a precursor for synthesizing antioxidant carbon CDRMs. Typically, the precursors undergo dehydration and carbonization via amidation reactions in organic solvents like formamide, ethylenediamine, and dimethyl sulfoxide.

The precursor candidates for antioxidant CDRMs range from small molecules to chemical compounds and even biomass substances. Small molecules such as citric acid, ascorbic acid, glutathione, and other antioxidants are excellent precursors. For instance, Zhu et al. [157] dissolved citric acid and urea in N,N-dimethylformamide (DMF) to prepare antioxidant CDRMs with remarkable ·OH scavenging ability in a concentration-dependent manner. Similarly, combining citric acid and glutathione can yield CDs that rapidly scavenge ·OH, $O_2^{\cdot-}$, and H_2O_2 [158]. Natural chemical compounds also serve as ideal candidates for antioxidant CDRM synthesis. For example, melatonin (N-acetyl-5-methoxy-tryptamine, MT), a secondary metabolite in plants and animals, was hydrothermally treated by Yu and Yang et al. to form CDRMs capable of effectively scavenging ·OH (Fig. 15a) [159]. These MT-derived CDs demonstrated lower toxicity, improved water solubility, and better biocompatibility, expanding their potential applications compared to MT itself. Furthermore, biomass substances such as traditional Chinese medicine (TCM) and food have been directly utilized as precursors. For example, *Scutellaria baicalensis* (*S. baicalensis*), a low-cost TCM with broad pharmacological effects and clinical applications, was used by Yang et al. [160] to produce CDs with exceptional scavenging abilities for ·OH and $O_2^{\cdot-}$, outperforming Vitamin C. In another study, Jiang et al. [161] synthesized antioxidant CDRMs (SB-HHD-CDs) using Scutellaria barbata (SB) and Herba Hedyotis diffusae (HHD), which effectively scavenged multiple radicals, including ·OH and $O_2^{\cdot-}$ (Fig. 15b).

Despite the diverse sources of precursors, the structural principles underlying antioxidant precursors for ROS-downregulating CDRMs remain unclear. This challenge could be addressed through advancements in molecular- and nanoscale-level observation technologies.

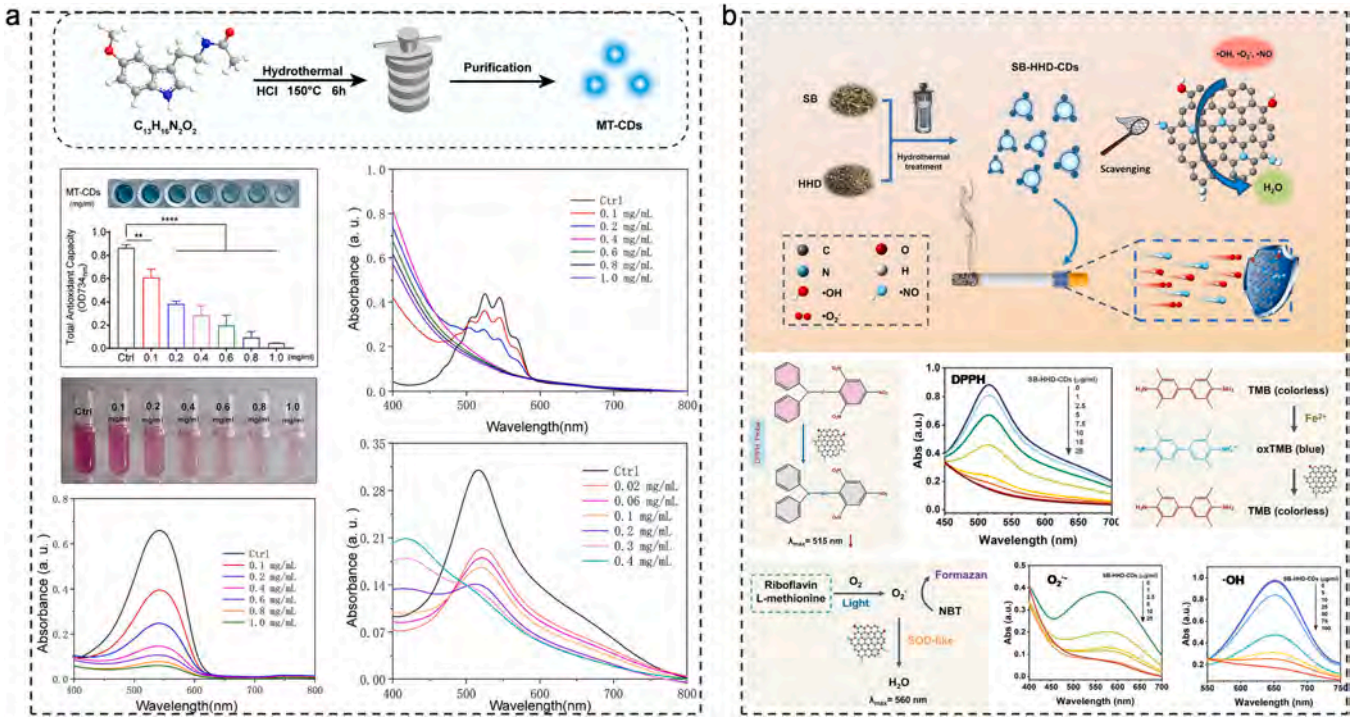

Fig. 15. Antioxidant precursor-inherited ROS downregulation. (a) Antioxidant CDRMs derived from natural small molecules. [159]. Copyright 2024, American Chemical Society. (b) Antioxidant CDRMs obtained from traditional Chinese medicine. [161]. Copyright 2023, Elsevier.
(a) Reproduced with permission from ref. (b) Reproduced with permission from ref.

Additionally, as the active sites in antioxidant precursor-derived CDRMs closely resemble the catalytic sites of SOD-mimicking CDRMs, establishing clearer criteria to differentiate between antioxidant CDRMs and SOD-like CDRMs is a critical area for future research.

4.2. Activity modulation

Although antioxidant CDRMs overcome the disadvantages of natural enzymes, such as rapid inactivation, low bioavailability, and expensive preparation, the unsatisfactory antioxidant performance of CDRMs is still limiting their broad application. Recently, strategies such as precursor screening, elements doping, surface electron transfer adjustment, and heterostructures construction have been proposed to boost antioxidant activity of antioxidant CDRMs.

4.2.1. Precursor screening

The selection of precursors plays a crucial role in determining the crystallinity and core size of CDRMs, which significantly influences their antioxidant activity. For instance, Gao et al. [61] compared the antioxidant activity of CDRMs synthesized from graphite powder, carbon black, and activated charcoal under identical conditions. The crystal structure, density, porosity, and hardness of activated charcoal provided optimal thermodynamic and kinetic conditions for oxidation and etching processes, resulting in CDRMs with exponentially superior antioxidant activity compared to those derived from the other two precursors. Moreover, even precursors with identical components but in different ratios can produce antioxidant CDRMs with varying efficiencies. Xu et al. [162] utilized gallic acid (GA) and polyethyleneimine (PEI) as carbon and active site sources to synthesize antioxidant CDRMs. A GA/PEI ratio of 3:4 yielded the best antioxidant activity, attributed to the higher oxygen content and lower redox potential of the resulting CDs-GA3/4, which facilitated the ROS scavenging process.

Due to the complex synthesis processes of CDRMs, establishing universal principles to guide the selection of reaction conditions and precursors remains challenging. However, exploring fundamental structural effects, such as core size and crystallinity, may offer a feasible approach to enhancing the antioxidant activity of CDRMs. Additionally, leveraging emerging machine learning techniques to screen and predict valuable precursor candidates represents a promising direction for future research.

4.2.2. Elemental doping

Doping with appropriate elements is a key strategy to enhance the antioxidant performance of CDRMs. For example, Naumov et al. [163] synthesized ten types of antioxidant CQDs with varying doping states and demonstrated that doped CQDs exhibited significantly higher antioxidant activity compared to undoped ones. Among the dopants, Al stood out, enabling CQDs with the highest activity, emphasizing the critical role of doping types. Furthermore, dual-element doping can enhance antioxidant activity by introducing additional active sites and improving interactions with substrates. Inspired by the natural occurrence of Cu/Zn in some SODs, Wu et al. [164] developed biocompatible CuZn-CDs featuring -Cu-O-Zn- bimetallic covalent doping, which endowed the CDs with both catalase (CAT)- and SOD-like activities (Fig. 16a). Notably, Cu helped balance the positive charge during the Zn doping process under low pH conditions, enabling CuZn-CDs to exhibit CAT-like catalysis. The dual doping of Cu and Zn also stabilized the antioxidation capability across a wide pH range (1.2–13.0) and at high temperatures (up to 150°C), making these nanozymes superior to natural antioxidant enzymes in terms of application, transport, and storage. Similarly, CDRMs doped with Ce and Pr exhibited stronger ·OH scavenging abilities compared to single-doped counterparts, owing to enhanced redox performance arising from dual doping [165].

4.2.3. Accelerating surface electron transfer

Since the antioxidant processes of CDRMs fundamentally rely on electron transfer between CDRMs and active ROS, enhancing electron transfer efficiency through surface modification with specific ligands and functional groups can significantly boost ROS-scavenging performance. For instance, Zhang et al. [166] demonstrated that an oligomeric nanozyme (O-NZ) synthesized using ethanol and o-phenylenediamine as precursors exhibited remarkable antioxidant activity (Fig. 16b). The high antioxidant performance was attributed to the semiconductor core and surface-active units of O-NZ, which facilitated ultrafast electron

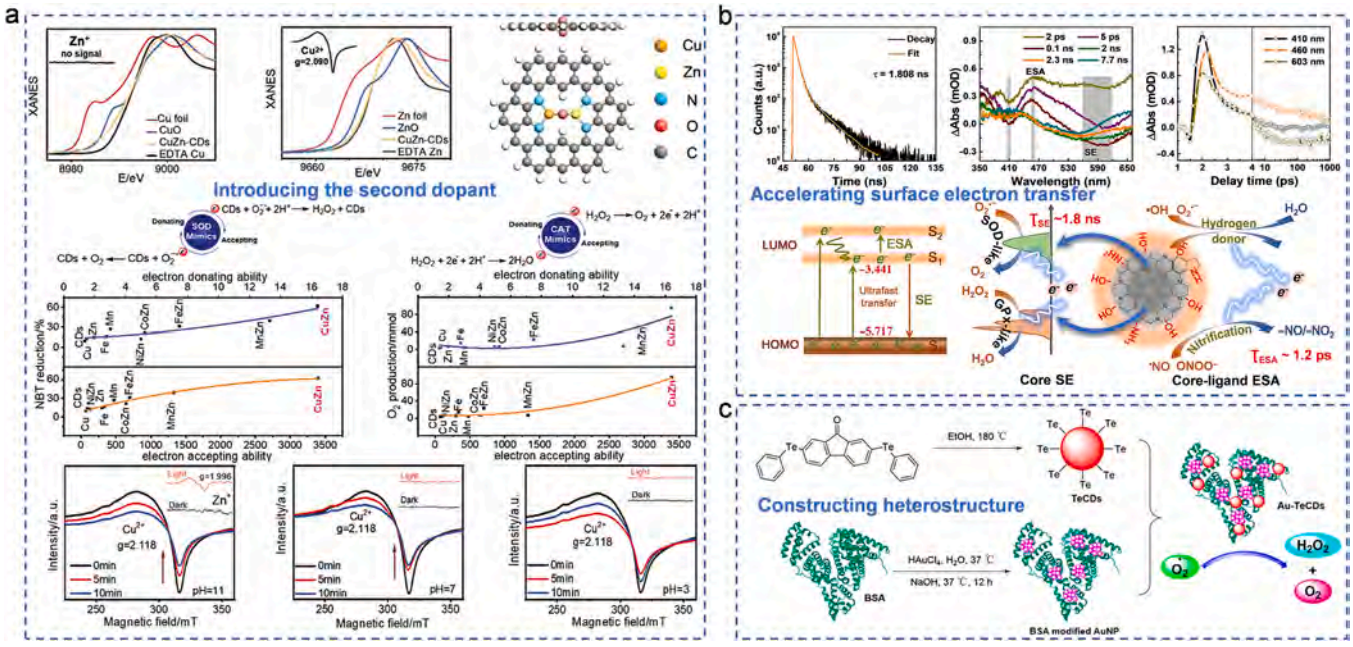

Fig. 16. Activity modulation of CDRMs to downregulate ROS. (a) Introduction of the second dopant. [164]. Copyright 2021, Wiley. (b) Surface electron transfer acceleration. [166]. Copyright 2021, The American Association for the Advancement of Science. (c) Antioxidant heterostructure construction. [169]. Copyright 2021, American Chemical Society.
(a) Reproduced with permission from ref. (b) Reproduced with permission from ref. (c) Reproduced with permission from ref.

transfer, achieving rates of 1.8 nanoseconds within the internal cores and 1.2 picoseconds between the core and ligand molecules. This efficiently electron transfer endowed O-NZ with ultrahigh SOD- and glutathione POD-like activities, comparable to those of natural enzymes. Beyond accelerating electron transfer speed, increasing the availability of surface electrons can further enhance the antioxidant capacity of CDRMs. For example, the semiconductor-like properties of CDRMs can be leveraged through photo or ultrasound stimulation to generate hot electrons, thereby amplifying their antioxidant activity [167,168].

4.2.4. Constructing heterostructure

The construction of heterostructures represents an advanced strategy to enhance the antioxidant performance of CDRMs by leveraging their electronic and structural synergies. Heterojunction structures modulate the electronic environment of the material, optimize charge transfer pathways, minimize energy losses, and accelerate charge migration, collectively boosting the efficiency of antioxidant reactions. Additionally, the interface regions formed within heterostructures often provide new active sites, further facilitating redox reactions and strengthening the antioxidant activity of CDRMs. For instance, Tang et al. [169] developed a heterostructure comprising Tellurium-containing carbon dots (TeCDs) decorated with gold nanoparticles (Au-TeCDs). In this system, the TeCDs served as active reaction sites, while the heterostructure with Au nanoparticles enhanced the elimination of $O_2^{\cdot-}$ (Fig. 16c). This demonstrates how the synergy between different components in a heterostructure can significantly improve antioxidant performance. Despite these advantages, the synthesis of CDRM-metal heterostructures still present challenges, including complex procedures and potential toxicity concerns. As an alternative, heterojunctions formed between different types of CDRMs (CDRM-CDRM heterojunctions) offer a simpler, safer, and equally effective way to improve antioxidant performance. These CDRM-CDRM heterojunctions exploit the intrinsic properties of each component, creating a cooperative effect that enhances overall redox activity [144].

4.2.5. Weaving surface functional groups

The antioxidant activity of CDRMs varies depending on the type of functional group involved. Hydroxyl (-OH) groups exhibit stronger electron-donating abilities than carboxyl (-COOH) groups due to their higher electron density. This results in the higher antioxidant activity for -OH-functionalized CDRMs compared to -COOH-functionalized ones. For example, Paoprasert et al. [170] synthesized different types of CDs using green tea and alpha-hydroxy acids as precursors. They found that CDs containing multiple hydroxyl groups exhibited superior antioxidant activity compared to those containing fewer hydroxyl groups.

4.3. Selectivity modulation

Selective scavenging of toxic ROS while preserving the beneficial ones is vital for maintaining intracellular ROS balance. The antioxidant selectivity of CDRMs is largely determined by the surface functional groups present, as they govern both the electron and hydrogen atom transfer processes essential for effective ROS scavenging.

For example, to achieve SOD-like activity and eliminate $O_2^{\cdot-}$, CDRMs need to facilitate hydrogen atom and electron transfer to convert reactive ROS into stable molecules like O_2, H_2O, and H_2O_2. Studies have shown that the active sites of SOD-like CDRMs often involve functional groups such as -OH, -COOH, and -NH_2, which are capable of donating hydrogen atoms to neutralize ROS. Similarly, to scavenge hydroxyl radicals (·OH), hydrogen atoms must also be provided by the CDRMs to react with ·OH. For instance, Lee et al. [171], synthesized SH-CQDs by hydrothermal pyrolysis of citric acid and reduced glutathione (GSH), showing that the -SH groups conferred the ability to scavenge H_2O_2 and ·OH.

Furthermore, the redox potential of CDRMs must align with that of the substrate for efficient electron transfer. The core and surface structure of the CDRMs play a significant role in determining their redox potential, which governs their ability to selectively scavenge specific ROS. For example, Li et al. [45] demonstrated selective ROS scavenging by tuning the surface states of herbal-derived CDs (Fig. 17). These CDs, such as those derived from honeysuckle (HOCD) and dandelion (DACD), had appropriate redox potentials to scavenge harmful ·OH and ONOO− while being inactive toward beneficial $O_2^{\cdot-}$, H_2O_2, and NO.

Other factors, such as surface charge and the reaction environment (e.g., acidic or alkaline conditions), also influence antioxidant selectivity. The surface charge of CDRMs can affect the adsorption of substrates through electrostatic interactions, thus altering the selectivity of ROS scavenging. Additionally, the reaction environment can alter the mechanism of ROS scavenging. For example, Pathak et al. [172] synthesized N, S co-doped CDs (NSCDs) and found that, under acidic conditions, the scavenging of free radicals occurred through a hydrogen atom transfer mechanism, while under alkaline conditions, proton-coupled electron transfer predominated.

To further enhance the antioxidant selectivity of CDRMs, various strategies can be employed, such as constructing electron locks, combining recognition molecules, and designing specific catalytic microenvironments around active centers. These approaches can help to better regulate ROS scavenging, improving the efficiency and selectivity of CDRMs in biological applications.

5. CDRMs to bidirectionally regulate ROS

Most CDRMs can regulate ROS levels either by upregulating them through enzymatic catalysis or physical excitation, or by downregulating them through antioxidant enzyme mimicry. In certain cases, these remarkable properties can be achieved using the same precursor, enabling bidirectional control of ROS. This section discusses strategies for achieving bidirectional ROS management, including the integration of both pro-oxidative and antioxidative active sites on individual CDRM nanozymes, and leveraging physical excitation to switch between antioxidant and pro-oxidative modes.

5.1. Nanozyme-catalyzed ROS bidirectional modulation

Metal doping introduces active sites onto CDRMs, enabling enzyme-like activity for managing intracellular ROS, with valence transitions of metal ions facilitating the shift between pro-oxidative and anti-oxidative states. For instance, Xu et al. [173] studied the catalytic dynamics of CDRMs based on the oxidation state of single atoms (Fig. 18a). Using ferrous and ferric ions in ethylenediamine tetraacetate (Fe^{2+}/Fe^{3+}-EDTA) as precursors, they synthesized Fe single-atom-incorporated CDs via a one-step low-temperature fabrication process. These CDs exhibited either pro-oxidative POD-like catalysis or multiple antioxidative enzyme-like activities, including POD, SOD, and CAT. Remarkably, when precisely coordinated with N and C atoms, the same Fe-CDs displayed multiple enzyme-like activities, such as pro-oxidative enzymes (POD and OXD), antioxidative enzymes (SOD and CAT), and glutathione peroxidase (GPx), enabling bidirectional modulation of intracellular ROS levels [174] (Fig. 18b). Similarly, Yang et al. [153] optimized reaction conditions to prepare Cu-doped CDs (Cu-CDs), which enhanced POD-catalyzed ROS production and CAT-catalyzed O_2 production, alleviating hypoxia effectively.

Since acidic conditions enhance the pro-oxidative capabilities of CDRMs while antioxidative nanozymes typically operate in neutral or alkaline environments, pH-responsive modulation holds promise for achieving bidirectional ROS regulation. For example, Xu et al. [175] developed celery-based CDs (CECDs, Fig. 18c), which exhibited photo-driven OXD-like activity at a pH of 5, closely matching the microenvironmental pH of infection sites. Conversely, CECDs displayed antioxidant activity at neutral or weakly alkaline pH levels, enabling intelligent, pH-responsive wound healing. However, the overlapping pH domains for pro-oxidation and antioxidation often complicate precise

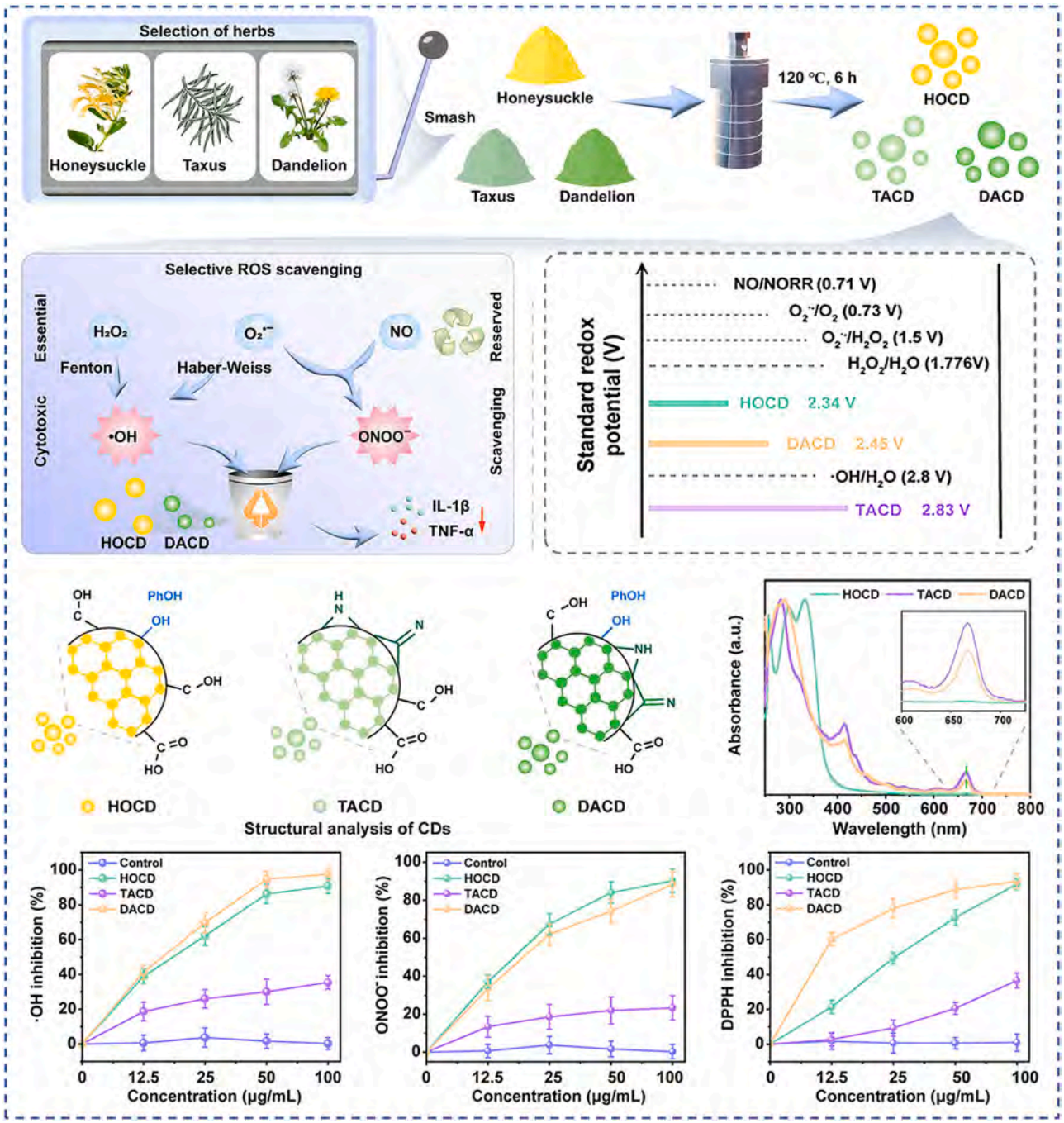

Fig. 17. Modulating surface states to manipulate the antioxidant selectivity of CDRMs. Reproduced with permission from ref. [45]. Copyright 2024, American Chemical Society.

control. This limitation can be overcome by reconstructing the electronic structure of CDRMs through strategies such as heteroatom doping, careful selection of precursors, and fine-tuning of reaction environments [176,177]. These approaches can enhance the adaptability and efficiency of CDRMs in diverse pathological settings.

5.2. *Physical field-switchable ROS bidirectional modulation*

Although physical fields such as photo energy can evoke both pro-oxidative and antioxidative activities, the energy required for each activity is often distinct. Thus, the conversion between pro-oxidation and antioxidation in CDRM nanozymes can be achieved by modulating the physical field in the reaction environment. For example, Yin et al. [178] synthesized GQDs via chemical oxidation and cutting methods, which could quench various antioxidant free radicals without external stimuli but induce a ROS burst under blue light irradiation. Similarly, in He's work [179] Au/N-doped CD nanozymes (Au/NC) exhibited intrinsic ROS-scavenging SOD-like activity but could generate ROS ($O_2^{\cdot-}$, ·OH, and $^1O_2$) through OXD-like activity under visible light, demonstrating light-induced redox conversion. Additionally, Huang et al. [180] prepared ultra-stable tellurium-doped CDs (Te-CDs) with intrinsic H_2O_2-scavenging activity, which could also generate ·OH upon NIR (808 nm) laser irradiation.

The above examples demonstrate the transformation from antioxidation to pro-oxidation using external photo energy, ranging from blue light to NIR. However, most applications of bidirectional CDRMs

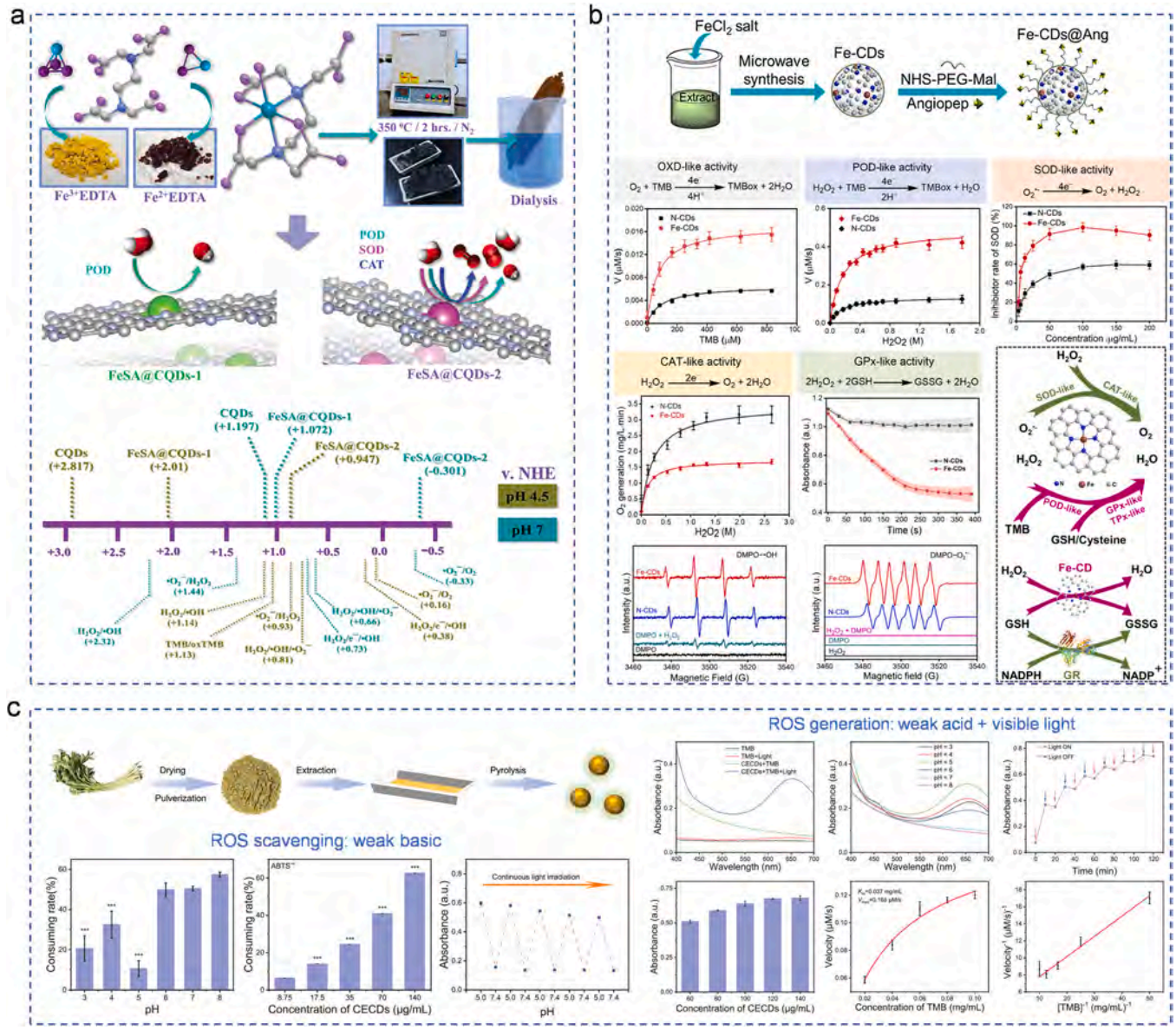

Fig. 18. Nanozyme-catalyzed ROS bidirectional modulation. (a) Modulation of the oxidation state of active sites to alter the catalytic microenvironment. [173]. Copyright 2022, Wiley. (b) Doping-induced coexistence of pro-oxidative and anti-oxidative activities. [174]. Copyright 2022, Elsevier. (c) Switchable enzymatic activities under acidic and weak basic conditions. [175]. Copyright 2024, Wiley.
(a) Reproduced with permission from ref. (b) Reproduced with permission from ref. (c) Reproduced with permission from ref.

aim to prevent excessive ROS production and prioritize the conversion of pro-oxidative nanozymes to antioxidative forms. For instance, Fang et al. [181] developed oxygen-nitrogen functionalized CQDs (O/N-CQDs) with intrinsic POD-like activity (ROS production) (Fig. 19). Interestingly, under appropriate visible light intensity, the CQDs could switch from POD-like activity to CAT-like catalysis (ROS scavenging). The mechanism underlying this photo-switchable enzymatic activity involved the polarization of quinoid nitrogen from the polyaniline precursor under visible light, which consumed ROS to produce O_2 and H_2O. Photo-switchable bidirectional ROS modulation shows great potential. However, its application faces challenges such as limited tissue penetration of light. This limitation could be addressed by employing alternative techniques such as ultrasound treatment to enable deeper tissue activation.

6. CDRM-dominated biomedical applications

ROS levels play a pivotal role in determining cellular fate. As emerging ROS modulators, CDRMs hold significant promises in biomedicine, enabling the development of diverse therapeutic strategies to treat severe diseases by precisely regulating ROS levels. On one hand, by harnessing physical fields or introducing enzyme-like active sites, CDRMs can upregulate ROS levels to induce irreversible oxidative stress within harmful bacteria and cancer cells, leading to structural damage and cell death. On the other hand, CDRMs can also scavenge excessive ROS to alleviate painful inflammation.

This section highlights the biomedical applications of CDRMs in wound healing, cancer treatment, and inflammation-related diseases. We delve into the pathological characteristics of these conditions, the therapeutic principles underlying ROS modulation, and the potential for synergistic therapies to enhance treatment outcomes.

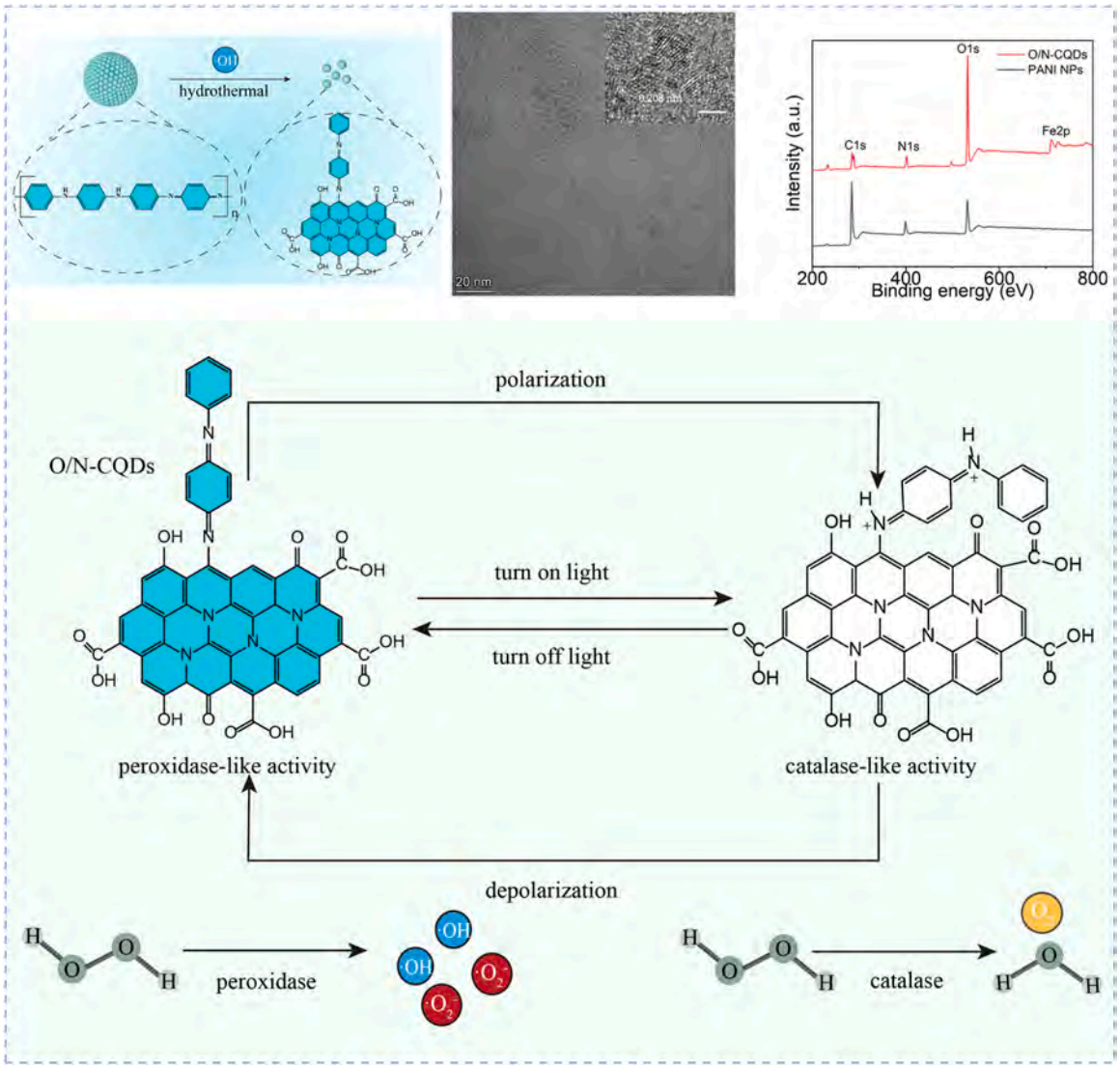

Fig. 19. Physical field-switchable ROS bidirectional modulation. Transformation of activity from POD to CAT upon visible light initiation. Reproduced with permission from ref. [181]. Copyright 2024, Wiley.

6.1. *Wound healing*

6.1.1. *Bacterial inactivation*

Bacterial infections are a significant barrier to wound healing, necessitating timely and effective elimination of bacteria to accelerate repair. While antibiotics remain the primary clinical approach to combat bacterial infections, their efficacy is diminishing due to the rapid emergence and evolution of antibiotic resistance [182–184]. Upregulating intracellular ROS to induce oxidative stress has emerged as a promising alternative to conventional antibiotics [185–187]. Under normal growth conditions, bacteria generate small amounts of ROS, including $O_2^{\cdot-}$, H_2O_2, and ·OH, which are neutralized by their intrinsic antioxidant defense systems. However, when exposed to ROS-upregulating CDRMs, the ROS levels overwhelm these defenses, leading to oxidative stress that damages bacterial lipids, proteins, and nucleic acids. This oxidative damage compromises cellular structures and metabolic pathways, ultimately resulting in bacterial death [188–192].

In infectious environments, bacteria and macrophages often overproduce H_2O_2. CDRMs with catalytic properties can exploit this, converting H_2O_2 into O_2 or ·OH via CAT- or POD-like activity, respectively. For instance, Lin et al. [193] designed O_2 self-supplying CDs (H-CDs) modified with the photosensitizer hemin to enhance photodynamic bacterial inactivation (Fig. 20a). H-CDs exhibited CAT-like activity, catalyzing endogenous H_2O_2 to O_2, and enhanced electron-hole separation efficiency during photodynamic therapy, producing more $^1O_2$. In a full-thickness infectious wound model, H-CDs combined with laser irradiation achieved an impressive wound closure rate of 92.8 %, surpassing other treatments. Similarly, Zhou and Liu et al. [95] utilized the POD-like activity of Fe-CDs to generate ·OH, causing severe oxidative damage to bacteria. Additionally, the photothermal effect of Fe-CDs under 808 nm laser irradiation enhanced POD-like activity, further boosting ROS generation and accelerating infectious wound healing within 10 days.

Chiral CDRMs have also been developed for selective bacterial inactivation. Xu and Wang et al. [194] fabricated chiral CDs using D- and L-cysteine as precursors (Fig. 20b). D-CDs demonstrated stronger fluorescence and greater efficacy against gram-positive bacteria compared to L-CDs. Under dual-light irradiation, D-CDs exhibited enhanced antimicrobial activity through a triple mechanism: membrane rupture in the absence of light, $^1O_2$ production during photodynamic therapy, and temperature elevation during photothermal therapy. *In vivo* studies confirmed the wound-healing potential of D-CDs under laser irradiation.

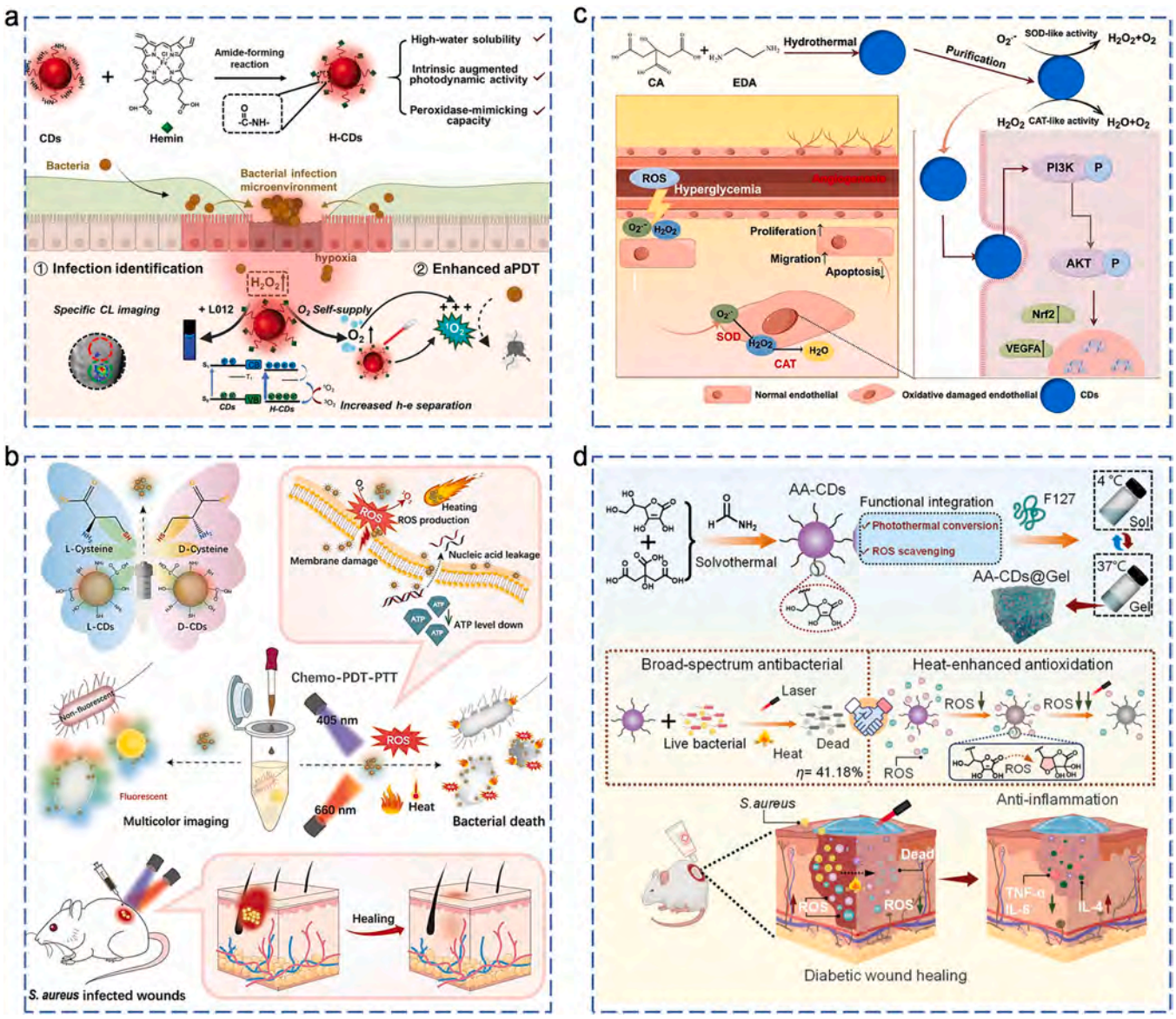

Fig. 20. CDRMs in managing intracellular ROS for wound healing. (a) O_2 self-supplying CDRMs for photodynamic therapy. [193]. Copyright 2023, Wiley. (b) Chiral CDRMs for bacteria-selective photodynamic therapy. [194]. Copyright 2024, Wiley. (c) Antioxidant CDRMs for anti-inflammatory therapy. [195]. Copyright 2024, Elsevier. (d) Antioxidant CDRMs for photothermal bactericidal and anti-inflammatory therapy. [197]. Copyright 2024, Wiley.
(a) Reproduced with permission from ref. (b) Reproduced with permission from ref. (c) Reproduced with permission from ref. (d) Reproduced with permission from ref.

While bacteria may attempt to counter oxidative stress by producing more antioxidant enzymes, excessive ROS production can overwhelm these defenses. Notably, resistance to oxidative stress is rarely reported, underscoring the promise of CDRM-based antibacterial strategies in addressing the global challenge of antibiotic resistance.

6.1.2. *Inflammation modulation*

Excessive inflammation arising from ROS is also a significant barrier to wound healing, causing oxidative injury to cells, impairing cell proliferation, and delaying the whole process. Antioxidant CDRMs, by downregulating overproduced ROS, can effectively transition wounds from the inflammatory phase to the cell proliferation phase, thereby promoting rapid repair. For example, Chen et al. [195] synthesized CDs with SOD- and CAT-like activities using anhydrous citric acid and ethanediamine as precursors (Fig. 20c). These CDs effectively scavenged $O_2^{\cdot-}$ and H_2O_2 with excellent biocompatibility, promoting the proliferation, migration, and angiogenesis of human umbilical vein endothelial cells. *In vivo* studies confirmed that these CDs acted as catalytic nano-antioxidant agents, significantly enhancing angiogenesis and facilitating repair in orthopedic disease models, including subcutaneous implants and diabetic wound healing. Similarly, Yang et al. [196] developed a Zn-SAzyme supported by ultra-small CDs (Zn/CDs) via a one-step hydrothermal method. This nanozyme exhibited antibacterial, angiogenic, and anti-inflammatory properties, aiding diabetic wound repair. Zn/CDs efficiently entered cells, localized to mitochondria, and scavenged overproduced ROS, thereby protecting cells from oxidative stress and reducing the release of pro-inflammatory cytokines. The synergistic effect of mild photothermal strategies and antioxidant CDRMs could further promote the wound-healing process. For instance, Lin et al. [197] prepared antioxidant CDs (AA-CDs) with notable photothermal effects using a straightforward solvothermal method with citric acid and ascorbic acid as precursors (Fig. 20d). AA-CDs demonstrated a photothermal conversion efficiency of 41.18 %, which simultaneously enhanced bacterial elimination and ROS scavenging. To

facilitate *vivo* application, AA-CDs were incorporated into a thermally responsive hydrogel. This hydrogel exhibited excellent anti-inflammatory properties by modulating inflammatory factors, significantly accelerating diabetic wound healing.

As the oxidative and antioxidative properties of CDRMs can separately promote antibacterial and anti-inflammatory processes, these two mechanisms often occur sequentially. Therefore, bidirectional CDRMs hold great promise in achieving an initial oxidation phase followed by antioxidation, restoring the natural healing state to the greatest extent. However, this hypothesis requires further investigation.

While numerous studies have highlighted the potential of CDRMs for intracellular ROS modulation in wound healing, several challenges must be addressed before clinical application. First, a deeper understanding of the repair mechanisms at the cellular and molecular levels is essential to move beyond superficial observations. Additionally, intracellular ROS level is critical for antibacterial efficiency but ROS are short-lived and readily react with surrounding substances, limiting their availability. Modifying CDRMs with bacteria-targeting molecules to improve their adherence to bacterial surfaces may help overcome these challenges and optimize antibacterial efficacy.

6.2. Cancer treatment

Malignant cancers remain one of the leading causes of death globally, particularly advanced cancers, which are more difficult to treat and have significantly lower survival rates due to their rapid spread and metastasis. Current anticancer strategies primarily focus on either directly inducing cancer cell death or modifying the tumor microenvironment, with ROS regulation playing a pivotal role in both approaches.

6.2.1. Monotherapy inducing cancer cell death

Excessive ROS accumulation induces oxidative stress, which can damage biological macromolecules and lead to cancer cell death. Pro-oxidant CDRMs have been extensively utilized to treat various tumors by regulating pathways such as apoptosis, autophagy, ferroptosis, and pyroptosis.

6.2.1.1. Apoptosis. ROS can activate apoptosis pathways by upregulating pro-apoptotic proteins, promoting the opening of mitochondrial permeability transition pore, and activating caspases [15,198–200]. For example, Zheng et al. [128] synthesized CDs with effective photodynamic anti-cancer activity. These CDs functioned as both NIR phosphorescence emitters (lifetime > 2.0 h) and ROS producers, enhancing photodynamic therapy under 685 nm laser irradiation. This approach effectively inhibited the growth of subcutaneous xenograft tumors in CT26 models, demonstrating remarkable therapeutic efficacy *in vivo*.

6.2.1.2. Autophagy. While autophagy is typically a cellular survival mechanism, excessive ROS accumulation can impair organelles and proteins, causing cell death. Shi et al. [174] rationally designed ultrasmall CD-supported Fe SAzymes (Fe-CDs) (Fig. 21a) with multiple enzymatic properties, including OXD, CAT, SOD, and peroxidase family activities (POD, TPx, and GPx). These CDs accumulated in acidic endosomes and lysosomes, where their OXD/POD-like activities produced toxic ROS, impairing lysosomal degradation and activating autophagic flux. Additionally, their SOD, CAT, and GPx-like activities disrupted redox homeostasis, directly enhancing autophagy and lysosome-mediated apoptosis.

6.2.1.3. Ferroptosis and Cuproptosis. Ferroptosis, a novel form of non-

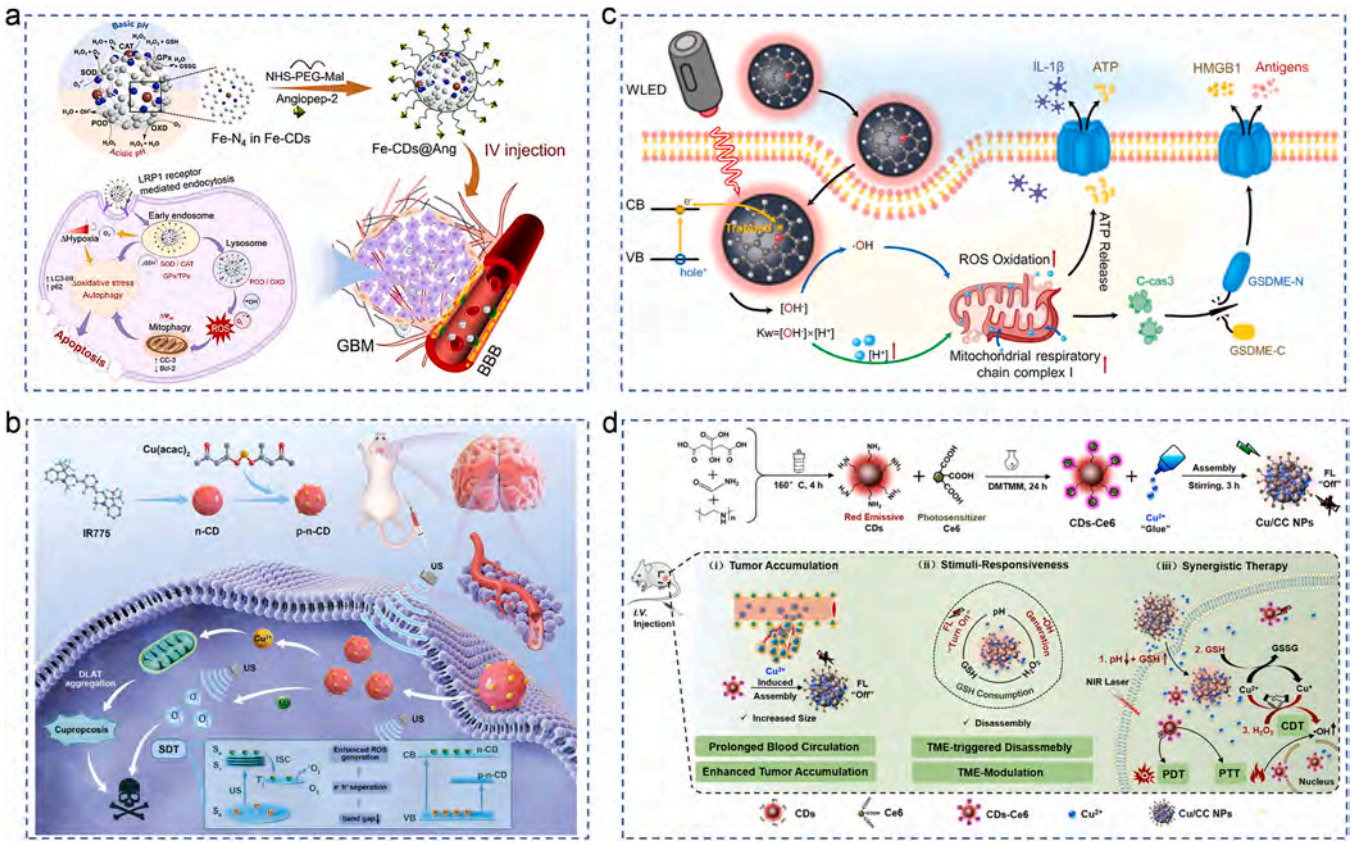

Fig. 21. CDRMs in managing intracellular ROS for malignant cancer treatment. (a) Autophagy targeting. [174]. Copyright 2022, Elsevier. (b) Cuproptosis pathway. [145]. Copyright 2024, Wiley. (c) Pyroptosis pathway. [205]. Copyright 2024, Wiley. (d) Multi-modal therapy. [206]. Copyright 2020, Wiley.
(a) Reproduced with permission from ref. (b) Reproduced with permission from ref. (c) Reproduced with permission from ref. (d) Reproduced with permission from ref.

apoptotic cell death, involves antioxidant defense collapse and lipid peroxidation, making it a promising cancer therapy strategy with minimal drug resistance. Leblanc et al. [201] developed copper chlorophyllin-based CDs (Chl-D CDs) with excellent biocompatibility. These CDs augmented photodynamic activity via Fenton-like reactions, increasing ROS levels and triggering ferroptosis in cancer cells *in vitro* and *in vivo*. Moreover, Chl-D CDs could synergize with temozolomide, combining photodynamic therapy with chemotherapy for enhanced efficacy. Similarly, cuproptosis is also an emerging therapeutic strategy, involving modulation of the tricarboxylic acid (TCA) cycle [202–204]. Cheng et al. [145] synthesized Cu-doped CDs (Cu-CDs) with a distinctive p-n junction and a narrow bandgap, enabling sonodynamic ROS generation (Fig. 21b). The doped Cu ions also induced cuproptosis, synergistically enhancing therapeutic efficacy against glioblastoma multiforme.

Pyroptosis, a highly immunogenic form of cell death, features membrane pore formation, cell swelling and lysis, and pro-inflammatory cytokine release, making it a promising approach in cancer immunotherapy. Qu et al. [205] developed photocatalytic ROS-upregulating CDs to induce pyroptosis for constructing whole cancer cell vaccines (Fig. 21c). Under white light irradiation, these CDs produced significant ·OH, increasing intracellular ROS and reducing cytoplasmic pH. This efficiently triggered pyroptosis through the ROS-mitochondria-caspase 3-gasdermin E pathway and proton-driven mitochondrial ATP synthesis.

The cancer-killing mechanisms of pro-oxidant CDRMs, whether acting independently or synergistically, effectively target tumor cells without inducing resistance, offering a powerful tool for advanced cancer therapies.

6.2.2. *Multimodal therapy*

Given the complexity, multiplicity, and unpredictability of malignant tumors, therapeutic strategies have evolved from monotherapy to multimodal therapy based on CDRMs. These approaches integrate tumor microenvironment (TME) targeting, intervention of the Warburg effect, and organelle-specific targeting to improve therapeutic efficacy.

6.2.2.1. TME targeting. The TME characterized by weak acidity, hypoxia, and abnormal metabolism, plays a critical role in tumor progression and therapeutic resistance. Leveraging these unique features allows targeted regulation of ROS for cancer therapy. For instance, Lin et al. [206] developed a TME stimulus-responsive nanoplatform for fluorescence (FL) imaging and synergistic cancer therapy. This platform consisted of photosensitizer-modified CDs (CDs-Ce6) and Cu^{2+} ions. The aggregation of CDs-Ce6 quenched FL and photosensitization, but their abilities were triggered under low pH, high glutathione (GSH), and H_2O_2 levels in the TME. Additionally, Cu^{2+} provided chemodynamic therapy (CDT) by reacting with H_2O_2 and depleted GSH, amplifying intracellular oxidative stress and enhancing ROS-based cancer therapy efficacy (Fig. 21d).

6.2.2.2. Intervention of the Warburg effect. The Warburg effect, a hallmark of cancer, involves glucose metabolism through aerobic glycolysis to sustain rapid ATP production and meet the energy demands of tumor growth. Starvation therapy has been proposed to deplete glucose in tumor tissues, synergizing with ROS-upregulated CDRMs to inhibit cancer cell proliferation. For example, Chang et al. [207] designed a multifunctional nano-catalyst, Cu,N,S-CQDs@GOx/CPT (CuCGC), combining Cu, N, S-doped carbon quantum dots, glucose oxidase (GOx), and camptothecin (CPT). The acidic TME facilitated the release of Cu^{2+} and S^{2-} ions, which catalyzed hydroxyl radical (·OH) and H_2S gas production for CDT and gas therapy (GT), respectively. Moreover, CuCGC reacted with glucose to produce gluconic acid and H_2O_2, supporting starvation therapy (ST) and enhancing CDT. CuCGC also showed ROS-responsive CPT release upon activation by H_2O_2 and glucose, achieving a 66 % drug release rate and improving its therapeutic efficacy.

6.2.2.3. Organelle targeting. Precise targeting of specific organelles minimizes side effects and enhances the bioavailability of pro-oxidant CDRMs. For example, Bi and Li et al. [208] developed lysosome-targeted CDs capable of light-controlled nitric oxide (NO) release for enhanced PDT. These CDs, synthesized via hydrothermal methods using metformin and methylene blue (MB), exhibited high singlet oxygen ($^1O_2$) quantum yield and NO generation efficiency upon LED light irradiation. The cascade reactions, including oxidation of NO to peroxynitrite ($ONOO^-$), disrupted lysosomal membrane integrity, achieving ~80 % HepG2 cell destruction under light excitation while maintaining low cytotoxicity in the dark. Similarly, Zhang et al. [133] constructed a mitochondrial-targeting CD photosensitizer derived from Hypericum perforatum extract. These red-emissive CDs (RCDs) effectively generated $^1O_2$ and $O_2^{\cdot-}$ under 635 nm irradiation. Their inherent mitochondrial-targeting ability enabled fluorescence-guided navigation for type I/II PDT, even under hypoxic conditions.

Despite the promising laboratory results, the clinical translation of CDRM-based therapies faces several challenges: **Selective ROS generation**: Achieving precise and adequate ROS generation in tumor cells while minimizing toxicity to normal cells remains a critical hurdle. **Stable and controlled ROS release**: The short lifespan of ROS necessitates strategies for controllable and stable release at tumor sites to ensure therapeutic efficacy. Additionally, the physiological stability of CDRMs must be improved for sustained ROS generation. **Balancing efficiency and biotoxicity**: While enhancing treatment efficiency, it is essential to ensure biocompatibility and avoid long-term toxicity and side effects, crucial for FDA approval. **Understanding mechanisms**: A deeper understanding of how ROS induce cancer cell death and mediate multimodal therapy is necessary. The precise action sites of CDRMs within malignant tumors also requires further elucidation based on evidence from multiple perspectives.

6.3. *Inflammation-related diseases*

Statistical research shows that over 50 % of global deaths are associated with inflammatory diseases, such as ischemic heart disease, neurodegenerative diseases, diabetes, and autoimmune disorders [209–212]. These diseases share a common pathology of cellular damage caused by excessive ROS production. Therefore, CDRMs with antioxidant properties have the potential to contribute to anti-inflammatory treatments by scavenging harmful ROS and reducing pro-inflammatory cytokines. Additionally, the fluorescent properties of CDRMs enable visible monitoring of therapeutic effects via *in vivo* imaging. CDRMs have shown promise in alleviating conditions such as visceral inflammation, periodontitis, and neurodegenerative diseases.

Inflammatory bowel disease (IBD) is primarily caused by excessive oxidative stress due to abnormally high ROS levels in the colon. Zhang et al. [213] developed red fluorescent C-dots with SOD-like antioxidant activity to scavenge excessive $O_2^{\cdot-}$ and treat IBD (Fig. 22a). Using glutathione (GSH) and biotin as precursors, these C-dots effectively reduced ROS levels, remodeling the redox microenvironment in the colon and downregulating pro-inflammatory cytokines, such as TNF-α, IL-6, and IL-1β. The fluorescent properties also enabled in situ imaging in mouse models. Symptomatically, C-dots alleviated colon inflammation by promoting epithelial repair, restoring colon length, and reducing inflammatory cell infiltration. Similarly, Luo et al. [149] created a CDRM nanoplatform for visual therapy aimed at ameliorating acute lung injury. These CDRMs demonstrated SOD-like activity (>4000 U/mg) and could accumulate in mitochondria to scavenge harmful ROS. They also emitted fluorescence at a wavelength of 683 nm, allowing for real-time imaging during therapy.

Periodontitis, a chronic inflammatory disease closely linked to excessive intracellular ROS, can benefit from ROS regulation. A reduced

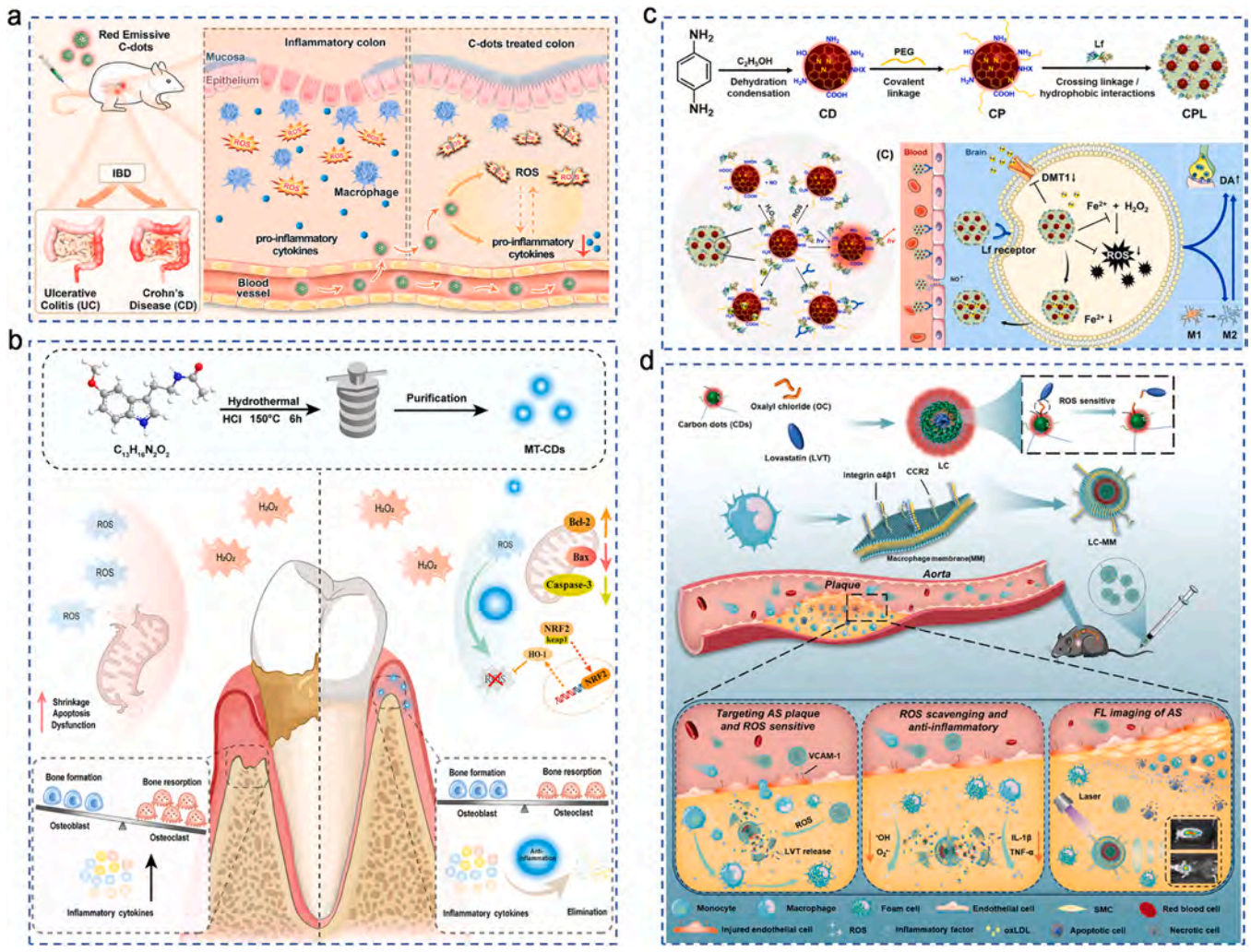

Fig. 22. CDRMs in managing intracellular ROS for treatment of inflammation-related diseases. (a) Inflammatory bowel disease. [213]. Copyright 2023, Elsevier. (b) Periodontitis. [159]. Copyright 2024, American Chemical Society. (c) Parkinson's disease. [214]. Copyright 2024, Elsevier. (d) Atherosclerosis. [218]. Copyright 2024, Wiley.
(a) Reproduced with permission from ref. (b) Reproduced with permission from ref. (c) Reproduced with permission from ref. (d) Reproduced with permission from ref.

ROS level can remodel the periodontal microenvironment and attenuate the inflammatory response. For instance, Yu and Yang et al. [159] hydrothermally synthesized melatonin-derived carbon dots (MT-CDs), which exhibited excellent solubility, biocompatibility, and ROS-scavenging capabilities (Fig. 22b). *In vitro* studies showed that MT-CDs effectively reduced intracellular ROS levels, maintained mitochondrial homeostasis, and inhibited the generation of inflammatory mediators. *In vivo* studies demonstrated that MT-CDs significantly promoted tissue regeneration by suppressing alveolar bone degradation, reducing osteoclast activation, and inhibiting the inflammatory response through the Nrf2/HO-1 signaling pathway.

CDRMs also show promise in treating neurodegenerative diseases such as Parkinson's disease (PD). Traditional PD drugs are often limited by the blood-brain barrier (BBB), leading to poor drug availability at the lesion sites. CDRMs have gained attention due to their unique physicochemical properties, which can facilitate BBB penetration. Studies suggest that CDRM size, surface charge, and chemical composition play pivotal roles in traversing the BBB. Smaller CDRMs can pass through the tissue gaps in the BBB, and surface functional groups can promote receptor-mediated interactions that enhance BBB permeability. Huang et al. [214] used a solvothermal method to prepare red-emitting N-doped CDRMs, which could eliminate ROS, produce nitric oxide (NO) to reversibly open the BBB, and chelate iron ions to inhibit the Fenton reaction (Fig. 22c). The addition of lactoferrin further improved BBB permeability and facilitated selective accumulation of CDRMs in dopaminergic neurons of the substantia nigra via receptor-mediated pathways. *In vivo* results confirmed improved behavioral performance in PD mice through reduced inflammation, and the biocompatibility of the CDRMs was demonstrated by their clearance from the brain via cerebrospinal fluid circulation.

Despite their remarkable antioxidant ability to treat inflammatory diseases, non-specific targeting of CDRMs may lead to adverse effects on normal tissues and organs following *in vivo* administration [215–217]. As macrophage recruitment by chemokines is a notable feature of inflammatory lesions, exploiting the natural chemotaxis of macrophages could provide a promising strategy for the localized delivery of CDRMs. For example, Wu et al. [218] designed a macrophage membrane (MM)-camouflaged, ROS-responsive nanotherapeutic platform (LC-MM) to treat atherosclerosis (AS) (Fig. 22d), a chronic progressive inflammatory disease that contributes to various cardiovascular conditions, including ischemic heart disease, coronary artery disease, and stroke. To inhibit pro-inflammatory cytokines, they grafted CDs with the classical cholesterol-lowering drug lovastatin (LVT), which could be released in a ROS-responsive manner via oxalyl chloride (OC). The key functional

membrane protein of MM, integrin α4β1, was capable of recognizing and interacting with the overexpressed vascular cell adhesion molecule 1 (VCAM-1) on inflammatory endothelial cells, enhancing both targeted accumulation and therapeutic efficacy. Additionally, Wu et al. [219] reported the development of phosphatidylserine-specific peptide--functionalized carbon dot nanozymes (pep-CDs) for the specific and efficient noninvasive therapy of atherosclerosis. The peptide, CLIKKPF, facilitated the targeting of foam cells by binding specifically to phosphatidylserine on their surface. This selective targeting significantly enhanced the accumulation of pep-CDs at plaques, thereby maximizing the therapeutic efficacy in treating AS.

As an emerging class of nanomaterials, CDRMs have demonstrated great potential in treating inflammation-related diseases, thanks to their exceptional antioxidant properties, targeting ability, imaging functionality, and biocompatibility. By scavenging free radicals, modulating antioxidant enzymes, and influencing related signaling pathways, CDRMs can effectively reduce inflammation and promote recovery in patients. However, research on the anti-oxidative mechanisms of CDRMs is still in its early stages, and further in-depth investigations are needed. Looking ahead, CDRMs hold great promise as a powerful tool in the fight against inflammation, with the potential to significantly improve human health.

7. Perspectives and summary

7.1. Summary

ROS plays a crucial role in regulating the physiological functions of cells. Carbon dots with advantages such as low preparation costs, excellent biocompatibility, and favorable electronic properties, are emerging as promising tools for manipulating intracellular ROS levels to combat various devastating diseases. Despite numerous reviews on carbon dots, few focus specifically on their regulation of ROS and the underlying mechanisms.

In this review, we aim to summarize the rapid advancements in carbon dots as ROS modulators (CDRMs). We first discuss classification criteria and common strategies for synthesizing and functionalizing CDRMs, such as doping and surface modifications. Next, we explore the mechanisms by which CDRMs regulate ROS, covering upregulation, downregulation, and bidirectional regulation, and examine methods to modulate their activity and selectivity in each state. For ROS upregulation, we detail how ROS stress is triggered through photo energy, ultrasound, and nanozyme catalysis. Regarding ROS scavenging and antioxidant functions, we highlight potential active sites and mechanisms, including nanozyme-catalyzed antioxidant activity and the ROS downregulation inherited from antioxidant precursors. Additionally, dynamic bidirectional ROS manipulation is achieved in CDRMs through the rational construction of enzymatic sites and the application of physical fields. To accelerate the clinical application of CDRMs in biomedicine, we review their potential applications in wound healing, cancer treatment, and inflammation-related diseases, with a focus on the pathological characteristics, therapeutic mechanisms, and lesion-targeting strategies.

7.2. Future perspectives

Despite the enormous potential and significant progress of CDRMs in intracellular ROS modulation, there is still a long way to go before they can be fully integrated into advanced healthcare management. The main challenges and potential solutions are as follows:

i) **Ambiguous structure-property relationship.** CDRMs exhibit a wide range of structures, from zero-dimensional dots to three-dimensional spheres, with the possibility of multiple structures coexisting in one-pot synthesis. This structural diversity complicates their characterization and makes it challenging to establish a unified structural model. Furthermore, the performance of CDRMs is closely linked to their size and morphology, but current synthesis methods struggle to precisely control size distribution and shape. This leads to poor reproducibility and inconsistent functionality. Additionally, CDRMs often feature a variety of surface functional groups, which significantly influence their solubility, stability, biocompatibility, and catalytic activity. Achieving precise control over these surface groups remains a significant challenge. Importantly, the relationship between specific structures and their corresponding performance, as well as how to optimize performance through structural manipulation, lacks standardized principles. To address these issues, high-precision structural analysis, in-situ characterization techniques, and advanced theoretical computational methods are essential. Moreover, machine learning could be leveraged to guide the selection of synthesis parameters (e.g., reaction solvent, precursors, temperature, and time), enabling more accurate predictions of structure and properties. For CDRMs to be successfully translated into practical applications, challenges related to standardization and industrial production must also be overcome. This involves ensuring structural consistency and performance stability during large-scale manufacturing.

ii) **Poor selectivity over ROS type management.** Different ROS have distinct roles and mechanisms of action in biological systems. Increasing evidence suggests that the management of ROS by CDRMs is closely linked to their surface properties. However, the impact of various surface functional groups on ROS regulation requires further in-depth study. Selectively managing specific ROS types necessitates precise control over both the electronic structure of the core and the surface of CDRMs. Unfortunately, current synthesis and modification techniques lack the precision needed for exact modulation of intracellular ROS types. A promising direction is to develop “smart” CDRMs, functionalized with stimulus-responsive molecules that can be activated by external or intracellular cues to regulate specific ROS types. Additionally, exploring the relationship between the redox potential (i.e., electron energy level) of CDRMs and their ROS-regulating properties could lead to the development of CDRMs with selective ROS-modulating capabilities.

iii) **Precise and on-demand ROS level modulation.** ROS serve as crucial cellular signaling molecules involved in various physiological processes, but excessive ROS production can trigger oxidative stress and cause cell damage. The key to effective ROS regulation using CDRMs lies in the precise and on-demand control of intracellular ROS levels to achieve therapeutic effectiveness without side effects. However, ROS management is complex, and accurately modulating ROS levels under specific pathological conditions remains challenging. Recently, researchers have designed multifunctional CDRMs that can both generate and scavenge ROS. For instance, ROS generators and scavengers can be incorporated into a single CDRM through structural design. Under light excitation, these CDRMs can produce ROS for sterilization or cancer cell killing, while simultaneously regulating ROS levels through antioxidants to prevent excessive production. Unfortunately, these systems lack the ability to sense when to upregulate or downregulate ROS levels. A promising approach is combining physical field-excited bidirectional regulation systems with ROS level-sensing platforms to enable controllable and timely ROS management. Additionally, developing intelligent, microenvironment-responsive CDRMs that respond to pH or enzyme changes could further enhance the accuracy of ROS regulation based on intracellular environmental shifts.

iv) **Superficial investigations on therapeutic mechanisms.** Currently, CDRMs in biomedical healthcare primarily focused on demonstrating their effectiveness in treating ROS-related diseases. It remains unclear how and why specific ROS contribute

most significantly to disease treatment. This issue may be addressed by loading CDRMs with agents that specifically scavenge certain ROS, allowing their contribution to be measured by changes in overall therapeutic efficiency. Additionally, establishing a robust system to evaluate the effectiveness of ROS regulation is essential. Advanced characterization techniques, such as electron spin resonance (ESR) and in-situ Raman spectroscopy, could assist in accurately assessing the types and quantities of specific radicals. Furthermore, interdisciplinary research should be conducted to better understand the action mechanisms of ROS-regulating CDRMs on signal transduction pathways. By integrating bioinformatics and systems biology, a model of ROS regulation and cellular signal transduction could be developed, providing a theoretical framework for designing more effective CDRM-based therapeutic drugs.

v) **Long-term safety evaluation.** While CDRMs generally exhibit good biocompatibility, their long-term *in vivo* safety remains a concern. The size, surface functional groups, and modifications of CDRMs can significantly affect their biotoxicity and *in vivo* behavior. Improper modifications or dosages may lead to toxicity, limiting their potential for biomedical applications. Therefore, comprehensive *in vitro* and *in vivo* safety evaluations should be conducted, addressing acute toxicity, long-term toxicity, and immunogenicity. By precisely controlling synthesis conditions and optimizing surface functional groups—such as increasing hydrophilic groups and reducing potentially toxic ones—the biocompatibility of CDRMs can be enhanced. Additionally, designing biodegradable CDRMs and investigating their metabolic pathways *in vivo* are promising strategies to ensure biosafety.

This review is important and timely because it addresses the growing interest in CDRMs as versatile tools for modulating reactive oxygen species (ROS) in disease treatment. While many reviews have focused on CDs in general, few have specifically examined their role in ROS regulation and the underlying mechanisms. This makes the review unique, offering in-depth insights into how CDRMs can be tailored for ROS upregulation, downregulation, and bidirectional manipulation, which are crucial for combating diseases linked to oxidative stress. The review also stands out by emphasizing strategies to optimize CDRM functionality through doping, surface modifications, and dynamic ROS control, filling a gap in current literature. Moreover, it provides a forward-looking perspective on the clinical potential of CDRMs in fields like cancer therapy, wound healing, and inflammation-related diseases, which are rapidly advancing but still face significant challenges in terms of targeted delivery and efficacy. By focusing on both the scientific mechanisms and real-world applications, offering challenges and potential solutions, this review provides a comprehensive overview that can inform future research and clinical strategies in ROS-based therapies.

CRediT authorship contribution statement

Paul K. Chu: Visualization, Supervision, Resources, Funding acquisition. **Ziyu Liu:** Formal analysis, Resources, Visualization. **Guomin Wang:** Writing – review & editing, Supervision, Project administration, Funding acquisition, Formal analysis, Conceptualization. **Guopeng Xu:** Writing – original draft, Visualization, Methodology, Investigation, Formal analysis, Conceptualization. **Yiheng Tang:** Investigation, Formal analysis. **Danfeng Xiong:** Formal analysis. **Wenkun Zhang:** Formal analysis.

Declaration of Competing Interest

The authors declare that they have no known competing financial interests or personal relationships that could have appeared to influence the work reported in this paper.

Acknowledgments

This work was supported by the National Natural Science Foundation of China (82302382), Shanghai Natural Science Foundation (23ZR1467100), the National Key Research and Development Program of China (2023YFB3809900 and 2023YFB3809901), City University of Hong Kong Donation Research Grants (DON-RMG 9229021 and 9220061), and Guangdong - Hong Kong Technology Cooperation Funding Scheme (TCFS, GHP/212/22GD and CityU 9440399).

Data availability

No data was used for the research described in the article.

References

[1] C. Glorieux, S. Liu, D. Trachootham, P. Huang, Nat. Rev. Drug Discov. 23 (2024) 583–606.
[2] X. Li, J. Gao, C. Wu, C. Wang, R. Zhang, J. He, Z.J. Xia, N. Joshi, J.M. Karp, R. Kuai, Sci. Adv. 10 (2024) eadl0479.
[3] H. Sies, V.V. Belousov, N.S. Chandel, M.J. Davies, D.P. Jones, G.E. Mann, M. P. Murphy, M. Yamamoto, C. Winterbourn, Nat. Rev. Mol. Cell Biol. 23 (2022) 499–515.
[4] L.L. Camargo, F.J. Rios, A.C. Montezano, R.M. Touyz, Nat. Rev. Cardiol. 1 (2024) 91–106.
[5] B. Halliwell, Nat. Rev. Mol. Cell Biol. 25 (2023) 13–33.
[6] P. Innocenzi, L. Stagi, Nano Today 50 (2023) 101837.
[7] M.P. Murphy, H. Bayir, V. Belousov, C.J. Chang, K.J.A. Davies, M.J. Davies, T. P. Dick, T. Finkel, H.J. Forman, Y. Janssen-Heininger, D. Gems, V.E. Kagan, B. Kalyanaraman, N.-G. Larsson, G.L. Milne, T. Nyström, H.E. Poulsen, R. Radi, H. Van Remmen, P.T. Schumacker, P.J. Thornalley, S. Toyokuni, C. C. Winterbourn, H. Yin, B. Halliwell, Nat. Metab. 4 (2022) 651–662.
[8] E.C. Cheung, K.H. Vousden, Nat. Rev. Cancer 22 (2022) 280–297.
[9] H. Dong, Q. Zeng, Y. Sheng, C. Chen, G. Yu, A. Kappler, Nat. Rev. Earth Environ. 4 (2023) 659–673.
[10] R. Mittler, S.I. Zandalinas, Y. Fichman, F. Van Breusegem, Nat. Rev. Mol. Cell Biol. 23 (2022) 663–679.
[11] H. Sies, D.P. Jones, Nat. Rev. Mol. Cell Biol. 21 (2020) 363–383.
[12] T. TeSlaa, M. Ralser, J. Fan, J.D. Rabinowitz, Nat. Metab. 5 (2023) 1275–1289.
[13] D. Kalyane, D. Choudhary, S. Polaka, H. Goykar, T. Karanwad, K. Rajpoot, R. Kumar Tekade, Prog. Mater. Sci. 130 (2022) 100974.
[14] C. Mao, S. Yeh, J.F. Fu, M. Porosnicu, A. Thomas, G.L. Kucera, K.I. Votanopoulos, S. Tian, X. Ming, Sci. Transl. Med. 14 (2022) eabh1261.
[15] R. Mathiyalagan, M. Murugesan, Z.M. Ramadhania, J. Nahar, P. Manivasagan, V. Boopathi, E.-S. Jang, D.C. Yang, J. Conde, T. Thambi, Mater. Sci. Eng. R. -Rep. 160 (2024) 100824.
[16] D.A. Gray, B. Wang, M. Sidarta, F.A. Cornejo, J. Wijnheijmer, R. Rani, P. Gamba, K. Turgay, M. Wenzel, H. Strahl, L.W. Hamoen, Nat. Commun. 15 (2024) 6877.
[17] Y. Kang, L. Xu, J. Dong, X. Yuan, J. Ye, Y. Fan, B. Liu, J. Xie, X. Ji, Nat. Commun. 15 (2024) 1042.
[18] T. Richards, J.H. Harrhy, R.J. Lewis, A.G.R. Howe, G.M. Suldecki, A. Folli, D. J. Morgan, T.E. Davies, E.J. Loveridge, D.A. Crole, J.K. Edwards, P. Gaskin, C. J. Kiely, Q. He, D.M. Murphy, J.-Y. Maillard, S.J. Freakley, G.J. Hutchings, Nat. Catal. 4 (2021) 575–585.
[19] A. Mohammad, M.A. Laboulaye, C. Shenhar, A.D. Dobberfuhl, Nat. Rev. Urol. 21 (2024) 433–449.
[20] J. Muri, M. Kopf, Nat. Rev. Immunol. 21 (2020) 363–381.
[21] K. Wu, A.E. El Zowalaty, V.I. Sayin, T. Papagiannakopoulos, Nat. Cancer 5 (2024) 384–399.
[22] Z. Zhang, R. Dalan, Z. Hu, J.W. Wang, N.W.S. Chew, K.K. Poh, R.S. Tan, T. W. Soong, Y. Dai, L. Ye, X. Chen, Adv. Mater. 34 (2022) 2202169.
[23] D. Zhong, D. Zhang, W. Chen, J. He, C. Ren, X. Zhang, N. Kong, W. Tao, M. Zhou, Sci. Adv. 7 (2021) eabi9265.
[24] T. Wei, T. Pan, X. Peng, M. Zhang, R. Guo, Y. Guo, X. Mei, Y. Zhang, J. Qi, F. Dong, M. Han, F. Kong, L. Zou, D. Li, D. Zhi, W. Wu, D. Kong, S. Zhang, C. Zhang, Nat. Nanotechnol. 19 (2024) 1178–1189.
[25] W. Xiu, H. Dong, X. Chen, L. Wan, L. Lu, K. Yang, L. Yuwen, Q. Li, M. Ding, Y. Zhang, Y. Mou, L. Wang, ACS Nano 18 (2024) 15204–15217.
[26] B. Zou, Z. Xiong, Y. Yu, S. Shi, X. Li, T. Chen, Adv. Mater. 36 (2024) 2401620.
[27] Y. Zuo, J. Ye, W. Cai, B. Guo, X. Chen, L. Lin, S. Jin, H. Zheng, A. Fang, X. Qian, Z. Abdelrahman, Z. Wang, Z. Zhang, Z. Chen, B. Yu, X. Gu, X. Wang, Nat. Nanotechnol. 18 (2023) 1230–1240.
[28] L. Đorđević, F. Arcudi, M. Cacioppo, M. Prato, Nat. Nanotechnol. 17 (2022) 112–130.
[29] H. Lei, A. Alu, J. Yang, X. He, C. He, W. Ren, Z. Chen, W. Hong, L. Chen, X. He, L. Yang, J. Li, Z. Wang, W. Wang, Y. Wei, S. Lu, G. Lu, X. Song, X. Wei, Nat. Commun. 14 (2023) 2678.
[30] B. Ma, A. Bianco, Nat. Rev. Mater. 8 (2023) 403–413.

[31] B. Sui, Y. Zhu, X. Jiang, Y. Wang, N. Zhang, Z. Lu, B. Yang, Y. Li, Nat. Commun. 14 (2023) 6782.
[32] J. Zhang, Y. Liu, C. Njel, S. Ronneberger, N.V. Tarakina, F.F. Loeffler, Nat. Nanotechnol. 18 (2023) 1027–1035.
[33] Y.-Y. Liu, N.-Y. Yu, W.-D. Fang, Q.-G. Tan, R. Ji, L.-Y. Yang, S. Wei, X.-W. Zhang, A.-J. Miao, Nat. Commun. 12 (2021) 812.
[34] N.C. Verma, A. Yadav, C.K. Nandi, Nat. Commun. 10 (2019) 2391.
[35] B. Zhao, Z. Wang, Z. Tan, Nat. Photonics 14 (2020) 130–136.
[36] N. Gong, X. Ma, X. Ye, Q. Zhou, X. Chen, X. Tan, S. Yao, S. Huo, T. Zhang, S. Chen, X. Teng, X. Hu, J. Yu, Y. Gan, H. Jiang, J. Li, X.-J. Liang, Nat. Nanotechnol. 14 (2019) 379–387.
[37] F. Li, T. Li, C. Sun, J. Xia, Y. Jiao, H. Xu, Angew. Chem. Int. Ed. 56 (2017) 9910–9914.
[38] Z. Zhang, D. Zhou, Z. Li, X. Luan, J. Yang, S. Tang, Y. Song, Angew. Chem. Int. Ed. 63 (2023) e202316007.
[39] S. Cong, J. Cai, X. Li, J. You, L. Wang, X. Wang, Adv. Funct. Mater. 34 (2024) 2401540.
[40] Y. Jiang, K. Pu, Acc. Chem. Res. 51 (2018) 1840–1849.
[41] T. Luo, H. Yang, R. Wang, Y. Pu, Z. Cai, Y. Zhao, Q. Bi, J. Lu, R. Jin, Y. Nie, X. Shuai, ACS Nano 17 (2023) 16715–16730.
[42] N. Tao, H. Li, L. Deng, S. Zhao, J. Ouyang, M. Wen, W. Chen, K. Zeng, C. Wei, Y.-N. Liu, ACS Nano 16 (2021) 485–501.
[43] B. Kong, T. Yang, F. Cheng, Y. Qian, C. Li, L. Zhan, Y. Li, H. Zou, C. Huang, J. Colloid Interface Sci. 611 (2022) 545–553.
[44] J. Li, C. Fu, B. Feng, Q. Liu, J. Gu, M.N. Khan, L. Sun, H. Wu, H. Wu, Adv. Sci. 11 (2024) 2400527.
[45] R. Nie, J. Zhang, Q. Jia, Y. Li, W. Tao, G. Qin, X. Liu, Y. Tao, Y. Zhang, P. Li, ACS Nano 18 (2024) 22055–22070.
[46] X. Xu, R. Ray, Y. Gu, H.J. Ploehn, L. Gearheart, K. Raker, W.A. Scrivens, J. Am. Chem. Soc. 126 (2004) 12736–12737.
[47] A. Döring, E. Ushakova, A.L. Rogach, Light Sci. Appl. 11 (2022) 75.
[48] H. Liu, X. Zhong, Q. Pan, Y. Zhang, W. Deng, G. Zou, H. Hou, X. Ji, Coord. Chem. Rev. 498 (2024) 215468.
[49] H. Cai, Y. Li, X. Wu, Y. Yang, A.C. Tedesco, Z. Li, H. Bi, Adv. Funct. Mater. 34 (2024) 2406096.
[50] J.X. Qin, C.L. Shen, L. Li, H. Liu, W.Y. Zhang, X.G. Yang, C.X. Shan, Adv. Mater. 36 (2024) 2404694.
[51] Y. Ru, G.I.N. Waterhouse, S. Lu, Aggregate 3 (2022) e296.
[52] B. Wang, G.I.N. Waterhouse, S. Lu, Trends Chem. 5 (2023) 76–87.
[53] Y. Yu, Q. Zeng, S. Tao, C. Xia, C. Liu, P. Liu, B. Yang, Adv. Sci. 10 (2023) 2207621.
[54] S. Chung, R.A. Revia, M. Zhang, Adv. Mater. 33 (2019) 1904362.
[55] Y. Li, L. Chen, S. Yang, G. Wei, X. Ren, A. Xu, H. Wang, P. He, H. Dong, G. Wang, C. Ye, G. Ding, Adv. Mater. 36 (2024) 2313639.
[56] J. Liu, D. Li, K. Zhang, M. Yang, H. Sun, B. Yang, Small 14 (2018) 1703919.
[57] C. Xia, S. Zhu, T. Feng, M. Yang, B. Yang, Adv. Sci. 6 (2019) 1901316.
[58] X. Li, C. Kang, S. Tao, B. Yang, Carbon 237 (2025) 120122.
[59] B. Wang, G.I.N. Waterhouse, B. Yang, S. Lu, Acc. Chem. Res. 57 (2024) 2928–2939.
[60] Z. Yang, T. Xu, H. Li, M. She, J. Chen, Z. Wang, S. Zhang, J. Li, Chem. Rev. 123 (2023) 11047–11136.
[61] W. Gao, J. He, L. Chen, X. Meng, Y. Ma, L. Cheng, K. Tu, X. Gao, C. Liu, M. Zhang, K. Fan, D.-W. Pang, X. Yan, Nat. Commun. 14 (2023) 160.
[62] B. Geng, J. Hu, Y. Li, S. Feng, D. Pan, L. Feng, L. Shen, Nat. Commun. 13 (2022) 5735.
[63] N. Dhas, M. Pastagia, A. Sharma, A. Khera, R. Kudarha, S. Kulkarni, S. Soman, S. Mutalik, R.P. Barnwal, G. Singh, M. Patel, J. Control. Release 348 (2022) 798–824.
[64] P. Zuo, X. Lu, Z. Sun, Y. Guo, H. He, Microchim. Acta 183 (2015) 519–542.
[65] A. Sharma, J. Das, J. Nanobiotechnol 17 (2019) 92.
[66] Y. Xian, K. Li, Adv. Mater. 34 (2022) 2201031.
[67] H. Yang, Y. Liu, Z. Guo, B. Lei, J. Zhuang, X. Zhang, Z. Liu, C. Hu, Nat. Commun. 10 (2019) 1789.
[68] M. Moniruzzaman, S. Deb Dutta, K.-T. Lim, J. Kim, Appl. Surf. Sci. 597 (2022) 153630.
[69] H. Yan, P. Li, F. Wen, Q. Xu, Q. Guo, W. Su, J. Mater. Res. Technol. 22 (2023) 17–34.
[70] Y. Feng, J. Jiang, Y. Xu, S. Wang, W. An, Q. Chai, U.H. Prova, C. Wang, G. Huang, Carbon 211 (2023) 118105.
[71] X. Miao, D. Qu, D. Yang, B. Nie, Y. Zhao, H. Fan, Z. Sun, Adv. Mater. 30 (2017) 1704740.
[72] P. Gong, L. Sun, F. Wang, X. Liu, Z. Yan, M. Wang, L. Zhang, Z. Tian, Z. Liu, J. You, Chem. Eng. J. 356 (2019) 994–1002.
[73] J. Li, S. Yang, Z. Liu, G. Wang, P. He, W. Wei, M. Yang, Y. Deng, P. Gu, X. Xie, Z. Kang, G. Ding, H. Zhou, X. Fan, Adv. Mater. 33 (2020) 2005096.
[74] J. Chen, T. Lian, S. Liu, J. Zhong, R. Cheng, X. Tang, P. Xu, P. Qiu, J. Colloid Interface Sci. 667 (2024) 450–459.
[75] Y. Cui, D. Yang, Q. Li, Z. Peng, Z. Zhong, Y. Song, Q. Han, Y. Yang, ACS Appl. Mater. Interfaces 16 (2024) 32619–32632.
[76] Y. Gong, J. Huang, X. Xing, H. Liu, Z. Zhou, H. Dong, Chem. Eng. J. 481 (2024) 148523.
[77] J. Liu, F. Gao, L. Zhao, Y. Wu, F. Wang, L. Dong, Y. Jiang, Ceram. Int. 49 (2023) 25253–25260.
[78] Y. Shi, Y. Xia, M. Zhou, Y. Wang, J. Bao, Y. Zhang, J. Cheng, J. Nanobiotechnol. 22 (2024) 88.
[79] H. Li, Y. Dou, H. Yang, H. Xing, C. Zhu, T. Wang, Z. Xuan, M. Yang, J. Nanobiotechnol. 22 (2024) 100.
[80] Q. Wang, T. Zhang, Q. Cheng, B. Wang, Y. Liu, G. Xing, Z. Tang, S. Qu, Adv. Funct. Mater. 34 (2024) 2402976.
[81] M. Vázquez-Nakagawa, L. Rodríguez-Pérez, N. Martín, M.Á. Herranz, Angew. Chem. Int. Ed. 61 (2022) e202211365.
[82] M. Zhang, C. Tong, J. Hazard. Mater. 472 (2024) 134558.
[83] S.-J. Jeon, P. Hu, K. Kim, C.M. Anastasia, H.-I. Kim, C. Castillo, C.B. Ahern, J. A. Pedersen, D.H. Fairbrother, J.P. Giraldo, Environ. Sci. Technol. 57 (2023) 19663–19677.
[84] Z. Wang, Y. Li, B. Zhang, X. Gao, M. Shi, S. Zhang, S. Zhong, Y. Zheng, X. Liu, Adv. Funct. Mater. 33 (2023) 2213143.
[85] Y.J. Chung, B.I. Lee, C.B. Park, Nanoscale 11 (2019) 6297–6306.
[86] A. Saengsrichan, P. Khemthong, W. Wanmolee, S. Youngjan, J. Phanthasri, P. Arjfuk, P. Pongchaikul, S. Ratchahat, P. Posoknistakul, N. Laosiripojana, K.C. W. Wu, C. Sakdaronnarong, Anal. Chim. Acta 1230 (2022) 340368.
[87] H. Wang, Q. Wang, Q. Wang, W. Dong, Y. Liu, Q. Hu, X. Song, S. Shuang, C. Dong, X. Gong, J. Clean. Prod. 411 (2023) 137337.
[88] L. Gao, J. Zhuang, L. Nie, J. Zhang, Y. Zhang, N. Gu, T. Wang, J. Feng, D. Yang, S. Perrett, X. Yan, Nat. Nanotechnol. 2 (2007) 577–583.
[89] J.M. Perez, Nat. Nanotechnol. 2 (2007) 535–536.
[90] H. Wei, E. Wang, Chem. Soc. Rev. 42 (2013) 6060.
[91] F. Cui, L. Li, D. Wang, L. Ren, J. Li, Y. Lu, Y. Meng, R. Ma, S. Wang, X. Li, T. Li, J. Li, Chem. Eng. J. 473 (2023) 145291.
[92] H. Zhang, L. Gao, X. Qi, H. Ma, S. Zhang, Z. Wang, L. Jin, Y. Shen, Colloids Surf., B 241 (2024) 114006.
[93] J. Dong, G. Liu, Y.V. Petrov, Y. Feng, D. Jia, V.E. Baulin, A.Y. Tsivadze, Y. Zhou, B. Li, ACS Mater. Lett. 6 (2024) 1112–1119.
[94] Y. Yang, J. Xu, R. Zhou, Z. Qin, C. Liao, S. Shi, Y. Chen, Y. Guo, S. Zhang, Carbon 219 (2024) 118831.
[95] Y. Liu, B. Xu, M. Lu, S. Li, J. Guo, F. Chen, X. Xiong, Z. Yin, H. Liu, D. Zhou, Bioact. Mater. 12 (2022) 246–256.
[96] S. Liu, J. Wang, X. Wang, Y. Guo, S. Guan, T. Zhang, Colloids Surf., B 239 (2024) 113950.
[97] G. Xu, Z. Ren, J. Xu, H. Lu, X. Liu, Y. Qu, W. Li, M. Zhao, W. Huang, Y.-Q. Li, ACS Appl. Mater. Interfaces 16 (2024) 21689–21698.
[98] D. Chu, H. Qu, X. Huang, Y. Shi, K. Li, W. Lin, Z. Xu, D. Li, H. Chen, L. Gao, W. Wang, H. Wang, Small 20 (2023) 2304968.
[99] G. Jiang, J. Fan, Y. Wan, J. Li, F. Pi, Chem. Eng. J. 480 (2024) 148216.
[100] Y. Tang, X. Liu, P. Qi, Y. Cai, H. Wang, Y. Qin, W. Gu, C. Wang, Y. Sun, C. Zhu, ACS Nano 18 (2024) 25685–25694.
[101] S. Wei, W. Ma, M. Sun, P. Xiang, Z. Tian, L. Mao, L. Gao, Y. Li, Nat. Commun. 15 (2024) 6888.
[102] K. Wang, Q. Hong, C. Zhu, Y. Xu, W. Li, Y. Wang, W. Chen, X. Gu, X. Chen, Y. Fang, Y. Shen, S. Liu, Y. Zhang, Nat. Commun. 15 (2024) 5705.
[103] J. Wu, X. Zhu, Q. Li, Q. Fu, B. Wang, B. Li, S. Wang, Q. Chang, H. Xiang, C. Ye, Q. Li, L. Huang, Y. Liang, D. Wang, Y. Zhao, Y. Li, Nat. Commun. 15 (2024) 6174.
[104] Y. Xu, Y. Ma, X. Chen, K. Wu, K. Wang, Y. Shen, S. Liu, X.J. Gao, Y. Zhang, Angew. Chem. Int. Ed. 63 (2024) e202408935.
[105] X. Li, S. Ding, Z. Lyu, P. Tieu, M. Wang, Z. Feng, X. Pan, Y. Zhou, X. Niu, D. Du, W. Zhu, Y. Lin, Small 18 (2022) 2203001.
[106] Y. Ma, M. Zhang, J. Wu, Y. Zhao, X. Du, H. Huang, Y. Zhou, Y. Liu, Z. Kang, Small 19 (2023) 2300883.
[107] Y. Han, K. Ge, Y. Zhao, M. Bottini, D. Fan, W. Wu, L. Li, F. Liu, S. Gao, X.J. Liang, J. Zhang, Small 20 (2023) 202306656.
[108] Q. Yang, J. Liu, W. Cai, X. Liang, Z. Zhuang, T. Liao, F. Zhang, W. Hu, P. Liu, S. Fan, W. Yu, B. Jiang, C. Li, D. Wang, Z. Xu, Nano Lett. 23 (2023) 8585–8592.
[109] H. Liu, Z. Deng, Z. Zhang, W. Lin, M. Zhang, H. Wang, Matter 7 (2024) 977–990.
[110] G. Wu, H. Qiu, C. Du, Z. Zheng, Q. Liu, Z. Wang, P. Luo, Y. Shen, J. Hazard. Mater. 474 (2024) 134707.
[111] W. Dong, L. Xu, M. Chen, T. Jiang, L. Su, J. Ma, C.-p Chen, G. Zhang, J. Mater. Chem. B 12 (2024) 1052–1063.
[112] Y. Shen, C. Nie, T. Pan, W. Zhang, H. Yang, Y. Ye, X. Wang, Acta Biomater. 168 (2023) 580–592.
[113] L. Cursi, G. Mirra, L. Boselli, P.P. Pompa, Adv. Funct. Mater. 34 (2024) 2315587.
[114] Y. Wu, Y. Qin, M. Muppidathi, R. Carmieli, M. Fadeev, W. Lei, M. Xia, I. Willner, Adv. Funct. Mater. 34 (2023) 2306929.
[115] H. Zhang, P. Wang, J. Zhang, Q. Sun, Q. He, X. He, H. Chen, H. Ji, Angew. Chem. Int. Ed. 63 (2023) e202316779.
[116] P. Jiang, L. Zhang, X. Liu, C. Ye, P. Zhu, T. Tan, D. Wang, Y. Wang, Nat. Commun. 15 (2024) 1010.
[117] G. Xu, K. Liu, B. Jia, Z. Dong, C. Zhang, X. Liu, Y. Qu, W. Li, M. Zhao, H. Zhou, Y.-Q. Li, ACS Nano 18 (2024) 3814–3825.
[118] H. Fan, R. Zhang, K. Fan, L. Gao, X. Yan, ACS Nano 18 (2024) 2533–2540.
[119] F. Li, S. Li, X. Guo, Y. Dong, C. Yao, Y. Liu, Y. Song, X. Tan, L. Gao, D. Yang, Angew. Chem. Int. Ed. 59 (2020) 11087–11092.
[120] K. Yang, C. Wang, X. Wei, S. Ding, C. Liu, F. Tian, F. Li, Bioconjugate Chem. 31 (2019) 595–604.
[121] P. Agostinis, K. Berg, K.A. Cengel, T.H. Foster, A.W. Girotti, S.O. Gollnick, S. M. Hahn, M.R. Hamblin, A. Juzeniene, D. Kessel, M. Korbelik, J. Moan, P. Mroz, D. Nowis, J. Piette, B.C. Wilson, J. Golab, Ca. Cancer J. Clin. 61 (2011) 250–281.
[122] Y. Zhang, C. Yang, D. Yang, Z. Shao, Y. Hu, J. Chen, L. Yuwen, L. Weng, Z. Luo, L. Wang, Phys. Chem. Chem. Phys. 20 (2018) 17262–17267.
[123] Y. Zhou, E.M. Zahran, B.A. Quiroga, J. Perez, K.J. Mintz, Z. Peng, P.Y. Liyanage, R.R. Pandey, C.C. Chusuei, R.M. Leblanc, Appl. Catal., B 248 (2019) 157–166.

[124] K. Luo, W. Sun, Y. Chi, S. Chai, C. Sun, W. Wu, J. Mol. Struct. 1294 (2023) 136525.
[125] X.-L. Guo, Z.-Y. Ding, S.-M. Deng, C.-C. Wen, X.-C. Shen, B.-P. Jiang, H. Liang, Carbon 134 (2018) 519–530.
[126] J. Feng, Y.-L. Yu, J.-H. Wang, N. J. Chem. 44 (2020) 18225–18232.
[127] M. Lan, L. Guo, S. Zhao, Z. Zhang, Q. Jia, L. Yan, J. Xia, H. Zhang, P. Wang, W. Zhang, Adv. Ther. 1 (2018) 1800077.
[128] Z. Li, Q. Pei, Y. Zheng, Z. Xie, M. Zheng, Chem. Eng. J. 467 (2023) 143384.
[129] F. Nichols, J.E. Lu, R. Mercado, M.D. Rojas-Andrade, S. Ning, Z. Azhar, J. Sandhu, R. Cazares, C. Saltikov, S. Chen, Langmuir 36 (2020) 11629–11636.
[130] W. Han, D. Li, X. Hu, W. Qin, H. Sun, S. Wang, X. Duan, Mater. Today Chem. 30 (2023) 101546.
[131] N. Liu, Y. Wang, Z. Wang, Q. He, Y. Liu, X. Dou, Z. Yin, Y. Li, H. Zhu, X. Yuan, Nanoscale 14 (2022) 8183–8191.
[132] C.-Y. Shih, W.-L. Huang, I.T. Chiang, W.-C. Su, H. Teng, Nanoscale 13 (2021) 8431–8441.
[133] Y. Zhang, Q. Jia, F. Nan, J. Wang, K. Liang, J. Li, X. Xue, H. Ren, W. Liu, J. Ge, P. Wang, Biomaterials 293 (2023) 121953.
[134] S. Wu, R. Zhou, H. Chen, J. Zhang, P. Wu, Nanoscale 12 (2020) 5543–5553.
[135] W. Yang, B. Wei, Z. Yang, L. Sheng, J. Inorg. Biochem 193 (2019) 166–172.
[136] L. Jiang, H. Cai, W. Qin, Z. Li, L. Zhang, H. Bi, Bioconjugate Chem. 34 (2023) 1387–1397.
[137] H. Li, J. Guo, A. Liu, Y. Chen, Y. He, J. Qu, W. Yan, J. Song, Adv. Funct. Mater. 33 (2023) 2212141.
[138] V. Juvekar, Y. Cao, C.W. Koh, D.J. Lee, S.Y. Kwak, S.M. Kim, T.J. Park, S. Park, Z. Liu, H.M. Kim, Chem. Eng. J. 493 (2024) 152796.
[139] H. Keum, D. Yoo, S. Jon, Adv. Drug Deliv. Rev. 182 (2022) 114134.
[140] M. Tavakkoli Yaraki, B. Liu, Y.N. Tan, Nano-Micro Lett. 14 (2022) 123.
[141] X. Chu, P. Zhang, Y. Wang, B. Sun, Y. Liu, Q. Zhang, W. Feng, Z. Li, K. Li, N. Zhou, J. Shen, Carbon 176 (2021) 126–138.
[142] C. He, P. Feng, M. Hao, Y. Tang, X. Wu, W. Cui, J. Ma, C. Ke, Adv. Funct. Mater. 34 (2024) 2402588.
[143] W. Ren, H. Wang, Q. Chang, N. Li, J. Yang, S. Hu, Carbon 184 (2021) 102–108.
[144] J. Tang, J. Hu, X. Bai, Y. Wang, J. Cai, Z. Zhang, B. Geng, D. Pan, L. Shen, Small 20 (2024) 2404900.
[145] M. Cheng, Y. Liu, Q. You, Z. Lei, J. Ji, F. Zhang, W.F. Dong, L. Li, Adv. Sci. 11 (2024) 2404230.
[146] C.-H. Fan, N. Wu, C.-K. Yeh, Ultrason. Sonochem. 94 (2023) 106342.
[147] Q. Meng, Q. Wang, Q. Zhang, J. Wang, Y. Li, S. Zhu, R. Liu, H. Zhu, Mater. Chem. Front 8 (2024) 1362–1372.
[148] T. Zhang, H. Xing, M. Xiong, M. Gu, Z. Xu, L. Zhang, Y. Kang, P. Xue, Chem. Eng. J. 488 (2024) 150819.
[149] C. Liu, W. Fan, W.X. Cheng, Y. Gu, Y. Chen, W. Zhou, X.F. Yu, M. Chen, M. Zhu, K. Fan, Q.Y. Luo, Adv. Funct. Mater. 33 (2023) 2213856.
[150] X. Gao, H. Wei, W. Ma, W. Wu, W. Ji, J. Mao, P. Yu, L. Mao, Nat. Commun. 15 (2024) 7915.
[151] Y. Qin, Q. Wang, M. Qian, R. Huang, Mater. Today 76 (2024) 28–39.
[152] Q. Wang, X. Zhu, B. Yin, K. Yan, G. Qiu, X. Liang, R. Jia, J. Chen, X. Wang, Y. Wu, J. Liu, J. Zhong, K. Zhang, D. Wang, Adv. Funct. Mater. 34 (2024) 2408141.
[153] M. Liu, L. Huang, X. Xu, X. Wei, X. Yang, X. Li, B. Wang, Y. Xu, L. Li, Z. Yang, ACS Nano 16 (2022) 9479–9497.
[154] F. Jing, Y. Zhu, F. Li, Y. Wang, X. Yu, K. Zhang, G. Xin, W. Huang, Chem. Eng. J. 465 (2023) 142675.
[155] Y. Rao, G. Xu, Z. Zhang, W. Wang, C. Zhang, M. Zhao, Y. Qu, W. Li, M. Ji, Y. Liu, Y.-Q. Li, Chem. Eng. J. 465 (2023) 142961.
[156] X. Tang, X. Yang, Y. Yu, M. Wu, Y. Li, Z. Zhang, G. Jia, Q. Wang, W. Tu, Y. Wang, X. Zhu, S. Li, J. Nanobiotechnol. 22 (2024) 125.
[157] Y. Xu, J. Chen, W. Jiang, Y. Zhao, C. Yang, Y. Wu, Q. Li, C. Zhu, Small 18 (2021) 2102848.
[158] W. Wang, X. Lin, X. Dong, Y. Sun, Acta Biomater. 148 (2022) 298–309.
[159] X. Xin, J. Liu, X. Liu, Y. Xin, Y. Hou, X. Xiang, Y. Deng, B. Yang, W. Yu, ACS Nano 18 (2024) 8307–8324.
[160] H. Wang, Y. Kang, N. Yang, H. Li, S. Huang, Z. Liang, G. Zeng, Y. Huang, W. Li, M. Zheng, R. Huang, B. Lei, X. Yang, Ecotoxicol. Environ. Saf. 246 (2022) 114177.
[161] F. Gao, J. Liu, P. Gong, Y. Yang, Y. Jiang, Chem. Eng. J. 462 (2023) 142338.
[162] J. Liu, X. Huang, F. Zhang, X. Luo, W. Yu, C. Li, Z. Qiu, Y. Liu, Z. Xu, Chem. Eng. J. 477 (2023) 147048.
[163] A. Bhaloo, S. Nguyen, B.H. Lee, A. Valimukhametova, R. Gonzalez-Rodriguez, O. Sottile, A. Dorsky, A.V. Naumov, Antioxidants 12 (2023) 1536.
[164] S. Xue, T. Zhang, X. Wang, Q. Zhang, S. Huang, L. Zhang, L. Zhang, W. Zhu, Y. Wang, M. Wu, Q. Zhao, P. Li, W. Wu, Small 17 (2021) 2102178.
[165] S. Zou, F. Guo, L. Wu, H. Ju, M. Sun, R. Cai, L. Xu, Y. Gong, A. Gong, M. Zhang, F. Du, Nanotechnology 31 (2020) 165101.
[166] X. Mu, J. Wang, H. He, Q. Li, B. Yang, J. Wang, H. Liu, Y. Gao, L. Ouyang, S. Sun, Q. Ren, X. Shi, W. Hao, Q. Fei, J. Yang, L. Li, R. Vest, T. Wyss-Coray, J. Luo, X.-D. Zhang, Sci. Adv. 7 (2021) eabk1210.
[167] D. Guo, H.-F. Wei, R.-B. Song, J. Fu, X. Lu, R. Jelinek, Q. Min, J.-R. Zhang, Q. Zhang, J.-J. Zhu, Nano Energy 63 (2019) 103875.
[168] H. Zhang, C. Casadevall, J.H. van Wonderen, L. Su, J.N. Butt, E. Reisner, L.J. C. Jeuken, Adv. Funct. Mater. 33 (2023) 2302204.
[169] C. Xu, W. Zhang, R. Wang, S. Tan, J.M. Holub, B. Tang, Anal. Chem. 93 (2021) 9111–9118.
[170] P. Nuntahirun, R. Hanchaina, A. Ratchatacharoensak, M. Supjaroenpisan, S. Suptawornkul, Y. Wang, T. Kangsamaksin, P. Paoprasert, ChemistrySelect 8 (2023) e202302541.
[171] B. Oh, C.H. Lee, Pharm. Res. 33 (2016) 2736–2747.
[172] M.A.S. Shaik, D. Samanta, M. Shaw, I. Mondal, R. Basu, A. Pathak, Sens. Actuators Rep. 4 (2022) 100127.
[173] A. Zeb, S. Sahar, S.Y. Lv, A.B. Yousaf, P. Kasak, X. Lin, Z. Tang, Y. Wu, G. Li, A. W. Xu, Small 18 (2022) 2202522.
[174] P. Muhammad, S. Hanif, J. Li, A. Guller, F.U. Rehman, M. Ismail, D. Zhang, X. Yan, K. Fan, B. Shi, Nano Today 45 (2022) 101530.
[175] L. He, Z. Li, M. Gu, Y. Li, C. Yi, M. Jiang, X. Yu, L. Xu, Adv. Sci. 11 (2024) 2406681.
[176] Y. He, A. Bianco, C. Ménard-Moyon, J. Colloid Interface Sci. 679 (2025) 930–938.
[177] N. Tao, S. Chen, S. Mahdinloo, Q. Zhang, T. Lan, Q. Saiding, S. Chen, Y. Xiong, W. Tao, J. Ouyang, Nano Today 57 (2024) 102371.
[178] Y. Chong, C. Ge, G. Fang, X. Tian, X. Ma, T. Wen, W.G. Wamer, C. Chen, Z. Chai, J.-J. Yin, ACS Nano 10 (2016) 8690–8699.
[179] J. Zhao, H. Wang, H. Geng, Q. Yang, Y. Tong, W. He, ACS Appl. Nano Mater. 4 (2021) 7253–7263.
[180] H. Chen, K. Wen, J. Chen, W. Xing, X. Wu, Q. Shi, A. Peng, H. Huang, Sci. Bull. 65 (2020) 1580–1586.
[181] W. Yang, T. Leng, W. Miao, X. Cao, H. Chen, F. Xu, Y. Fang, Angew. Chem. Int. Ed. 63 (2024) e202403581.
[182] T.F. Durand-Reville, A.A. Miller, J.P. O'Donnell, X. Wu, M.A. Sylvester, S. Guler, R. Iyer, A.B. Shapiro, N.M. Carter, C. Velez-Vega, S.H. Moussa, S.M. McLeod, A. Chen, A.M. Tanudra, J. Zhang, J. Comita-Prevoir, J.A. Romero, H. Huynh, A. D. Ferguson, P.S. Horanyi, S.J. Mayclin, H.S. Heine, G.L. Drusano, J.E. Cummings, R.A. Slayden, R.A. Tommasi, Nature 597 (2021) 698–702.
[183] X. Huang, L. Li, Z. Chen, H. Yu, X. You, N. Kong, W. Tao, X. Zhou, J. Huang, Adv. Mater. 35 (2023) 2302431.
[184] C. Zampaloni, P. Mattei, K. Bleicher, L. Winther, C. Thäte, C. Bucher, J.-M. Adam, A. Alanine, K.E. Amrein, V. Baidin, C. Bieniossek, C. Bissantz, F. Boess, C. Cantrill, T. Clairfeuille, F. Dey, P. Di Giorgio, P. du Castel, D. Dylus, P. Dzygiel, A. Felici, F. García-Alcalde, A. Haldimann, M. Leipner, S. Leyn, S. Louvel, P. Misson, A. Osterman, K. Pahil, S. Rigo, A. Schäublin, S. Scharf, P. Schmitz, T. Stoll, A. Trauner, S. Zoffmann, D. Kahne, J.A.T. Young, M.A. Lobritz, K.A. Bradley, Nature 625 (2024) 566–571.
[185] G. Wang, K. Tang, W. Jiang, Q. Liao, Y. Li, P. Liu, Y. Wu, M. Liu, H. Wang, B. Li, J. Du, P.K. Chu, Adv. Mater. 35 (2023) 2212315.
[186] G. Wang, W. Jiang, S. Mo, L. Xie, Q. Liao, L. Hu, Q. Ruan, K. Tang, B. Mehrjou, M. Liu, L. Tong, H. Wang, J. Zhuang, G. Wu, P.K. Chu, Adv. Sci. 7 (2020) 1902089.
[187] G. Wang, H. Feng, L. Hu, W. Jin, Q. Hao, A. Gao, X. Peng, W. Li, K.-Y. Wong, H. Wang, Z. Li, P.K. Chu, Nat. Commun. 9 (2018) 2055.
[188] Y. Gao, Y. Deng, W. Geng, S. Xiao, T. Wang, X. Xu, M. Adeli, L. Cheng, L. Qiu, C. Cheng, Adv. Mater. 36 (2024) 2408787.
[189] R. Wang, M. Shi, F. Xu, Y. Qiu, P. Zhang, K. Shen, Q. Zhao, J. Yu, Y. Zhang, Nat. Commun. 11 (2020) 4465.
[190] Y. Weng, H. Chen, X. Chen, H. Yang, C.-H. Chen, H. Tan, Nat. Commun. 13 (2022) 4712.
[191] G. Wang, K. Tang, Z. Meng, P. Liu, S. Mo, B. Mehrjou, H. Wang, X. Liu, Z. Wu, P. K. Chu, Adv. Mater. 32 (2020) 2003616.
[192] G. Wang, W. Jin, A.M. Qasim, A. Gao, X. Peng, W. Li, H. Feng, P.K. Chu, Biomaterials 124 (2017) 25–34.
[193] K. Cheng, H. Wang, S. Sun, M. Wu, H. Shen, K. Chen, Z. Zhang, S. Li, H. Lin, Small 19 (2023) 2207868.
[194] W. Song, X. Wang, S. Nong, M. Wang, S. Kang, F. Wang, L. Xu, Adv. Funct. Mater. 34 (2024) 2402761.
[195] R. Zhang, C. Miao, X. Lin, R. Lin, X. Deng, J. Huang, Y. Wang, Y. Xu, S. Weng, M. Chen, Carbon 217 (2024) 118617.
[196] S. Dai, L. Yao, L. Liu, J. Cui, Z. Su, A. Zhao, P. Yang, Acta Biomater. 186 (2024) 454–469.
[197] H. Wang, S. Sun, Y. Zhao, P. Wang, Y. Zhou, H. Sun, J. Yang, K. Cheng, S. Li, H. Lin, Small 20 (2024) 2403160.
[198] D.-Y. Hou, D.-B. Cheng, N.-Y. Zhang, Z.-J. Wang, X.-J. Hu, X. Li, M.-Y. Lv, X.-P. Li, L.-R. Jian, J.-P. Ma, T. Sun, Z.-Y. Qiao, W. Xu, H. Wang, Nat. Commun. 15 (2024) 454.
[199] M. Liu, Y. Chen, Y. Guo, H. Yuan, T. Cui, S. Yao, S. Jin, H. Fan, C. Wang, R. Xie, W. He, Z. Guo, Nat. Commun. 13 (2022) 2179.
[200] J. Yan, R. Bhadane, M. Ran, X. Ma, Y. Li, D. Zheng, O.M.H. Salo-Ahen, H. Zhang, Nat. Commun. 15 (2024) 3684.
[201] E. Kirbas Cilingir, O. Besbinar, L. Giro, M. Bartoli, J.L. Hueso, K.J. Mintz, Y. Aydogan, J.M. Garber, M. Turktas, O. Ekim, A. Ceylan, M.A. Unal, M. Ensoy, F. Arı, O. Ozgenç Çinar, B.I. Ozturk, C. Gokce, D. Cansaran-Duman, M. Braun, J. Wachtveitl, J. Santamaria, L.G. Delogu, A. Tagliaferro, A. Yilmazer, R. M. Leblanc, Small 20 (2024) 2309283.
[202] L. Yang, Z. Zhao, B. Tian, M. Yang, Y. Dong, B. Zhou, S. Gai, Y. Xie, J. Lin, Nat. Commun. 15 (2024) 7499.
[203] X. Zhang, J. Zhu, S. Wang, S. Li, E. J, J. Hu, R. Mou, H. Ding, P. Yang, R. Xie, Adv. Funct. Mater. 34 (2024) 2402022.
[204] G. Zhu, Y. Xie, J. Wang, M. Wang, Y. Qian, Q. Sun, Y. Dai, C. Li, Adv. Mater. 36 (2024) 2409066.
[205] Q. Cheng, T. Zhang, Q. Wang, X. Wu, L. Li, R. Lin, Y. Zhou, S. Qu, Adv. Mater. 36 (2024) 2408685.
[206] S. Sun, Q. Chen, Z. Tang, C. Liu, Z. Li, A. Wu, H. Lin, Angew. Chem. Int. Ed. 59 (2020) 21041–21048.
[207] A. Wibrianto, G. Getachew, W.B. Direrssa, A.S. Rasal, C.-C. Huang, T.-C. Kan, J. Chang, J.-Y. Chang, Carbon 208 (2023) 191–207.
[208] H. Cai, X. Wu, L. Jiang, F. Yu, Y. Yang, Y. Li, X. Zhang, J. Liu, Z. Li, H. Bi, Chin. Chem. Lett. 35 (2024) 108946.

[209] A. Aich, A. Boshnakovska, S. Witte, T. Gall, K. Unthan-Fechner, R. Yousefi, A. Chowdhury, D. Dahal, A. Methi, S. Kaufmann, I. Silbern, J. Prochazka, Z. Nichtova, M. Palkova, M. Raishbrook, G. Koubkova, R. Sedlacek, S.E. Tröder, B. Zevnik, D. Riedel, S. Michanski, W. Möbius, P. Ströbel, C. Lüchtenborg, P. Giavalisco, H. Urlaub, A. Fischer, B. Brügger, S. Jakobs, P. Rehling, Nat. Commun. 15 (2024) 6914.
[210] Z. He, W. Chen, K. Hu, Y. Luo, W. Zeng, X. He, T. Li, J. Ouyang, Y. Li, L. Xie, Y. Zhang, Q. Xu, S. Yang, M. Guo, W. Zou, Y. Li, L. Huang, L. Chen, X. Zhang, Q. Saiding, R. Wang, M.-R. Zhang, N. Kong, T. Xie, X. Song, W. Tao, Nat. Nanotechnol. 19 (2024) 1386–1398.
[211] M. Kawamura, C. Parmentier, S. Ray, S. Clotet-Freixas, S. Leung, R. John, L. Mazilescu, E. Nogueira, Y. Noguchi, T. Goto, B. Arulratnam, S. Ganesh, T. Tamang, K. Lees, T.W. Reichman, A.C. Andreazza, P.K. Kim, A. Konvalinka, M. Selzner, L.A. Robinson, Nat. Commun. 15 (2024) 8086.
[212] P. Liu, T. Zhang, Y. Wu, Q. Chen, T. Sun, C. Jiang, Adv. Mater. 36 (2024) 2408729.
[213] Y. Ma, J. Zhao, L. Cheng, C. Li, X. Yan, Z. Deng, Y. Zhang, J. Liang, C. Liu, M. Zhang, Carbon 204 (2023) 526–537.
[214] W. Guo, M. Ji, Y. Li, M. Qian, Y. Qin, W. Li, H. Nie, W. Lv, G. Jiang, R. Huang, C. Lin, H. Li, R. Huang, Biomaterials 309 (2024) 122622.
[215] J. Cheng, S. Zhang, C. Li, K. Li, X. Jia, Q. Wei, H. Qi, J. Zhang, Nat. Commun. 13 (2022) 7166.
[216] X. Tang, Y. Shang, H. Yang, Y. Song, S. Li, Y. Qin, J. Song, K. Chen, Y. Liu, D. Zhang, L. Chen, Nat. Commun. 15 (2024) 1673.
[217] J. Wang, P. Shangguan, X. Chen, Y. Zhong, M. Lin, M. He, Y. Liu, Y. Zhou, X. Pang, L. Han, M. Lu, X. Wang, Y. Liu, H. Yang, J. Chen, C. Song, J. Zhang, X. Wang, B. Shi, B.Z. Tang, Nat. Commun. 15 (2024) 705.
[218] X. Duan, X. Yang, N. Mou, Y. Cao, Z. He, L. Zhu, Y. Zhong, K. Zhang, K. Qu, X. Qin, Q. Chen, Y. Luo, W. Wu, Adv. Funct. Mater. 34 (2024) 2405629.
[219] Q. Chen, X. Duan, Y. Yu, R. Ni, G. Song, X. Yang, L. Zhu, Y. Zhong, K. Zhang, K. Qu, X. Qin, W. Wu, Adv. Sci. 11 (2023) 2307441.

Guopeng Xu is a PhD candidate in School of medicine, Tongji University. He obtained his bachelor's and master's degree in Physics from Lanzhou University and Shandong University, respectively. His research interest is focused on the design of physical/chemical antibacterial interfaces and wireless-charging bactericidal devices based on functional carbon dots.

Prof. Paul K. Chu is Chair Professor of Materials Engineering in the Department of Physics, Department of Materials Science & Engineering, and Department of Biomedical Engineering at City University of Hong Kong. He received his BS in mathematics (cum laude) from The Ohio State University in 1977 and his MS and PhD in chemistry from Cornell University in 1 979 and 1982, respectively. In addition to being a Fellow and Council Member of the Hong Kong Academy of Engineering, he is a Fellow of the American Physical Society (APS), American Vacuum Society (AVS), Institute of Electrical and Electronics Engineers (IEEE), Materials Research Society (MRS), and Hong Kong Institution of Engineers (HKIE). He has received more than 30 research/technical awards, including the IEEE NPSS Merit Award and two first-class natural science awards from Shanghai (China) and the Chinese Ministry of Education. He has been granted more than 30 patents and his papers have been cited more than 120,000 times (h-index ~150). He is a highly cited researcher in materials science/cross-field (Web of Science, 2016 to present).

Guomin Wang is a professor at School of Medicine, Tongji University, China. She earned her B.S., M.S., and Ph.D. degrees from Nankai University, Peking University, and City University of Hong Kong, respectively. With over a decade of research experience in surface modification, she has authored more than 20 publications as first and/or corresponding author in prestigious journals such as Nature Communications, Advanced Materials, Advanced Science, and Biomaterials. Her work has been cited over 2,900 times, contributing to an h-index of 28 (Google Scholar). As a principal investigator, she has secured research funding exceeding HK$8 million from various agencies, including the Hong Kong Health and Medical Research Fund and the National Natural Science Foundation of China.